T.R.
ÜSKÜDAR UNIVERSITY
INSTITUTE OF SCIENCE

BIOTECHNOLOGY DEPARTMENT

BIOTECHNOLOGY MASTER'S THESIS PROGRAM

MASTER'S DEGREE THESIS

VIRTUAL FUNCTIONAL PROFILING OF VARIANTS OF UNKNOWN SIGNIFICANCE IN THE GABRB3 GENE ASSOCIATED WITH EPILEPSY

Derya TÜRKMEN DELİOĞLU

Thesis Advisor
Asst. Prof. Dr. Ayla ARSLAN

İSTANBUL-2024

T.R.
ÜSKÜDAR UNIVERSITY
INSTITUTE OF SCIENCE

BIOTECHNOLOGY DEPARTMENT

BIOTECHNOLOGY MASTER'S THESIS PROGRAM

MASTER'S DEGREE THESIS

VIRTUAL FUNCTIONAL PROFILING OF VARIANTS OF UNKNOWN SIGNIFICANCE IN THE GABRB3 GENE ASSOCIATED WITH EPILEPSY

Derya TÜRKMEN DELİOĞLU

Thesis Advisor
Asst. Prof. Dr. Ayla ARSLAN

İSTANBUL-2024

ÖZET

EPİLEPSİ İLE İLİŞKİLİ GABRB3 GENİNDEKİ ÖNEMİ BİLİNMEYEN VARYANTLARIN SANAL FONKSİYONEL PROFİLİ

GABA (A) reseptörleri beyindeki birincil inhibisyona aracılık eden, kimyasal kapılı heteropentamerik klorür kanallarıdır. GABA (A) reseptörlerinin beta 3 (β3) alt birimi, epilepsi dahil bir dizi bozuklukla ilişkilidir. Spesifik olarak, β3 alt birimini kodlayan gendeki (GABRB3) varyant konumu, epilepsi fenotip şiddeti ve hücresel patoloji mekanizmalarıyla ilişkilidir. Bu, GABRB3'ün önemi bilinmeyen varyantlarından (VUS) herhangi birinin bu bulgularla uyumlu olup olmayacağı ve ilgili patojeniteyi gösterip göstermeyeceği sorusuna yol açmaktadır. Bu soruya cevaben, çoklu algoritmalar kullanan araştırmamız, ClinVar veritabanından elde edilen ve β3 alt birimini kodlayan VUS arasında 141 nokta mutasyonunu hesaplamalı yöntemlerle derinlemesine incelemeyi amaçlayarak, β3 alt birimi kodlama bölgesinde bulunan 17 genetik varyantı patojenik olarak belirlemiştir. Bu varyantlardan on tanesi β3 alt biriminin (Y48C, D49E, D73H, M80R, D94E, H132Y, R142C, P169L, C175W, Y182H) N-terminal hücre dışı alanında haritalanmıştır; bir tanesi (S264F) birinci transmembran (TM1) alanda, iki tanesi (T281A, R294Q) ikinci transmembran (TM2) alanda, iki tanesi (R294Q, P298S) ikinci ve üçüncü transmembran alanın arasındaki bölgede (TM2-TM3 arasındaki bölge) ve iki tanesi de (Y467S, Y467H) β3 alt biriminin dördüncü transmembran (TM4) alanında bulunmaktadır. Bu sonuçlar, literatür verileri ışığında değerlendirildiğinde, varyantların β3 alt birimindeki pozisyonuna göre epilepsi fenotip şiddeti ve hücresel patoloji mekanizmalarının tahmin edilmesine olanak sunabilir. Ek olarak, çalışmanın ikinci aşamasında GABA bağlanma bölgesinde bulunan 6 VUS, varyantın GABA ligandına bağlanma afinitesi üzerindeki etkisi açısından da incelenmiştir. Bu çalışma için seçilen tüm VUS seti (141) arasından GABA molekülüne bağlandığı deneysel çalışmalarla gösterilmiş aminoasitlere tekabül eden 6 VUS seti tespit edilmiş (Y182H (PDB aralığında Y157), Y182C (PDB aralığında Y157), F225V (PDB aralığında F200), T227A (PDB aralığında T202), T227P (PDB aralığında T202), Y230C (PDB aralığında Y205)) ve bunların GABA bağlanma afinitesi üzerindeki değişken etkisi moleküler kenetlenme simülasyonları kullanılarak hesaplanmıştır. Kenetlenme simülasyonları sonucunda 6 VUS'un herbiri için serbest enerji değişim değeri (ΔΔG), yabanıl tipteki (WT: -5.3 Kcal/mol) konformasyonun ΔΔG'sinden daha yüksek olduğu bulunmuştur: Y182C>

Y182H> T227P= T227A> F225V= Y230C> WT. Ayrıca yabanıl tip (WT) ve beş varyant (Y182H, T227P, T227A, F225V, Y230C) 182. pozisyonda GABA ile hidrojen bağına sahipken, yalnızca Y182C varyantı 182. pozisyonda GABA ile herhangi bir hidrojen bağı etkileşimi göstermemiştir. Y182C varyantının bağlanma afinitesinde en kritik düşüşü sergilediği gözlenmiştir. Sonuç olarak özellikle Y182C (ΔΔG, -4.8 Kcal/mol) ve Y182H (ΔΔG, -4.9 Kcal/mol) varyantlarının, diğer varyantlara göre daha yüksek enerjili ligand pozu sunması sebebiyle, reseptöre GABA'nın bağlanmasını olumsuz etkileyerek reseptör ligand etkileşimini bozması ve reseptör kanalının açılmasını olumsuz yönde etkileyerek fonksiyonunda dejenerasyona yol açacağı muhtemeldir. Bu çalışmanın sonuçları ACMG (Amerikan Tıbbi Genetik Koleji) PP3 varyant yorumlama kriteri doğrultusunda, GABRB3 geni varyantlarının (VUS) epilepside hassas tıp uygulamaları açısından anlamlıdır. Aynı zamanda GABRB3 varyantlarının epilepsi gibi sinir ağı bözukluklarında moleküler ve hücresel seviyede patolojisini incelemeyi amaçlayan laboratuvar araştırmalarına rehberlik etme açısından da önem taşımaktadır.

Keywords: Epilepsi, GABA (A) reseptör, GABRB3, İn siliko, SNP

ABSTRACT

VIRTUAL FUNCTIONAL PROFILING of VARIANTS of UNKNOWN SIGNIFICANCE in the GABRB3 GENE ASSOCIATED with EPILEPSY

GABA (A) receptors are heteropentameric chloride channels mediating the primary inhibition in the brain. Beta 3 (β3) subunit of GABA (A) receptors are associated with a range of disorders including epilepsy. Specifically, the variant location in the β3 subunit encoding gene (GABRB3), correlates with various epilepsy phenotype and cellular pathology. This leads to the question to ask if any of the variants of unknown significance (VUSs) of the GABRB3 would align with these findings and manifest relevant pathogenicity. Employing multiple algorithms, our investigation delved into 141 GABRB3 VUS sourced from ClinVar, pinpointing 17 notably pathogenic ones within the β3 subunit. Ten of these variants were mapped on the N-terminus extracellular domain of the β3 subunit (Y48C, D49E, D73H, M80R, D94E, H132Y, R142C, P169L, C175W, Y182H), one (S264F) is located in the first transmembrane domain (TM1), two variants (T281A, R294Q) were located in the second trasnmembrane domain (TM2), two (R294Q, P298S) in the linker between the second and third transmembrane domains (TM2-TM3 linker) and two (Y467S, Y467H) were in the fourth transmembrane domain (TM4) of the β3 subunit. These results, when evaluated in the light of literature data, enable the prediction of epilepsy phenotype severity and cellular pathology mechanisms according to the position of the variants in the β3 subunit. Additionally, in the second phase of the study, variants, which were selected from those matching with the experimentally determined residues located in the GABA binding site, were computationally studied to assess the variant impact on GABA binding affinity. Among the entire set of 141 GABRB3 VUS identified in this study, these variants (6) were Y182H (Y157 in PDB range), Y182C (Y157 in PDB range), F225V (F200 in PDB range), T227A (T202 in PDB range), T227P (T202 in PDB range), Y230C (Y205 in PDB range), which were analyzed by docking simulations to investigate the variant impact on binding affinity to the GABA molecule. Docking simulations showed that the double free energy difference (ΔΔG) of these 6 variants were higher than the ΔΔG of the wild type (WT: -5.3 Kcal/mol) conformation, i.e., Y182C> Y182H> T227P= T227A> F225V= Y230C> WT. It was significant in terms of molecular docking results that Y182H (ΔΔG, -4.9 Kcal/mol) and Y182C (ΔΔG, -4.8 Kcal/mol) variants presented a higher energy ligand pose to GABA

compared to rest of the variants analyzed by docking simulations. In addition, while wild type (WT) and five variants (Y182H, T227P, T227A, F225V, Y230C) had hydrogen bonds with GABA at codon 182, only the variant Y182C did not show any hydrogen bond interaction with GABA at codon 182. It was observed that variant Y182C exhibited the most critical decrease of binding affinity. Thus, the Y182H (ΔΔG, -4.9 Kcal/mol) and especially Y182C (ΔΔG, -4.8 Kcal/mol) presented a higher energy ligand pose than the other variants, thus negatively affecting GABA binding, possibly disrupting the receptor-ligand interaction and negatively affecting the opening of the receptor. The results of this study are significant in emphasizing the importance of GABRB3 gene VUSs for the precision medicine in epilepsy, in line with the PP3 variant interpretation criteria of the American College of Medical Genetics (ACMG). Our results are also important to guide laboratory studies aimed at defining the molecular and cellular pathology of GABRB3 variants in network disorders.

Keywords: Epilepsy, GABA (A) receptor, GABRB3, In silico, SNP

FORWORD

I am sincerely grateful to my scientific advisor, Asst. Prof. Dr. Ayla Arslan, whose support and guidance throughout the project was invaluable.You have been a fantastic primary advisor. I would like to thank all the academicians who helped me reach this stage, especially Professor Dr. Tunç Çatal. I would like to thank my dear Asst. Prof. Dr. Gizem Köprülü Küçük, who noticed my interest in science and guided me on this way.

I am grateful to my grandmother, Gülen Sezgin, for the care and support she gave me, even though she was in a period of life when she needed more attention. I also hope this thesis will inspire my son.

DECLARATION FORM

I declare that this study is my own thesis work, that I obtained the information in all processes of the thesis by adhering to academic and ethical rules, and that I cite all information and comments that were not obtained through the thesis study. I also declare that this thesis has been written in accordance with the Üsküdar University Institute of Science Thesis Writing Guide.

January, 2024

Derya Türkmen Delioğlu

TABLE OF CONTENTS

INDEX of TABLES

INDEX of FIGURES

ICONS and INDEX of ABBREVIATIONS

ΔΔG: Change in Binding Free Energy

Å: Angstrom

ACMG: The American College of Medical Genetics and Genomics.

AMP: Association for Molecular Pathology

ASD: Anti-seizure drug

CNS: Central Nervous System

CI: Confidence Interval

ECA: Epilepsy, Childhood Absence

ECD: Extracellular Domain (N terminus)

DEE: Developmental and Epileptic Encephalopathy

EOEE: Early-Onset Epileptic Encephalopathy

FS: Febrile Seizures

GABRB3: Gamma-aminobutyric acid A receptor beta 3 subunit gene

$GABA_ARs$: Gamma-aminobutyric acid A receptors

CADD: Computer-Aided Drug Design

GGE: Genetic Generalized Epilepsy

GEFS: Generalized Epilepsy with Febrile Seizures

GWAS: Genome-Wide Association Studies

HGP: Human Genome Project

JME: Juvenile Myoclonic Epilepsy

LOF: Loss of Function

MTLEHS: Mesial Temporal Lobe Epilepsy with Hippocampal Sclerosis

NCBI: National Library of Medicine

NGS: Next-Generation Sequencing

NHGRI: National Human Genome Research Institute

SBDD: Structure-Based Drug Design

SNP: Single Nucleotide Polymorphisms

TM1: First transmembrane domain

TM2: Second transmembrane domain

TM2-TM3 Loop: Segment between the first and the second transmembrane domains

VUS: Variants of Uncertain (Unknown) Significance

1. INTRODUCTION

Epilepsy is one of the most common chronic neurological diseases affecting all age groups. Recurrent epileptic seizures not only affect the quality of life of patients and even their families, but can also lead to the death of patients. In addition, when factors such as total annual health expenditures and absenteeism from work and school are taken into consideration, it can be understood how much the disease increases the economic burden of countries (*Libby et al., 2012*). Epilepsy, which occurs when cells in a part of the brain send abnormal electrical signals, manifests itself with seizures. There are various experimental and theoretical studies aimed at understanding the mechanisms underlying the onset and propagation of this electrical activity (*Ben-Ari et al., 2012; Ghit et al., 2021*). With the advent of pharmacological treatment of epilepsy at the beginning of the 19th century, human and animal research continued to provide hope for treatment for many years, but our understanding of the mechanisms that cause neuronal hyperactivity remains incomplete (*Kaculini et al., 2021*). Epilepsy is a disease that may occur as a result of an imbalance in inhibitory and excitatory signal transmission in the brain (*Treiman, 2001*). Therefore, it is not surprising that research has focused on gamma aminobutyric acid (GABA) receptors, the major inhibitory neurotransmitter in the brain. It will be easier to develop therapeutic solutions when the genetic causes of disorders in the relevant mechanisms are better understood. In addition, the underlying reasons why approximately one-third of individuals with epilepsy do not respond to treatment are still being investigated, and this pharmacoresistance has not yet been fully explained (*Lerche, 2020*). Given that GABA receptors have become therapeutic targets in epilepsy in recent years, it would be logical to identify the pathogenic effects of gamma-aminobutyric acid type A receptor subunit beta3 (GABRB3) mutations when trying to explain why individuals respond differently to drugs.

In recent years, the rapid expansion of genomic data with genome-wide association studies (GWAS) and next-generation sequencing (NGS) has revealed the need to accelerate experimental research. Genome-wide association studies (GWAS) compare the genome of individuals with a particular phenotype, such as epilepsy, with individuals without the disease phenotype. In this way, it becomes possible to use it as a genetic marker, in addition to contributing to studies on association with the phenotype of

epilepsy (*Wang et al., 2017a; Perucca and Perucca, 2019)*. In this context, prediction of possible molecular effects of variants has begun to be made using statistical methods as well as experimental approaches. Bioinformatic prediction tools have become frequently used, becoming one of the popular strategies to reveal the genetic basis of complex diseases in humans.

In this study, the computational approach was performed on variants of the ligand-gated ion channel receptor GABRB3. These variants may be associated with the underlying cellular pathology of epilepsy and may provide valuable information in understanding the genetic mechanism underlying epilepsy (*Löscher, 2020*). Resistance to antiepileptic drugs in different individuals may be due to the presence of SNPs that alter the expression of GABA receptors in brain tissue. Therefore, identifying the functional effects of SNPs in silico will open the door to understanding the complex mechanisms of epileptic seizures.In this context, estimating the pathogenicity of GABRB3 variants with bioinformatics prediction tools will contribute to personalized treatments with the contribution of experimental studies while creating treatment strategies for individuals with epilepsy. Additionally, the results of this study have implications for guiding wet laboratory experiments in the field of epilepsy.

2. GENERAL INFORMATION

2.1. Genetic Polymorphism

Genomic polymorphism is two or more variant forms of a specific DNA sequence that can occur between different individuals. It has been shown in many studies that some polymorphisms in genes mediate abnormal expression or production of an abnormal form of the protein (*Shastry, 2009*). According to National Human Genome Research Institute (NHGRI, 2021), the incidence of the gene polymorphism in the population is estimated to be ≥1%. If the polymorphism is shown to be associated with disease, it is often called a genetic mutation. The most common type of polymorphism involves variation in a single nucleotide. Other polymorphisms may be much larger and involve longer sections of DNA. DNA polymorphism types are classified as tandem repeat polymorphisms, short tandem repeats, copy-number polymorphism and single nucleotide polymorphism (SNP). SNPs are the most common type of genetic variation among humans (*Azizzadeh-Roodpish et al., 2021*).

A single nucleotide polymorphism (SNP) is a variation in the genetic sequence that affects only one of the bases adenine (A), guanine (G), thymine (T), or cytosine (C), the base part of the nucleotide in a section of a DNA molecule (*fig. 1, Mila et al., 2022*). For example, a SNP can replace the nucleotide adenine (A) with the nucleotide guanine (G) in a particular section of DNA. In order to be defined as a polymorphism, it must occur in more than 1 percent of the population (*Katsonis et al., 2022*). There are pathogenic or nonpathogenic SNPs in the human genome that occur in exon or intron regions (*Cargill et al., 1999*). By scanning the entire genome of a large number of individuals with Genome-Wide Association Study (GWAS), millions of genetic variants in these individuals and their relationships with heart diseases, metabolic diseases, autoimmune diseases, neurodegenerative and psychiatric disorders were investigated. Only a few of the SNPs that have pathogenic effects on these diseases have been identified. These findings facilitated the pathogenesis of the disease and the development of personalized therapies (*Visscher et al., 2017*).

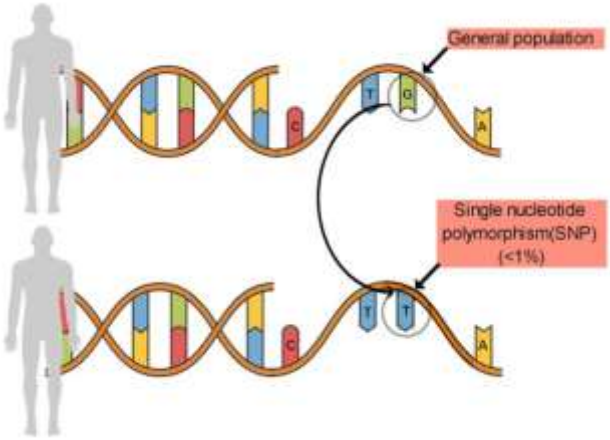

Figure 1. The schema of single nucleotide polymorphism (SNP) .
(Image reproduced based on Mila et al., 2022)

2.2. Role of GABAergic Inhibition in Epilepcy Treatment

Considering that approximately 1-2% of the world's population is affected by epilepsy today, it is very important to identify and treat the molecular mechanisms that cause epilepsy (*Staley, 2015*). Although there have been significant advances in our knowledge of pathophysiological development and prognosis in the last 20 years, drug-resistant patient groups are still untreated, meaning one-third of the total patient burden is still untreated. It is understandable that anti-seizure drugs, which are frequently preferred today, do not provide complete seizure control and have side effects, in terms of researching new drug targets.

The first option tried in the treatment of epilepsy is seizure prevention. Although the number of approved drugs is more than 20, one third of patients cannot benefit from the treatment (*Devinsky et al., 2018*). For patient groups that cannot benefit from drug treatment, surgery, neurostimulation devices, dietary treatments or clinical trials of new anti-seizure drugs (ASDs) are being tried as alternative options for seizure control. In addition to the completion of the human genome project, the increasing number of mouse experiments and human studies in recent years and studies on the molecular genetics of epilepsies need to be transformed into precise therapies and treatments. The most effective way to improve the effectiveness of personalized epilepsy treatments will undoubtedly be to try to identify genetic variations that cause variation in response to antiepileptic drug treatment.

An imbalance between excitation (E) and inhibition (I) in the brain is known to cause impairment in GABAergic inhibition (*Tang et al., 2021; Righes Marafiga et al., 2021*).

A considerable part of neurodevelopmental disorders (NDDs) risk genes encode $GABA_ARs$, which are one of the critical components of the GABAergic inhibition system (*Satterstrom et al., 2020*).

2.2.1 Gamma-Aminobutyric Acid

In experiments conducted in 1950, it was determined that the unknown compound (ninhydrin-reactive substance) in the brain extract was definitely γ-aminobutyric acid, and with this study, GABA (*fig. 2*) was discovered for the first time (*Bowery and Smart, 2006*). Contributed by experiments with mouse brain homogenates, washed residues, and acetone powders, it has been shown that γ-aminobutyric acid is synthesized from glutamic acid in the brain (*Roberts and Frankel, 1950*). With this discovery, studies on GABA's relationship with neuronal activity began to gain momentum.

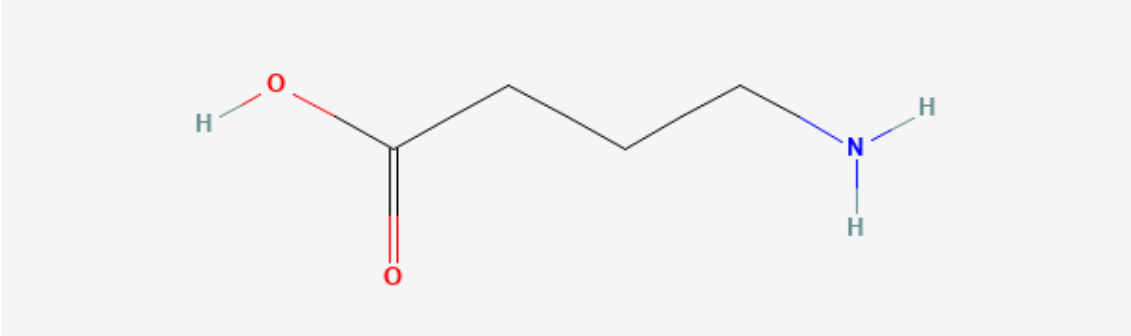

Figure 2. 2D structure of GABA

The chemical structure depiction of GABA, whose molecular formula is C4H9NO2, was taken from the PubChem website; Last accessed on January 20th, 2023 (PubChem CID: 119)

GABA and glutamate are respectively the primary inhibitory (I) and excitatory (E) neurotransmitters in the central nervous system. The opposing functions of these two neurotransmitters ensure that their activities are balanced under normal physiological conditions. Since glutamate is the precursor of GABA, an increase in glutamate levels causes an increase in GABA synthesis (*Nikolaus et al., 2010; Lee et al., 2019*).

In GABA production (*fig. 3, Mead et al., 2013*), α-ketoglutarate, obtained from glucose metabolism in the Krebs cycle, is first converted to glutamate by GABA α-

oxoglutarate transaminase (GABA-T). Glutamate decarboxylase (GAD) catalyzes the decarboxylation of glutamate to form GABA. GABA is metabolized by GABA transaminase to form succinic semialdehyde. Succinic semialdehyde can be oxidized to succinic acid by the enzyme succinic semialdehyde dehydrogenase (SSADH) and enter the Krebs cycle again (*Ghit et al., 2021*). GABA produced by glutamate is transported to secretory vesicles and released into the synaptic gap by depolarization of the presynaptic neuron. From here it binds to its receptor on the membrane surface of the postsynaptic neuron. It continues its function here until it is taken back by presynaptic nerve terminals and glial cells (*Treiman, 2001*).

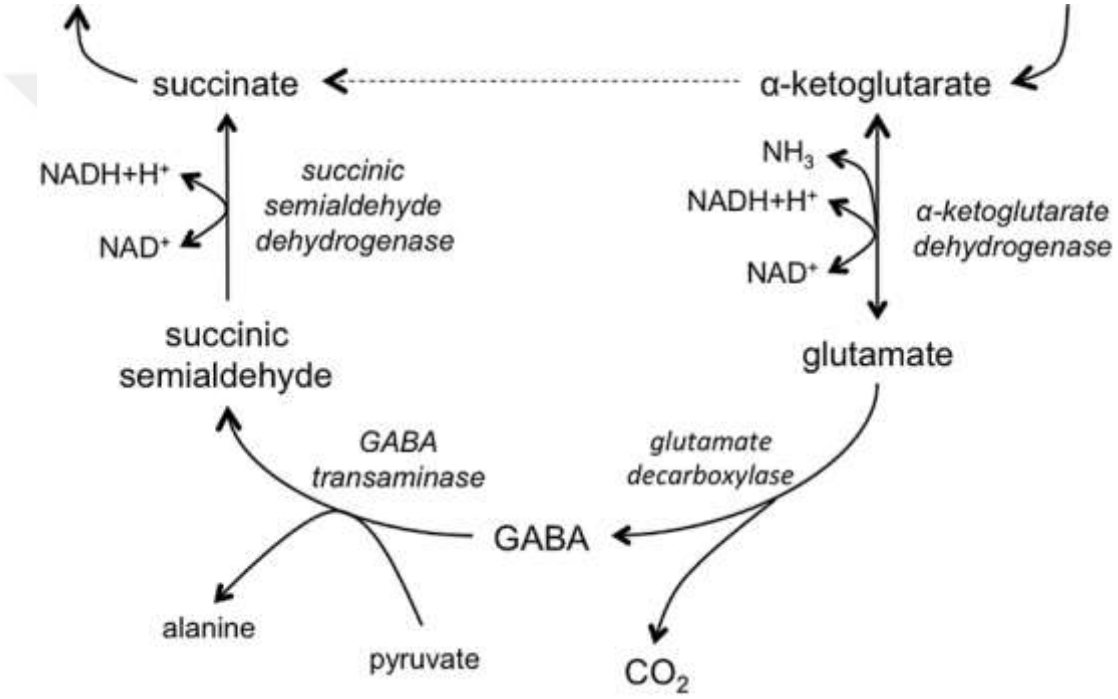

Figure 3. The GABA shunt.

(Scheme reproduced based on Mead et al., 2013)

With the understanding that epileptic seizures in epilepsy occur as a result of sudden and temporary synchronization of neuronal activity, the course of treatment of seizures has changed to the receptors that affect the major neurotransmitters in the brain (*Cloix, 2009*). Healthy brain functions depend on the balance of signals created by both excitatory and inhibitory neurotransmitters on target neurons. Epileptic seizures may occur following increased neuronal excitability as a result of an imbalance in the signaling

levels of γ-aminobutyric acid (GABA) and glutamate neurotransmitters, which are inhibitory and excitatory, respectively (*Treiman, 2001*). Two types of GABA receptors, $GABA_A$ and $GABA_B$, lead to inhibition of neuronal activity. While the $GABA_A$ receptor mediates fast inhibitory signals through postsynaptic membrane hyperpolarization, the $GABA_B$ receptor mediates slow and long-lasting inhibitory signals linked G proteins. $GABA_A$ receptors induce the inflow of chloride ions, while $GABA_B$ receptors induce the efflux of K+ ions (*Terunuma, 2018*). Drug active substances such as benzodiazepines, anesthetics and barbiturates are also used in the treatment of epilepsy by binding to specific binding sites of $GABA_A$ receptor.

In general, the causes of epilepsy include structural, genetic, metabolic, infectious, immune and other unknown factors (*Scheffer et al., 2017*). Sequencing approaches such as whole exome sequencing (WES) and whole genome sequencing (WGS) have accelerated new gene discovery in epilepsy (*Perucca et al., 2020*). The discovery of nearly 3000 genes associated with epilepsy has been very useful for focusing on targeted therapies. Many associations have been found with GABRB3, one of the genes related to ion channels, in idiopathic/genetic epilepsies were found based on literature information obtained from National Center for Biotechnology Information (NCBI-last accessed: September 2023). As mentioned before, this research will focus on single nucleotide polymorphisms (SNPs) in the γ-aminobutyric acid receptor subunit beta-3 (GABRB3), which is included in the classification of genetic factors.

2.2.2. GABA (A) Receptors

The importance of γ-aminobutyric acid (GABA) is that, in addition to being the most common inhibitory neurotransmitter in the mammalian brain, it plays an important role in the pathogenesis or expression of many neurological diseases, including epilepsy (*Ben-Ari et al., 2012*). Gamma-aminobutyric acid (GABA), which is most prevalent distributed in the brain, is capable of producing hyperpolarizing inhibition in almost all neurons (*Ghit et al., 2021*). With the presence of GABA, $GABA_A$ receptors ($GABA_A$ and $GABA_B$) are activated and the increased chloride ion flow causes membrane hyperpolarization. As a result, GABA-dependent neuronal excitability decreases. It is thought to play a key role in the basis of epilepsy due to its effect on neuronal inhibition.

Two receptors that play a role in the inhibitory effect on neuron function through GABA; They are GABA type A ($GABA_A$) receptors ($GABA_ARs$) and GABA type B

($GABA_B$) receptors ($GABA_BRs$). $GABA_ARs$ are more associated with epilepsy because they mediate a more rapid inhibitory effect than $GABA_BRs$ (*Bryson and Petrou, 2023*).

The $GABA_A$ receptor is a member of the ligand-gated ion channels superfamily. This family also includes the nicotinic acetylcholine receptor, 5-hydroxytryptamine type 3 receptor, and glycine receptor (*Cecchini and Changeux, 1995*). $GABA_A$ receptors consist of pentameric combinations of different subunits. In humans, there are a total of 19 $GABA_A$ receptor subunit genes; six α (alpha1-6), three β (beta1-3), three γ (gamma1-3), three ρ (rho1-3) and δ (delta), ε (epsilon), π (pi) and θ (theta) (Siegart et al., 1999). The most commonly expressed subunits are α1, α2, α3, β2, β3, and γ2.

$GABA_ARs$ can be distributed in the central nervous system (CNS), different types of immune cells, liver cells, pancreatic islet β cells, and airway smooth muscle.

The $GABA_ARs$ can realize its inhibition response to the neurotransmitter GABA by phasic and tonic modalities (*Arslan, 2015*). GABA, an inhibitory neurotransmitter, is released into the synaptic gap and activates postsynaptic receptors, which open for a relatively short period of time, increasing the permeability of the postsynaptic membrane to chloride (Cl^-) ions (*Brickley and Mody, 2012*). These two inhibitory modalities may have both common and distinct effects on the network activity of the nervous system through changes in $GABA_AR$ composition (*Joo et al., 2014; Farrant and Nusser, 2005; Kasugai et al., 2010*). Based on laboratory studies it is predicted that altering extrasynaptic $GABA_ARs$ function may cause epilepsy and various neurological diseases (*Wang and Kriegstein, 2008; Arslan et al., 2014).* While synaptic receptors show low affinity to GABA, it is estimated that extrasynaptic receptors show higher affinity (*Brickley and Mody, 2012*). With the increasing number of experimental data for various neurological diseases, tonic inhibition has emerged as a pathological factor in protein dysfunctions (*Hines et al., 2012*). In this context, the finding that receptors containing α2, α3 and β3 subunits are approximately (~) 100 times more abundant in synapses than in extrasynaptic membranes encouraged us to focus on variants of the gene encoding GABRB3 (Gamma-Aminobutyric Acid Type A Receptor Subunit Beta3) (*Kasugai et al., 2010; Ghit et al., 2021; Egawa and Fukuda, 2013).*

GABRB3 (*Gene ID: 2562*) is a structurally and functionally important member of the gamma-aminobutyric acid-A ($GABA_A$) receptor gene family of heteromeric pentameric ligand-gated ion channels (*Arslan, 2023*). The most common combination of

$GABA_A$ receptors; it is formed by combining 2α, 2β and 1γ subunits. GABRB3 is a protein coding gene. According to data from NCBI/Gene, cytogenetic location of $GABA_A$ receptor subunit β3 gene is 15q12 and genomic coordinates (GRCh38): 15:26,543,552-26,773,763. The GABRB3 gene is 5767 bp long and contains nine exons. The $GABA_A$ receptor β3 subunit isoform 1 precursor contains 473 amino acids as shown in *figure 4.*

$GABA_A$ receptor β3 subunits, which are widely expressed in the developing and adult brain (cortex, hippocampus, and thalamic reticular nucleus), are also expressed in some other human tissues, such as gallbladder, prostate, stomach, adrenal gland, gallbladder, testis, and thyroid. Embryonic and postnatal expression of $GABA_A$ receptor subunit genes in the rat CNS was examined by in situ hybridization study (*Laurie et al., 1992*). With this study, it is known that the $GABA_A$ receptor β3 gene emerges in the early stages of the embryonic and neonatal brain.

```
  1 mwglaggrlf gifsapvlva vvccaqsvnd pgnmsfvket vdkllkgydi rlrpdfggpp
 61 vcvgmnidia sidmvsevnm dytltmyfqq ywrdkrlays giplnltldn rvadqlwvpd
121 tyflndkksf vhgvtvknrm irlhpdgtvl yglritttaa cmmdlrrypl deqnctleie
181 sygyttddie fywrggdkav tgverielpq fsivehrlvs rnvvfatgay prlslsfrlk
241 rnigyfilqt ympsilitil swvsfwinyd asaarvalgi ttvltmttin thlretlpki
301 pyvkaidmyl mgcfvfvfla lleyafvnyi ffgrgpqrqk klaektakak ndrsksesnr
361 vdahgnillt slevhnemne vsggigdtrn saisfdnsgi qyrkqsmpre ghgrflgdrs
421 lphkkthlrr rssqlkikip dltdvnaidr wsrivfpftf slfnlvywly yvn
```

Figure 4. GABRB3 amino acid sequence.

*Protein encoded by the gamma-aminobutyric acid receptor subunit beta-3 isoform 1 precursor, according to NCBI/*Protein (NCBI Reference Sequence: NP_000805.1) *data.*

The subject of research is γ-aminobutyric acid receptor subunit beta-3 (GABRB3), the receptor that acts on γ-aminobutyric acid (GABA), one of the most abundant neurotransmitters in the central nervous system (CNS). GABRB3, a subunit of $GABA_A$ receptors that mediates inhibition, is the receptor to be discussed in this study.

2.2.3. GABRB3 Variants

NCBI/ClinVar, which we use as a data source, utilize standard terms recommended by an authoritative source for the clinical significance of variants. Five terms for Mendelian diseases are used as suggested by The American College of Medical

Genetics and Genomics (ACMG) / the Association for Molecular Pathology (AMP) (*Richards et al., 2015*). According to ACMG/AMP's proposed standards, it is recommended to use standard terminology such as "pathogenic," "likely pathogenic," "of uncertain significance," "likely benign," and "benign" to describe variants in genes linked to Mendelian disorders. In this study, variants with missense molecular consequence for the SNP variant type were analyzed in order to understand the genetic mechanisms underlying epilepsy.

The availability of the human genome sequence has made it possible to understand how SNP variants are distributed in different individuals and populations. These differences occur most commonly among genetic variations (rare variant, insertion and duplication, deletion, inversion). As mentioned before to define a variant as an SNP, it must be present in at least 1 percent (%1) of the population. Thanks to the Human Genome Project, we can use SNPs in our genetic code as biological markers and find genes associated with disease. To explain genetic factors in a common and complex disease like epilepsy, we can pool together thousands of people with epilepsy and compare their SNP patterns with thousands of people without epilepsy. Furthermore, SNPs can occur in a regulatory region near a gene, affecting the function of the gene, resulting in a critical impact in disease. This undoubtedly shows that, although SNPs do not have a direct impact on diseases, some of these genetic differences are very important in human health research. The fact that SNPs help predict an individual's response to certain medications has spurred research to identify SNPs associated with complex diseases such as epilepsy. Therefore, the main motivation of this research is to understand the pathogenic effect of SNPs on epilepsy.

The literature review for the *NM_000814.6(GABRB3):c.905A>G (p.Tyr302Cys)* variant, given the RNA reference sequence (r.) and protein reference sequence (p.), will be an explanatory model in understanding the source of this study. Nucleotide and amino acid sequence information of the Tyr302Cys variation, a pathogenic SNP in GABRB3 associated with Epilepsy, childhood absence, susceptibility (ECA) *(Epi4K Consortium, 2013, Moller et al., 2017)* according to NCBI/ClinVar data, is shown in *table 1*.

Table 1. Variant details of GABRB3 pathogenic SNP associated with epilepsy

(The data was taken from NCBI/ClinVar, last accessed on January 25th, 2023)

Name: NM_000814.6:c.905A>G Accession	**Position**	**Sequence**
NM_000814.6	NM_000814.6:r.1009	AAAATCCCCTATGTCAAAGCC
NP_000805.1	NP_000805.1:p.302	HLRETLPKIPYVKAIDMYLMG

2.2.4. Clinical Highlights of GABRB3

Clinical studies reviewing the literature as well as data in the NCBI/Clinvar database have provided evidence that GABRB3 plays a role in developmental neurological disorders, including epilepsy (*Lü et al., 2004; Kim et al., 2006*).

According to NCBI/ClinVar data (last accessed: September 14th, 2023) , there are 12 pathogenic missense single nucleotide polymorphisms (SNPs) in the γ-aminobutyric acid receptor subunit beta-3 (GABRB3) gene that have been associated with developmental and epileptic encephalopathy-43 (DEE43) and childhood absence epilepsy (ECA5 or CAE) as shown in *table 2*. Mutations that did not meet the claim criteria were not included in the list. In this study, it was logical to focus on missense single nucleotide polymorphisms (SNPs) that mediate inhibition at the γ-aminobutyric acid (GABA) receptor while targeting the biological mechanisms responsible for epilepsy, which may be different in each individual.

Table 2. GABRB3 missense pathogenic SNPs found in epilepsy

(Linked literatures cited in NCBI- last accessed on September 14th, 2023)

AA change	***Protein***	***Origin of inheritance***	***Phenotype***	***Reference***
L310R	*NP_000805.1:p.Leu310Arg*	*de novo*	*DEE43*	*Absalom et al., 2020; Richards et al., 2015*

Continued table 2.

M308R	*NP_000805.1:p.Met308Arg*	*germline*	*ECA1, ECA5*	*Nykamp et al., 2017*
K304R	*NP_000805.1:p.Lys304Arg*	*germline*	*ECA1, ECA5*	*Denommé-Pichon et al., 2021*
Y302C	*NP_000805.1:p.Tyr302Cys*	*germline*	*ECA1, ECA5*	*Billakota et al., 2019; Epi4K Consortium 2013; Absalom et al., 2019*
T287I	*NP_000805.1:p.Thr287Ile*	*germline*	*DEE43, ECA1, ECA5*	*Papandreou et al., 2016; Trump et al., 2016*
S254F	*NP_000805.1:p.Ser254Phe*	*germline*	*ECA1, ECA5*	*Parrini et al., 2017; Nykamp et al., 2017; Liu et al., 2018*
P253T	*NP_000805.1:p.Pro253Thr*	*germline*	*ECA1, ECA5*	*Nykamp et al., 2017*
R232Q	*NP_000805.1:p.Arg232Gln*	*germline*	*ECA1, ECA5*	*Le et al., 2017; Møller et al., 2017; Nykamp et al., 2017*
T157M	*NP_000805.1:p.Thr157Met*	*germline*	*ECA1, ECA5*	*Epi4K Consortium 2016, Absalom et al., 2019; Nykamp et al., 2017; Møller et al., 2017*
D120N	*NP_000805.1:p.Asp120Asn*	*maternal,germline*	*DEE43, ECA1, ECA5*	*Janve et al., 2016; Epi4K Consortium 2016; Møller et al., 2017; Nykamp et al., 2017*
R96S	*NP_000805.1:p.Arg96Ser*	*germline*	*ECA1, ECA5*	*Nykamp et al., 2017*
L52V	*NP_000805.1:p.Leu52Val*	*germline*	*ECA1, ECA5*	*Zhang et al., 2020; Nykamp et al., 2017*

In an in vitro study conducted on GABRB3 for the first time in 1997, Homanics and friends proved that $GABA_AR$ density was reduced and $GABA_AR$ function was impaired in the brain of Beta3-deficient mice (*Homanics et al., 1997*). Cases of epilepsy associated with variants in the GABRB3 gene were first reported by Tanaka and friends in 2008 (*Tanaka et al., 2008*). One of the main motivations of this thesis was the demonstration that GABRB3 mutations can reduce GABA-induced current density in this research. In vitro studies showed that the P11S, S15F and G32R variant reduced current due to

abnormal N-linked glycosylation. In addition, experiments in human and mouse cells have proven that some of the GABRB3 missense SNPs affect promoter activities by changing transcription binding motifs (*Tanaka et al., 2012*). One of the another critical study showed that GABRB3 variants, providing strong evidence that missense variants of the $GABA_ARs$ can lead to a variety of clinical manifestations, were strongly associated with functional outcome of patients' clinical phenotypes (*Absalom et al., 2022*). Therefore, the structure and molecular pharmacology of GABRB3, the target gene of the research, will be examined under the next headings.

2.2.5. Hot-Spot Domains of GABRB3

Until the 3D structure of $GABA_ARs$ were elucidated by X-RAY DIFFRACTION with a resolution of 2.97 Å, analogy information with related proteins was used. The first 3D crystal structure of human $GABA_AR$, which allowed us to better understand the signaling mechanisms of pentameric ligand-gated ion channels, was discovered by Miller and Aricescu in 2014 (*Miller and Aricescu, 2014*). This first structure has a homopentameric feature (*PDB ID: 4COF*). RCSB Protein Data Bank (RCSB.org) is an easily and freely accessible database of protein three-dimensional structures. Since 2014, the number of 3D biostructures in the PDB has reached approximately 200.000. 105.000 of these are Eukaryotic protein structures, and more than half of them are known to be of human origin.

With the increasing availability of newly discovered 3D protein structure data, the discovery of heteromeric structures has become possible. It is theoretically possible for receptor subunits to come together in many different combinations. However, when the structures of receptor in various organisms were searched, it was seen that these combinations had some structural requirements in order to leave the endoplasmic reticulum (ER) and reach the neuronal cell surface. It has been noticed that most of the $GABA_ARs$ localized on the surface of neurons consist of 2α, 2β and 1γ subunits. In this study, the structure combining 2α, 2β and 1γ subunits, which is the most common heteromeric organization in the brain, was preferred for the GABRB3 3D structure according to *PDB ID: 6HUO* (*Masiulis et al., 2019*). After the 3D image of the structure was downloaded from PDB, it was edited to show the domains with the BIOVIA Discovery Studio Visualizer (DSV, 2021) program (*fig. 5*).

$GABA_AR$ subunits all have in common a basic scaffold consisting of a N-terminal extracellular domain of approximately 200 amino acids, four transmembrane domains, a cytoplasmic loop of variable size and amino acid sequence, and a shorter extracellular COOH-terminal sequence compared to the N-terminal. In figure 5C, the extracellular domain (ECD) containing β sheets, the transmembrane domain (TMD) containing α helices, and the intracellular domain (ICD) are shown schematically in $GABA_AR$, which contains two β3 subunits. Cys Loop, β1–β2 (Loop 2) and TM2-TM3 Loop, which are key regions in receptor activation, are shown (*fig. 5C*). Subunit organization and major (+) and complementary (-) subunit interfaces in cross-section of the extracellular domain are shown in *figure 5A*. The TM2 ion channel is shown in the cross section taken from the intracellular domain region (*fig. 5B*).

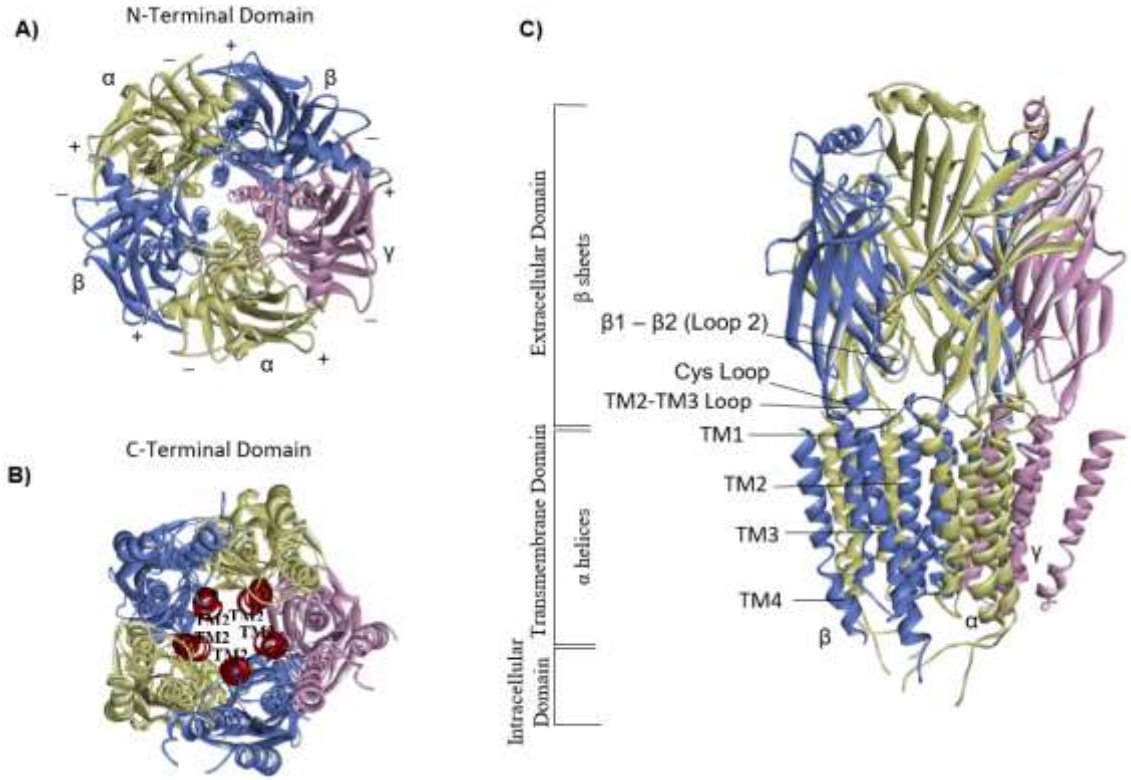

Figure 5. ***CryoEM structure of human heteromeric alpha1beta3gamma2 $GABA_AR$.***

The model of PDB ID: 6HUO (Masiulis et al., 2019) reference, resolution of 3.26 Å (electron microscopy) has been rearrenged in BIOVIA Discovery Studio Visualizer (DSV). Blue color represents β, yellow color represents α and purple color represents γ subunit. A, the layout of the subunits is shown in the cross-sectional image obtained from the N- Terminal Domain. C, structurally and functionally important regions of the ECD, TMD, ICD domains are shown. B, the layout of the subunits is shown in the cross-sectional image obtained from the C- Terminal Pore Domain. It shows the TM2 domain of each subunit in $GABA_AR$ that aligns the ion pores (red color).

Undoubtedly, in order to discover how β3 subunit variants that can cause epilepsy change the activation properties of the receptor, it is necessary to first understand the harmony of the $GABA_A$ receptor structure-function relationship. In this context, there is empirical evidence in the literature that opens the door. Our understanding of the assembly, trafficking and function of the N-terminal extracellular domain of $GABA_AR$ subunits has improved with experimental datas (*Wong et al., 2015; Goetz et al., 2007; Jacob et al., 2008*). The N terminus is a critical region for GABAergic signalling. The N-terminal extracellular domain of the GABRB3 protein is the area where the receptor initiates activation by binding to GABA. Subunit interfaces located at extracellular domains contain binding sites for barbiturates, benzodiazepines, and other allosteric modulators, in addition to GABA.

The coupling region between the extracellular and transmembrane domains also plays a critical role in stabilizing the receptor. A study by *Velisetty et al*, proposed a working model about conformational changes at the intra- and intersubunit interfaces. The energy resulting from GABA binding in the extracellular space moves towards the channel pore, and at this stage, the β1-β2 Loop, β6-β7 Loop and TM2-TM3 loop change the conformation of the motifs in the extracellular space. Interface loops consist of β1-β2 (Loop2), β6-β7 (Cys Loop) and β8-β9 segments in ECD, pre-TM1 and TM2-TM3, and the C-terminal end of TM4 in TMD (*Velisetty et al., 2014*). In the binding mechanism of an important neurotransmitter such as GABA, the signal is transmitted to the channel gate (TM2) via the ECD-TMD interface. Given the importance of this interface for signal transduction, it is possible that β3 subunit variants at this interface cause attenuation of signaling events and thus play a functional role in epilepsy.

TM2 segments define the pore space. The TM2 subunit is an important structural component in an ion channel pore that selects anion (mostly Cl-) permeability (*fig. 5B*).

The intracellular large loop between TM3 and TM4 (ICD) is the domain that interacts with intracellular proteins and ensures receptor trafficking and synaptic clustering. ICD is one of the regions where specific proteins bind to $GABA_AR$ and undergo post-translational modifications such as phosphorylation (Lorenz-*Guertin et al., 2018*).

2.2.6. Molecular Pharmacology of GABRB3

GABA binds at the extracellular interface between the β3 subunit on the principal (+) and the α1 on the complementary (-) sides. To activate the $GABA_AR$, two GABA molecules bind to the β3-α1 interfaces in the extracellular space (*fig. 6*). This activation process begins in the ligand binding region and continues with sequential conformational movements starting in the TM2-TM3 regions. As a result of these sequential movements, the TM2 regions bend and the pore opens.

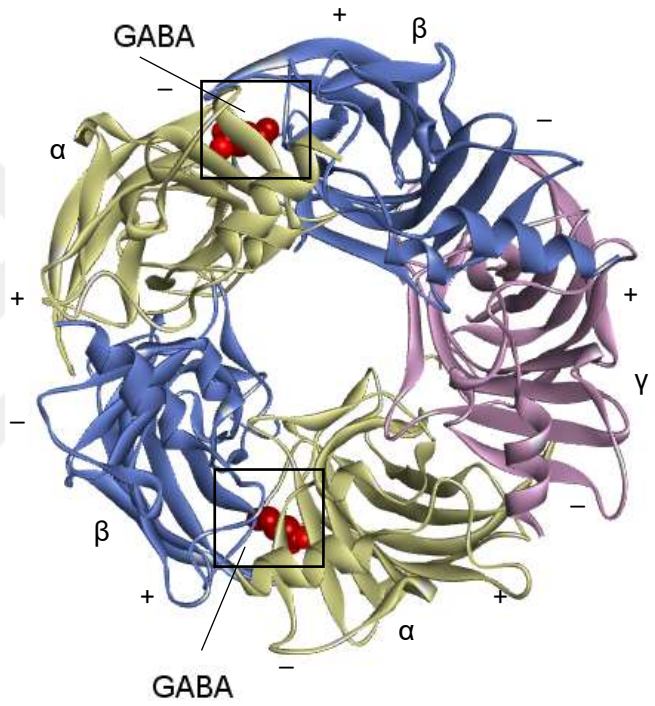

Figure 6. GABA binding sites at β +/α− interfaces

The model of PDB ID: 6HUO (Masiulis et al., 2019) (3.26 Å) was recolored in BIOVIA DSV. Top views of the 3D structure of the $GABA_A$ receptor-GABA complex, colored by subunit; α, yellow; β, blue; γ, purple and GABA is shown as red balls. TMD and ICD areas were removed and then imaged from above by N-Terminal to show two GABA-binding sites in $GABA_A$ receptor at β +/α− interfaces.

GABRB3 conformational dynamics is an important factor determining allosteric mechanisms and biological function. The GABA binding site, the active site, is where orthosteric agonists and antagonists bind. Apart from GABA, some of the other ligands that bind to and regulate various parts of $GABA_AR$ are; Orthosteric agonists such as gabox-adol, isoguvacin, muscimol and progabid activate the receptor, causing an increase

in Cl- conductance. Orthosteric antagonists such as bicu-culline and gabazine inhibit the effect of GABA and act by reducing Cl- conductance. Allosteric modulators bind to any part of the receptor. For example, barbiturates, benzodiazepines, alcohol, anesthetics and some neurosteroids show their effects by causing positive conformational changes in the receptor (*Zhu et al., 2018*). Examples of allosteric modulators with negative effects are pregnenolone sulfate and zinc. Non-competitive chloride channel blockers, such as picrotoxin, are ligands that block Cl- conductance. Preferred ligands for receptor activation are commonly; It is used as an anxiolytic, anticonvulsant, sedative and muscle relaxant (*Ghit et al., 2021*).

In Cys-loop receptors, neurotransmitter binding sites are located at the extracellular interface. Since the affinity of GABA molecule to GABRB3 mutations will be examined in this study, visualization was made only for GABA molecule. GABA typically binds between two adjacent subunits (*fig. 6*). The most common among $GABA_ARs$, the αβγ subtype (2α:2β:1γ), is characterized by two GABA binding sites at β +/α− interfaces (*Miller and Aricescu, 2014; Ghit et al., 2021*). While binding GABA to a location is sufficient for channel opening; when both spaces are occupied, the probability of the channel opening increases significantly.

2.3. Computational Approaches

Computational approaches began to be used in scientific studies starting from the mid-1990s, largely by elucidating the human genome map with the Human Genome Project (HGP) (*Collins and Fink, 1995*). Computational approaches have become among the popular research techniques in the discovery of new drug candidates with the contribution of interdisciplinary research. Nowadays, various computational approaches are widely used in the drug discovery process, which is quite complex, time-consuming and costly, due to its effectiveness in designing a suitable algorithm framework and predicting complex problems.

In general, the goal of in silico prediction methods in drug discovery is to produce more effective drug substance compounds by managing intense data flow with various algorithms. Computational tools commonly used to predict pathogenicity each have their own strengths and weaknesses. The purposes and methods used of these programs vary.

2.3.1. Prediction Methods

As DNA sequencing costs have decreased in recent years, the number of sequencing data sets obtained from individuals representing a population has increased inversely. Many prediction tools with high accuracy scores continue to be designed to process these large data sets correctly and help disease discovery with the right target-oriented algorithms.

Prediction tools are frequently used methods to detect different types of traits such as single nucleotide polymorphisms (SNPs), small insertions and deletions (indels), and duplications.

2.3.2. Molecular Docking

Computer-aided drug design (CADD), which has become widely used in personalized drug development, includes structure-based drug design (SBDD) for binding affinity predictions (*Kroemer, 2007*). It obtains the structural data necessary for the prediction of the interaction strength between target proteins and small molecules (ligands) either from experimental data (electron microscopy, x-ray diffraction) or from homology modeling if the structure is unknown.

Molecular docking involves the prediction of ligand conformation and orientation within a targeted binding site when a ligand and a target bind together to form a stable complex (*Lengauer and Rarey, 1996; Kitchen et al., 2004*). By using molecular docking in drug development, accurate structural modeling and accurate prediction of activity can be achieved.

Binding affinity is the strength of the binding interaction between a biomolecule such as a protein and its ligand such as a drug. The stronger the binding interaction, the more the ligand will affect the physiological function of target proteins. Therefore, in this study, in order to contribute to the development of individual treatment methods, the weaker binding affinities that may occur between the target protein, that is, GABRB3 variants and the GABA molecule in this study, were calculate.

3. EQUIPMENT and METHOD

3.1. Retrieval of Missense SNPs

The National Center for Biotechnology Information (NCBI) - ClinVar database *(https://www.ncbi.nlm.nih.gov/clinvar/)* was used to retrieve missense SNPs of the GABRB3 gene (*NCBI Gene ID: 2562*) in December 2th, 2022. ClinVar is a freely accessible, public archive of reports on relationships between human variations and phenotypes, with advanced search options and supporting evidence (*Landrum et al. 2014*). The FASTA format sequence of the protein, UniProt entry name (GBRB3_HUMAN) and UniProtKB number (P28472) of gamma-aminobutyric acid receptor subunit beta-3 was retrieved from the UniProt *(https://www.uniprot.org/)* database in December, 2023. UniProt Knowledge Base (UniProtKB) is a freely accessible resource that serves to collect functional information about proteins with comprehensive descriptions.

3.2. Analysis of Variant Effect

3.2.1. Functional Impacts

Six different bioinformatics tools (*SIFT, PolyPhen-2, PANTHER-PSEP, SNAP2, FATHMM-XF, PhD-SNP*) were used for functional analysis and disease-related of missense SNPs. Methods that reference protein sequence homology assume that frequent substitutions between branches are benign and that homologous proteins share the same functions. However, in this study, amino acid positions that are important for the function to be called pathogenic must be preserved in the protein family sequence.

The SIFT (Sorting Intolerant From Tolerant), PhD-SNP (Predictor of human Deleterious Single Nucleotide Polymorphisms), and PANTHER-PSEP (Protein Analysis Through Evolutionary Relationships / position-specific evolutionary preservation) prediction methods used in this in silico study for variant effect are primarily based on protein sequence homology.

The SIFT *(https://sift.bii.a-star.edu.sg/)* predicts, using sequence homology, whether an amino acid substitution will alter protein function and phenotype (*Ng and Henikoff, 2001*). The SIFT algorithm focuses on the evolutionary conservation of amino acids within protein families. The PhD-SNP *(https://snps.biofold.org/phd-snp/phd-snp.html)* is based a SVM (Support Vector Machines)-based classifier (*Capriotti et al. 2006*). PhD-SNP combines multiple sequence alignment data and the mutation environment within the surrounding protein sequence to produce an output in the same SVM classifier. The PANTHER-PSEP *(https://www.pantherdb.org/)* is another method that based on sequence homology to predict whether the variant causes a functional effect on the protein (*Tang and Thomas, 2016*). The homologous sequences of the protein of interest are collected, aligned, and a measure of conservation is calculated based on the weighted frequencies of the different amino acids observed at the target location in the alignment (in millions of years).

To improve the accuracy of the prediction, prediction tools PolyPhen-2 (Polymorphism Phenotyping v2), FATHMM-XF (FATHMM with extended features) and SNAP2, which use multiple features as well as sequence homology, were used. These tools exploit multiple properties such as molecular functions and physicochemicals. To obtain reliable results, it is inevitable to introduce machine learning methods at this stage. The PolyPhen 2 *(http://genetics.bwh.harvard.edu/pph2/)* extracts the sequence and structure-based features of that region for amino acid replacement and classifies these features in a probabilistic manner using a Bayesian approach (*Adzhubei et al., 2010*). The PolyPhen-2 is based on a number of features comprising the sequence of protein, phylogenetic and structural information. The user can choose between two types of data sets: HumDiv (trained using rare alleles causing Mendelian disease) that is used in this study and HumVar (trained using more common alleles and nonsynonymous SNPs) (*Adzhubei et al. 2013*). The FATHMM-XF *(http://fathmm.biocompute.org.uk/fathmm-xf/)* predicts whether single nucleotide polymorphisms (SNPs) in the human genome will be functional in inherited diseases (*Rogers et al., 2018*). The SNAP2 *(https://www.rostlab.org/services/snap/)* is a trained classifier based on a neural network-based machine learning device that predicts the functional effects of mutations. Besides the evolutionary information from multiple sequence alignment, structural features such as predicted secondary structure and solvent accessibility are also taken into account (*Hecht et al., 2015*).

3.2.2. Protein Stability Analysis

There is a possibility that missense SNPs may change the stability of the protein and therefore it is important to evaluate impact of variants on protein function. In this study, two web-based tools were used to evaluate whether there was a possibility of stabilizing or destabilizing the protein structure, and these were I-Mutant 3.0 and MUpro. The I-Mutant 3.0 tool *(http://gpcr2.biocomp.unibo.it/cgi/predictors/I-Mutant3.0/I-Mutant3.0.cgi/)* is used to determine the effect of nsSNPs on protein stability (*Capriotti et al. 2005*). The MUpro web server *(http://www.igb.uci.edu/servers/servers.html.)* uses support vector machines that predict protein stability changes for single amino acid mutations, using sequence and structural information of the protein (*Cheng et al., 2006*).

3.2.3. Phylogenetic Conservation

The evolutionary conservation of residues in GABRB3 is predicted via the ConSurf *(https://consurf.tau.ac.il/)* server (*Ashkenazy et al., 2016, Armon et al., 2001*). The ConSurf server is a homology-based prediction method which provide a "conservation" score for each protein residue rather than for each amino acid substitution

3.2.4. Molecular Mechanisms

MutPred2 *(http://mutpred.mutdb.org/)*, a web tool that uses many features such as structure, function description, and evolutionary features, was used to predict the pathogenicity that may be caused by missense SNPs of GABRB3 (*Pejaver et al. 2020*). MutPred2 uses a machine learning-based method for the prediction of specific molecular changes of SNPs that affect the phenotype.

3.3. Structural Properties and Modeling

The HOPE *(https://www.cmbi.umcn.nl/hope/)* collects and combines available information from various web services and databases to present the structural effects of a point mutation in a protein sequence (*Venselaar et al., 2010*). HOPE presents the results by creating a report full of figures and animations. The inclusion of HOPE in this study also allows validating structural performance in SWISS-MODEL and UCSF Chimera 1.17.3.

Homology model of the wild type (wt) of GABRB3 and the mutant type (mt) of pathogenic missense SNPs superimposed proteins were performed by the Swiss-Model database *(https://swissmodel.expasy.org/)* and the UCSF Chimera 1.17.3 program *(https://www.cgl.ucsf.edu/chimera/download.html/).* The reason for using the homology model, even though the protein structure was known, was to validate the superimposed molecular image of WT and MT. SWISS-MODEL was used to create homology modeling of pathogenic missense SNPs found in this study (*Waterhouse et al., 2018*). The UCSF Chimera 1.17.3 program was used to visualize three-dimensional models of the molecular structures of WT and MT protein (*Pettersen et al., 2004*). It can be downloaded free of charge for non-commercial use.

3.4. Molecular Docking

In the study, the MGLTools software package, supporting AutoDockTools-1.5.7, was used for visualization and analysis of molecular structures. Moleculer Graphics Laboratory (MGL), founden by Arthur Olson in 1981. AutoDock Vina *(https://ccsb.scripps.edu/mgltools/downloads/)*, a program for molecular docking and virtual screening, was used for binding affinity values. AutoDock Vina (*Trott and Olson, 2010; Eberhardt et al., 2021*) was used to demonstrate binding affinity interactions between variants predicted as GABRB3 pathogenic missense SNPs and gamma-aminobutyric acid examined as ligand. Visualization of hydrogen bond interactions and generating the graphical results were performed with BIOVIA Discovery Studio Visualizer (Discovery Studio Visualizer 2021, v21.1.0.20298). *(https://discover.3ds.com/discovery-studio-visualizer-download).*

4. FINDINGS

4.1. Workflow

In this study, various computational methods were used to identify the pathogenic missense SNPs of gamma-aminobutyric acid receptor subunit beta-3 (GABRB3) / Isoform 1 precursor (Homo sapiens) to better understand the pathophysiology of epilepsy (*fig. 7*). In the continuation of the study, changes in ligand-protein binding affinities are shown along with variants of all reported binding sites compatible with the literature using a molecular docking approach.

Multiple computational methods were used to estimate pathogenicity in this study. The purpose of using two or more algorithms for the prediction of the most deleterious missense SNPs is to increase the confidence level of the prediction analysis. Some tools used in the study are based on protein sequence homology (*SIFT, PhD-SNP, PANTHER-PSEP, FATHMM-XF*) and prediction is strengthened with function annotations and structural information when necessary (*Ng and Henikoff, 2001; Capriotti et al., 2006; Tang and Thomas, 2016; Rogers et al., 2018*). Some prediction methods (*ConSurf*) provide a "conservation" score for each protein residue rather than each amino acid substitution (*Ashkenazy et al., 2016; Armon et al., 2001*), some prediction methods (*MutPred2, PolyPhen-2, SNAP2*) are based on molecular functions (*Adzhubei et al., 2010; Hetch et al., 2015; Pejaver et al., 2020*) and physicochemical properties (*Stone and Sidow, 2005*) and some (*MUPro, I-Mutant 3.0*) based on the folding stability of the protein (*Cheng et al., 2006; Capriotti et al., 2005*).

While scanning the literature, the purpose and scope of the thesis topic were determined and accordingly, only English sources were used in PubMed. PubMed is a widely used search engine for biomedical literature, developed and maintained by the US National Library of Medicine/National Center for Biotechnology Information.

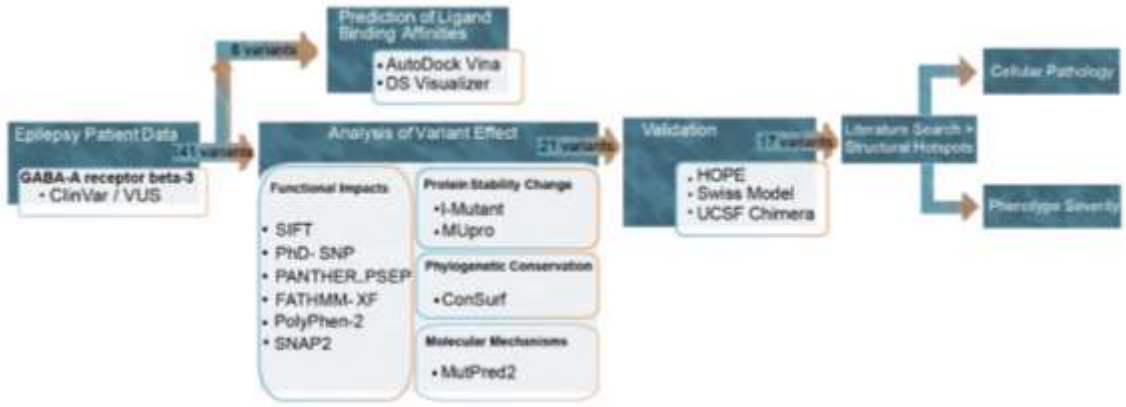

Figure 7. Workflow

Workflow diagram of in silico analysis steps taken to predict the effect of gamma-aminobutyric acid receptor subunit beta-3 (GABRB3) / Isoform 1 precursor (Homo sapiens) pathogenic VUSs on protein structure and function. Five VUSs (Y182C, F225V, T227A, T227P, Y230C) are included in the molecular docking study, because they are found in the GABA binding site expressed in the gaba-aminobutyric acid receptor subunit beta-3 (GABRB3). *Four VUSs, which are not associated with epilepsy, are not included in the study (NCBI/ClinVar). This schema was created by Adobe Illustrator Artwork 22.0.*

4.2. Retrieving GABRB3 Gene Variants

The gamma-aminobutyric acid type A receptor subunit beta3 (GABRB3) gene (*NCBI Gene ID: 2562*) is a protein-coding gene that is located at 15q12.

When the number of variation types was screened, 852 variation types were obtained from the NCBI/ClinVar database in the GABRB3 gene (accessed in December, 2022). Among these variants, there were 465 single nucleotide, 190 deletion, 161 duplication, 32 insertion and 4 indel variants (*fig. 8A*). 238 missense SNPs were selected from the total of variants for further analysis because they may change the function of the receptor by affecting the protein structure or increase susceptibility to different diseases (*fig. 8B*). The distribution of total missense SNPs reported in human GABRB3 was as follows; 152 were uncertain significance, 42 were probably pathogenic, 17 were pathogenic, 16 were probably benign, 14 had conflicting interpretations, and 6 were benign (*fig. 8C*). The uncertain significance of SNPs in gamma-aminobutyric acid receptor subunit beta-3 may cause complex changes in receptor properties, resulting in loss of function. Therefore, 152 uncertain significances were chosen to understand how they affect the function of GABRB3. Only missense SNPs belonging to *NCBI Reference Sequence: NM_000814.6* were included in the study (number of uncertain significance SNPs=141).

Bioinformatics tools to be used for pathogen effect analysis on protein in this in silico study will require amino acid sequencing. The FASTA (canonical) format of protein sequence of the gamma-aminobutyric acid subunit beta-3 isoform 1 precursor human gene (*NCBI Reference Sequence: NP_000805.1*) was retrieved from the UniProt database (*P28472.GBRB3_HUMAN*). The FASTA sequence of GABRB3, which has 473 amino acids, was obtained from the *https://rest.uniprot.org/uniprotkb/P28472.fasta* website (*fig. 9*).

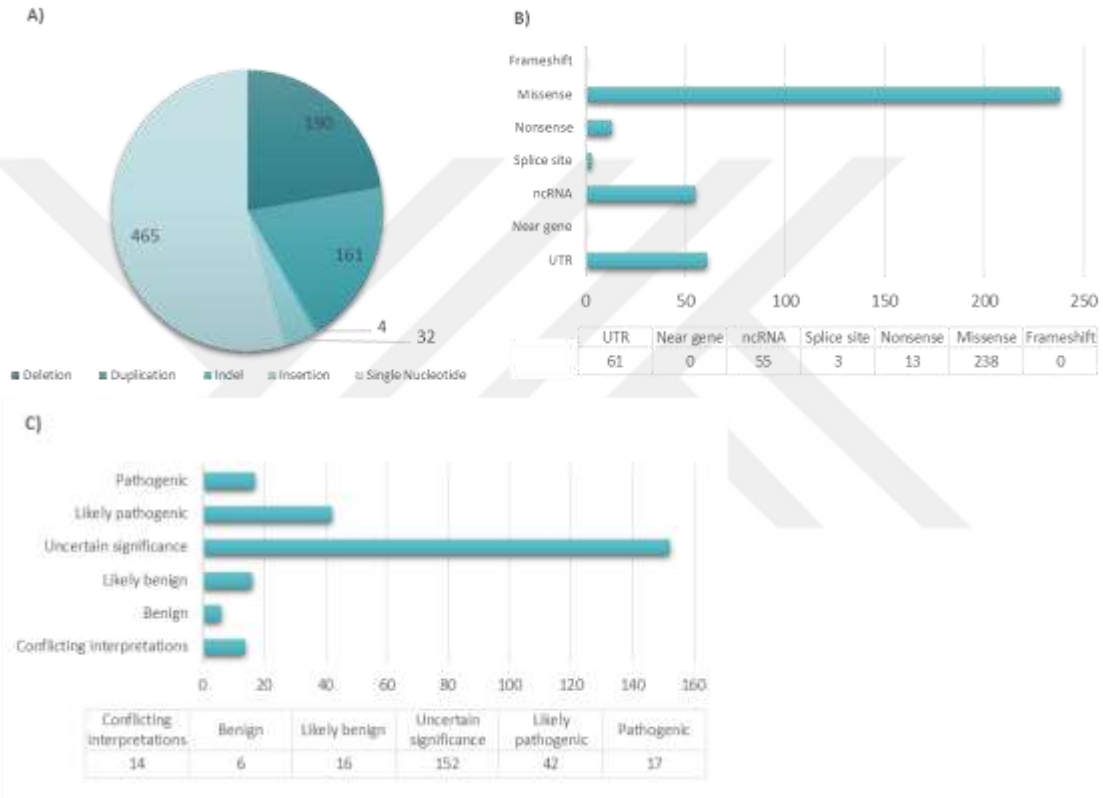

Figure 8. Distribution of GABRB3 SNPs

The graphs display the distribution of GABRB3 SNPs based on the ClinVar/NCBI database. (A) The pie chart displaying the total number (n= 852) of variation types of gamma-aminobutyric acid subunit beta-3 (GABRB3) human gene [Single nucleotide (n=465), Deletion (n=190), Duplication (n=161), Insertion (n=32) and Indel (n=4)] . (B) The graphic displays number of UTR (n=61), Near gene (n=0), ncRNA (n=55), Splice site (n=3), Nonsense (n=13), Missense (n=238) and Frameshift (n=0) SNPs in human GABRB3 gene. (C) Graphical representation of the number of missense variations (n=238) classified according to their clinical significance as reported on ClinVar ; Conflicting interpretations (n=14), Benign (n=6), Likely benign (n=16), Uncertain significance Only missense SNPs belonging to NCBI Reference Sequence: NM_000814.6 were included in the study (n=141), Likely pathogenic (n=42) and Pathogenic (n=17).

```
>sp|P28472|GBRB3_HUMAN Gamma-aminobutyric acid receptor subunit beta-3
MWGLAGGRLFGIFSAPVLVAVVCCAQSVNDPGNMSFVKETVDKLLKGYDIRLRPDFGGPP
VCVGMNIDIASIDMVSEVNMDYTLTMYFQQYWRDKRLAYSGIPLNLTLDNRVADQLWVPD
TYFLNDKKSFVHGVTVKNRMIRLHPDGTVLYGLRITTTAACMMDLRRYPLDEQNCTLEIE
SYGYTTDDIEFYWRGGDKAVTGVERIELPQFSIVEHRLVSRNVVFATGAYPRLSLSFRLK
RNIGYFILQTYMPSILITILSWVSFWINYDASAARVALGITTVLTMTTINTHLRETLPKI
PYVKAIDMYLMGCFVFVFLALLEYAFVNYIFFGRGPQRQKKLAEKTAKAKNDRSKSESNR
VDAHGNILLTSLEVHNEMNEVSGGIGDTRNSAISFDNSGIQYRKQSMPREGHGRFLGDRS
LPHKKTHLRRRSSQLKIKIPDLTDVNAIDRWSRIVFPFTFSLFNLVYWLYYVN
```

Figure 9. The FASTA format of GABRB3

4.3. Identification of the Pathogenic Missense SNPs

4.3.1. Analysing Functional Impacts of Missense SNPs

The results of the missense SNPs whose functional effects we analyzed in six programs (*SIFT, PANTHER-PSEP, FATHMM-XF, PolyPhen-2, SNAP2 and PhD-SNP*) were compared. According to these thresholds given by six prediction tools, 43 out of 141 missense SNPs were analyzed as the pathogenic. Variants with the highest score in all six tools were selected for the further study (*table 3*).

Table 3. Pathogenity outputs.

Results of gamma-aminobutyric acid receptor subunit beta-3 (GABRB3) missense SNPs analysis using SIFT, PolyPhen-2, PANTHER-PSEP, FATHMM-XF, PhD-SNP and SNAP2.

AA Change	SIFT	PolyPhen-2	PANTHER-PSEP	FATHMM-XF	PhD-SNP	SNAP2
Y471C	intolerant	PROBABLY DAMAGING	PROBABLY DAMAGING	pathogenic	Disease	Effect
Y467S	intolerant	PROBABLY DAMAGING	PROBABLY DAMAGING	pathogenic	Disease	Effect
Y467H	intolerant	PROBABLY DAMAGING	PROBABLY DAMAGING	pathogenic	Disease	Effect
Y329H	intolerant	PROBABLY DAMAGING	PROBABLY DAMAGING	pathogenic	Disease	Effect
A320T	intolerant	PROBABLY DAMAGING	PROBABLY DAMAGING	pathogenic	Disease	Effect
V317A	intolerant	PROBABLY DAMAGING	PROBABLY DAMAGING	pathogenic	Disease	Effect
K304E	intolerant	PROBABLY DAMAGING	PROBABLY DAMAGING	pathogenic	Disease	Effect
P298S	intolerant	PROBABLY DAMAGING	PROBABLY DAMAGING	pathogenic	Disease	Effect

Continued Table 3

R294Q	intolerant	PROBABLY DAMAGING	PROBABLY DAMAGING	pathogenic	Disease	Effect
L293P	intolerant	PROBABLY DAMAGING	PROBABLY DAMAGING	pathogenic	Disease	Effect
V283M	intolerant	PROBABLY DAMAGING	PROBABLY DAMAGING	pathogenic	Disease	Effect
T282A	intolerant	PROBABLY DAMAGING	PROBABLY DAMAGING	pathogenic	Disease	Effect
T281A	intolerant	PROBABLY DAMAGING	PROBABLY DAMAGING	nf*	Disease	Effect
G279R	intolerant	PROBABLY DAMAGING	PROBABLY DAMAGING	pathogenic	Disease	Effect
N268K	intolerant	PROBABLY DAMAGING	PROBABLY DAMAGING	pathogenic	Disease	Effect
S264F	intolerant	PROBABLY DAMAGING	PROBABLY DAMAGING	pathogenic	Disease	Effect
S234L	intolerant	PROBABLY DAMAGING	PROBABLY DAMAGING	pathogenic	Disease	Effect
Y230C	intolerant	PROBABLY DAMAGING	PROBABLY DAMAGING	pathogenic	Disease	Effect
T227P	intolerant	PROBABLY DAMAGING	PROBABLY DAMAGING	pathogenic	Disease	Effect
D188V	intolerant	PROBABLY DAMAGING	PROBABLY DAMAGING	pathogenic	Disease	Effect
Y182H	intolerant	PROBABLY DAMAGING	PROBABLY DAMAGING	pathogenic	Disease	Effect
C175W	intolerant	PROBABLY DAMAGING	PROBABLY DAMAGING	pathogenic	Disease	Effect
P169L	intolerant	PROBABLY DAMAGING	PROBABLY DAMAGING	pathogenic	Disease	Effect
A160E	intolerant	PROBABLY DAMAGING	PROBABLY DAMAGING	pathogenic	Disease	Effect
A160V	intolerant	PROBABLY DAMAGING	PROBABLY DAMAGING	pathogenic	Disease	Effect
L153P	intolerant	PROBABLY DAMAGING	PROBABLY DAMAGING	pathogenic	Disease	Effect
Y151C	intolerant	PROBABLY DAMAGING	PROBABLY DAMAGING	pathogenic	Disease	Effect
V149M	intolerant	PROBABLY DAMAGING	PROBABLY DAMAGING	pathogenic	Disease	Effect
D146A	intolerant	PROBABLY DAMAGING	PROBABLY DAMAGING	pathogenic	Disease	Effect
L143R	intolerant	PROBABLY DAMAGING	PROBABLY DAMAGING	pathogenic	Disease	Effect
R142C	intolerant	PROBABLY DAMAGING	PROBABLY DAMAGING	pathogenic	Disease	Effect
N138T	intolerant	PROBABLY DAMAGING	PROBABLY DAMAGING	pathogenic	Disease	Effect
H132Y	intolerant	PROBABLY DAMAGING	PROBABLY DAMAGING	pathogenic	Disease	Effect
Y99C	intolerant	PROBABLY DAMAGING	PROBABLY DAMAGING	pathogenic	Disease	Effect
D94E	intolerant	PROBABLY DAMAGING	PROBABLY DAMAGING	pathogenic	Disease	Effect
Y82S	intolerant	PROBABLY DAMAGING	PROBABLY DAMAGING	pathogenic	Disease	Effect
Y82C	intolerant	PROBABLY DAMAGING	PROBABLY DAMAGING	pathogenic	Disease	Effect
M80R	intolerant	PROBABLY DAMAGING	PROBABLY DAMAGING	pathogenic	Disease	Effect
D73H	intolerant	PROBABLY DAMAGING	PROBABLY DAMAGING	pathogenic	Disease	Effect
G57R	intolerant	PROBABLY DAMAGING	PROBABLY DAMAGING	pathogenic	Disease	Effect
R51G	intolerant	PROBABLY DAMAGING	PROBABLY DAMAGING	pathogenic	Disease	Effect
D49E	intolerant	PROBABLY DAMAGING	PROBABLY DAMAGING	pathogenic	Disease	Effect
Y48C	intolerant	PROBABLY DAMAGING	PROBABLY DAMAGING	pathogenic	Disease	Effect

*** nf: not found**

The SIFT prediction score ranges from 0 to 1 and is the scaled probability of tolerating an amino acid. The amino acid substitution is predicted damaging is the score is <= 0.05, and tolerated if the score is > 0.05. If the score in the SIFT program is below 0.05, the substituted amino acid is predicted to be related with pathogenic (Scores greater than 0.01 were not included in the study). According to the results (accessed on February

20th, 2023), 73 were predicted as deleterious, 64 were as tolerated, and 4 had low confidence. Phd-SNP algorithm produces two types of predictions, Disease or Neutral. In the study, all amino acid variations that resulted in disease were classified as pathogenic, regardless of the reliability index (RI) score that accompanies the output. In PhD-SNP out of 141 uncertain significance SNPs, 80 were found as disease and 61 were found as neutral (accessed on March 3th, 2023). The PANTHER-PSEP result is classified as possibly damaging, probably damaging, and likely benign. Results with a Pdel score of PANTHER-PSEP of 0.74 ≤ probably damaging ≤ 1 were taken into account in the study. This corresponds to a preservation time (P.Time) of over 750 years as seen in the *table 3* (accessed on March 12th, 2023).

The study included different prediction algorithms to support the results. PolyPhen-2 uses phylogenetic and structural information of the receptor (GABRB3) to predict the possible impact of found missense SNPs on GABRB3 structure and function. HumDiv results from one of the two datasets in PolyPhen-2, were analyzed in this study. Outputs are classified as Probably Damaging, Possibly Damaging, or Benign. PolyPhen-2 prediction results consist of a score starting from zero (neutrality) and increasing towards positive numbers (damaging effect). Out of 141 uncertain significance SNPs, 69 were determined as probably damaging, 18 as possible damaging and 54 as benign (accessed on March 15th, 2023). Predictions are scored (p-value) in the range of 0-1 in FATHMM-XF. Predictions are scored (p-value) in the range of 0-1. If the p-value is above 0.5 (>0.5), it is predicted as pathogenic, and values below 0.5 (<= 0.5) are predicted as neutral or benign. According to the results, 114 uncertain significance SNPs were predicted as pathogenic, 6 were as nf (not found) and 21 were as benign (accessed on March 19th, 2023). SNAP2, another tool that predicts the effect of single amino acid substitutions on protein function, was included in the analysis. It presents the output as neutral or effect by giving a score between -100 and +100 with expected accuracy. SNAP2 results that were both effective and had an expected accuracy rate of over 50 percent were selected. According to the uncertainly significant SNP results of GABRB3, 72 were found to be effective and 69 were neutral (accessed on March 25, 2023).

4.3.2. Impact of Missense SNPs on Protein Stability

To make protein stabilization predictions for missense SNPs, the results predicted as pathogenic in step 1 (n=43) were sent to the I-Mutant 3.0 and MUpro softwares.

I-Mutant 3.0 predicts the effect of missense SNPs on the free energy change Delta Delta G (ΔΔG) value. The resulting outputs are reported using SVM2 (support vector machine) binary classification (ΔΔG <0: Decrease Stability and ΔΔG >0: Increase Stability). These 43 SNPs predicted as pathogen were further analyzed by the I-Mutant 3.0 server; this determined that all 43 of the SNPs decreased protein stability (accessed on April 4th, 2023). MUpro and I-Mutant 3.0 results are shown in *Data Sheet 1*.

MUpro predict protein stability changes on Gibbs free energy (Delta Delta G: ΔΔG). MUpro outputs binary classification as ΔΔG < 0 (decreases the structural stability of the protein) and ΔΔG > 0 (increases the structural stability of the protein). MUpro output also gave the same results with I-Mutant 3.0 server for 43 SNPs (accessed on April 4th, 2023).

4.3.3. Identification of Functional and Structural Regions

ConSurf server determines conservation scores by coloring the value between 1 (the least conserved) and 9 (the most conserved). An amino acid is a functional residue if it is preserved and exposed, meaning it is highly conserved. If preserved and buried, it is a structural residue and again means highly conserved. The predicted conservation score revealed that 25 amino acids of the GABRB3 are located in the highly conserved region as shown in *table 4*.

Table 4. Conservation analysis

Identification of Higly Conserved Functional and Structural Regions on ConSurf Server is shown (Date: March 12th,2023). ***** *Amino acid names in bold are the names filtered on the ConSurf server (N=25).* ****X2 : 2 amino acid changes in the same substitution.*

A.A Change	Conservation score	Location	Prediction	A.A Change	Conservation score	Location	Prediction
Y471	9 (preserved)	exposed	**functional**	**C175**	9 (preserved)	buried	**structural**
Y467 x 2	9 (preserved)	buried	**structural**	**P169**	9 (preserved)	exposed	**functional**
Y329	7 (preserved)	buried	-	A160 x 2	6 (average)	exposed	-
A320	8 (preserved)	buried	**structural**	L153	7 (preserved)	buried	-
V317	8 (preserved)	buried	**structural**	**Y151**	8 (preserved)	buried	**structural**
K304	9 (preserved)	exposed	**functional**	V149	7 (preserved)	buried	-
P298	9 (preserved)	exposed	**functional**	D146	7 (preserved)	exposed	-
R294	8 (preserved)	exposed	**functional**	L143	7 (preserved)	buried	-
L293	6 (average)	buried	-	**R142**	8 (preserved)	exposed	**functional**
V283	8 (preserved)	buried	**structural**	**N138**	9 (preserved)	exposed	**functional**
T282	9 (preserved)	buried	**structural**	**H132**	9 (preserved)	exposed	**functional**

(Continued table 4)

T281	9 (preserved)	buried	**structural**	Y99	5 (average)	buried	-
G279	8 (preserved)	buried	**structural**	**D94**	9 (preserved)	exposed	**functional**
N268	7 (preserved)	exposed	-	Y82 x 2	7 (preserved)	buried	-
S264	9 (preserved)	buried	**structural**	**M80**	9 (preserved)	buried	**structural**
S234	5(average)	exposed	-	**D73**	8 (preserved)	exposed	**functional**
Y230	7 (preserved)	buried	-	G57	5 (average)	exposed	-
T227	7 (preserved)	exposed	-	R51	7(preserved)	exposed	-
D188	7 (preserved)	exposed	-	**D49**	8 (preserved)	exposed	**functional**
Y182	8 (preserved)	exposed	**functional**	**Y48**	9 (preserved)	exposed	**functional**

4.3.4. Pathogenicity of GABRB3 by Prediction of Molecular Mechanisms

The pathogenicity of predicted missense SNPs of GABRB3 and their molecular mechanisms were determined by MutPred2. The average of the scores from all neural networks in MutPred2 gives the overall pathogenicity score (g), which is the score output of MutPred2. A value of g >=0.5 (a score threshold of 0.50) expresses the probability that the amino acid substitution is pathogenic.

In MutPred2, 21 missense SNPs (N=21) with the score greater than 0.75 ($g > 0.75$) and top molecular feature score p value less than 0.01 ($p < 0.01$) were filtered as very confident hypotheses (*table 5*).

Table 5. Alterations of molecular mechanisms

*21 amino acid changes filtered (N=21) with '' g > 0.75 and p < 0.01 '' as very confident hypotheses (Date: March 18th, 2023). * Mutpred score >0.50 is considered pathogenic.** Pr: Posterior probability of molecular mechanism. *** P-value : The top molecular properties score. The predictions which are very confident hypotheses shown in bold font.*

Substitution	Mutpred score *	Molecular mechanism	Pr**	*P*-value***	Prediction
Y471C	0.933	Altered Ordered interface	0.33	3.2e-03	**very confident hypotheses**
		Altered Transmembrane protein	0.38	1.5e-05	**very confident hypotheses**
		Loss of Strand	0.27	0.03	confident hypotheses
		Loss of Sulfation at Y470	0.04	0 .01	confident hypotheses
Y467S	0.931	Altered Ordered interface	0.48	2.9e-04	**very confident hypotheses**
		Altered Transmembrane protein	0.29	2.1e-04	**very confident hypotheses**
		Loss of Sulfation at Y470	0.04	0.01	confident hypotheses
Y467H	0.916	Altered Ordered interface	0.55	8.8e-05	**very confident hypotheses**

(Continued table 5)

Substitution	Mutpred score	Molecular mechanism	Pr	*P*-value	Prediction
		Altered Transmembrane protein	0.31	9.7e-05	**very confident hypotheses**
		Altered Metal binding	0.09	0.01	confident hypotheses
		Loss of Sulfation at Y470	0.04	0.01	confident hypotheses
A320T	0.825	Altered Ordered interface	0.25	0.02	confident hypotheses
V317A	0.845	Gain of Helix	0.27	0.03	confident hypotheses
		Loss of Strand	0.26	0.04	confident hypotheses
		Altered Transmembrane protein	0.12	0.03	confident hypotheses
K304E	0.911	Loss of Strand	0.26	0.04	confident hypotheses
		Altered Transmembrane protein	0.10	0.04	confident hypotheses
P298S	0.877	Altered Transmembrane protein	0.26	1.2e-03	**very confident hypotheses**
		Gain of Strand	0.26	0.04	confident hypotheses
R294Q	0.843	Altered Transmembrane protein	0.29	2.9e-04	**very confident hypotheses**
		Gain of GPI-anchor amidation at N290	0.04	5.3e-03	**very confident hypotheses**
V283M	0.870	Altered Transmembrane protein	0.28	4.1e-04	**very confident hypotheses**
		Loss of Strand	0.27	0.02	confident hypotheses
T282A	0.901	Altered Transmembrane protein	0.32	7.8e-05	**very confident hypotheses**
		Altered Ordered interface	0.28	0.04	confident hypotheses
		Gain of Strand	0.28	7.6e-03	**very confident hypotheses**
T281A	0.886	Altered Transmembrane protein	0.35	2.4e-05	**very confident hypotheses**
		Loss of Strand	0.27	0.02	confident hypotheses
G279R	0.960	Altered Ordered interface	0.35	4.3e-03	**very confident hypotheses**
		Altered Transmembrane protein	0.29	3.8e-04	**very confident hypotheses**
		Loss of Strand	0.27	0.02	confident hypotheses
S264F	0.926	Altered Disordered interface	0.27	0.05	confident hypotheses
		Altered Ordered interface	0.26	0.02	confident hypotheses
		Altered Transmembrane protein	0.24	1.8e-03	**very confident hypotheses**
Y182H	0.909	Altered Ordered interface	0.42	8.0e-04	**very confident hypotheses**
		Altered Transmembrane protein	0.30	1.5e-04	**very confident hypotheses**
		Gain of Relative solvent accessibility	0.24	0.04	confident hypotheses
		Gain of Catalytic site at E180	0.12	0.03	confident hypotheses
		Loss of Sulfation at Y184	0.07	4.5e-03	**very confident hypotheses**
C175W	0.952	Altered Metal binding	0.69	1.1e-03	**very confident hypotheses**
		Altered Transmembrane protein	0.33	5.4e-05	**very confident hypotheses**

(Continued table 5)

Substitution	Mutpred score	Molecular mechanism	Pr	*P*-value	Prediction
		Altered Ordered interface	0.31	0.01	confident hypotheses
		Gain of Strand	0.26	0.05	confident hypotheses
		Gain of N-linked glycosylation at N174	0.16	4.9e-03	**very confident hypotheses**
		Loss of Catalytic site at E180	0.11	0.03	confident hypotheses
P169L	0.927	Altered Transmembrane protein	0.40	4.9e-06	**very confident hypotheses**
		Altered Ordered interface	0.32	0.01	confident hypotheses
		Gain of Helix	0.27	0.03	confident hypotheses
		Altered Metal binding	0.25	9.8e-03	**very confident hypotheses**
		Gain of N-linked glycosylation at N174	0.13	7.3e-03	**very confident hypotheses**
Y151C	0.931	Altered Transmembrane protein	0.34	5.4e-05	**very confident hypotheses**
		Altered Ordered interface	0.32	3.5e-03	**very confident hypotheses**
		Loss of Strand	0.27	0.03	confident hypotheses
		Altered Metal binding	0.25	0.01	confident hypotheses
		Gain of Catalytic site at R154	0.25	4.5e-03	**very confident hypotheses**
		Loss of Allosteric site at R154	0.25	0.02	confident hypotheses
		Altered DNA binding	0.24	0.01	confident hypotheses
R142C	0.935	Altered Ordered interface	0.29	0.03	confident hypotheses
		Altered Metal binding	0.24	0.01	confident hypotheses
		Altered Transmembrane protein	0.24	2.0e-03	**very confident hypotheses**
		Altered DNA binding	0.19	0.03	confident hypotheses
N138T	0.938	Altered Transmembrane protein	0.16	0.01	confident hypotheses
H132Y	0.918	Altered Metal binding	0.49	8.6e-04	**very confident hypotheses**
		Altered Ordered interface	0.35	8.3e-04	**very confident hypotheses**
		Loss of Relative solvent accessibilit	0.28	0.02	confident hypotheses
		Altered Transmembrane protein	0.21	4.0e-03	**very confident hypotheses**
		Gain of Methylation at K128	0.10	0.04	confident hypotheses
D94E	0.851	Altered Transmembrane protein	0.27	4.9e-04	**very confident hypotheses**
		Altered Ordered interface	0.25	0.02	confident hypotheses
M80R	0.968	Altered Metal binding	0.30	4.3e-03	**very confident hypotheses**
		Altered Transmembrane protein	0.30	1.8e-04	**very confident hypotheses**
		Altered Ordered interface	0.29	0.02	confident hypotheses
		Gain of Allosteric site at Y82	0.29	3.0e-03	**very confident hypotheses**
		Altered Stability	0.11	0.04	confident hypotheses
		Loss of Sulfation at Y82	0.06	5.6e-03	**very confident hypotheses**

(Continued table 5)

Substitution	Mutpred score	Molecular mechanism	Pr	*P*-value	Prediction
D73H	0.919	Altered Ordered interface	0.34	6.3e-03	**very confident hypotheses**
		Altered Transmembrane protein	0.32	5.8e-05	**very confident hypotheses**
		Altered Metal binding	0.29	4.5e-03	**very confident hypotheses**
		Gain of Strand	0.29	5.7e-03	**very confident hypotheses**
D49E	0.887	Altered Metal binding	0.34	1.4e-03	**very confident hypotheses**
		Altered Disordered interface	0.27	0.04	confident hypotheses
		Altered DNA binding	0.26	8.1e-03	**very confident hypotheses**
		Altered Transmembrane protein	0.25	1.3e-03	**very confident hypotheses**
		Gain of Allosteric site at P54	0.25	9.9e-03	**very confident hypotheses**
		Loss of Acetylation at K46	0.21	0.03	confident hypotheses
		Gain of Catalytic site at R53	0.10	0.04	confident hypotheses
Y48C	0.934	Altered Disordered interface	0.47	1.5e-03	**very confident hypotheses**
		Altered Metal binding	0.41	7.8e-03	**very confident hypotheses**
		Altered Transmembrane protein	0.32	7.3e-05	**very confident hypotheses**
		Loss of Allosteric site at R53	0.32	2.5e-03	**very confident hypotheses**
		Altered Ordered interface	0.30	4.3e-03	**very confident hypotheses**
		Altered DNA binding	0.29	3.5e-03	**very confident hypotheses**
		Loss of Strand	0.27	0.02	confident hypotheses
		Loss of Acetylation at K46	0.24	0.02	confident hypotheses
		Gain of Catalytic site at R53	0.10	0.04	confident hypotheses

Among the variants found to be pathogenic in this study, variants that were not associated with epilepsy in the literature were not included in the final pathogenic variant *table 6*. In this case, 4 missense SNPs were removed from the list of 21 missense SNPs that will go to 3D visualization, and a total of 17 missense SNPs were obtained for further study.

Table 6. List of pathogenic VUSs

	AA Change	Protein	ClinVar Variant ID	Clinical significance
1	**Y467S**	NP_000805.1:p.Tyr467Ser	1999008	*CAE
2	**Y467H**	NP_000805.1:p.Tyr467His	1038688	CAE
3	**P298S**	NP_000805.1:p.Pro298Ser	2011043	CAE
4	**R294Q**	NP_000805.1:p.Arg294Gln	2419058	CAE
5	**T281A**	NP_000805.1:p.Thr281Ala	548619	*DEE, CAE
6	**G279R**	NP_000805.1:p.Gly279Arg	1042138	CAE
7	**S264F**	NP_000805.1:p.Ser264Phe	1701763	DEE, CAE
8	**Y182H**	NP_000805.1:p.Tyr182His	2010195	CAE
9	**C175W**	NP_000805.1:p.Cys175Trp	2103323	CAE
10	**P169L**	NP_000805.1:p.Pro169Leu	537288	CAE
11	**R142C**	NP_000805.1:p.Arg142Cys	1696530	DEE, CAE
12	**H132Y**	NP_000805.1:p.His132Tyr	1038248	CAE
13	**D94E**	NP_000805.1:p.Asp94Glu	1320972	CAE
14	**M80R**	NP_000805.1:p.Met80Arg	559623	CAE
15	**D73H**	NP_000805.1:p.Asp73His	409958	CAE
16	**D49E**	NP_000805.1:p.Asp49Glu	834156	CAE
17	**Y48C**	NP_000805.1:p.Tyr48Cys	1474854	CAE

The 17 missense SNPs to be analyzed for molecular docking and the pathogenic variant identified in the literature (NCBI/ClinVar) are shown schematically on the protein domains (*fig. 10*).

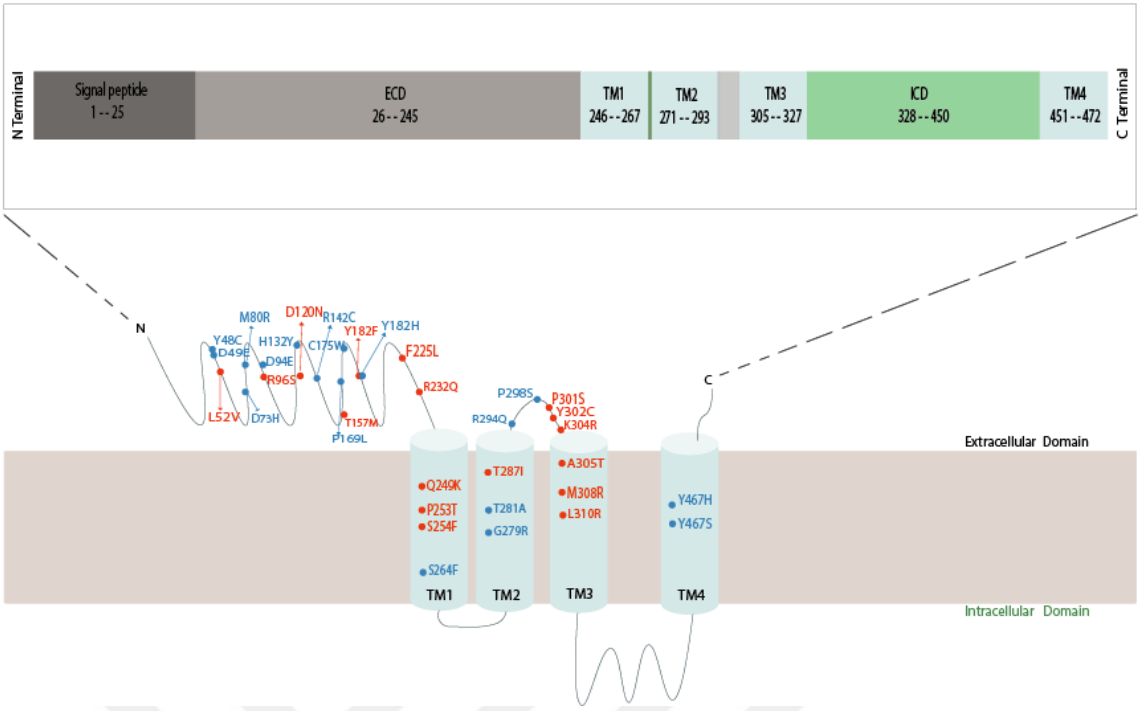

Figure 10. GABRB3 structure and variant location

Representation of the type A gamma-aminobutyric acid GABA(A) receptor subunit beta-3 (GABRB3) 2D protein structure (a) and the location of GABRB3 variants in membran (b), previously described as pathogenic (marked in red) in the literature and predicted to be the pathogenic (marked in blue) by filtering from uncertain significance in the study. N: Amino (N)-Terminal Domain, TM1-TM4: Transmembran Domain, C: Carboxy (C)-Terminal Domain, ECD: Extracellular Domain, ICD: Intracellular Domain.

In the NCBI database, the ECD of the beta-3 subunit is located in the region between the amino acids 26-245, thus Y48C, D49E, D73H, M80R, D94E, H132Y, R142C, P169L, C175W and Y182H variants fall into the region of large extracellular N terminus of the beta3 subunit, while S264F is located in the TM1, G279R is located in the TM2 and R294Q and P298S are located in the TM2-TM3 loop, Y467H and Y467S are located in the TM4 (*fig. 11*).

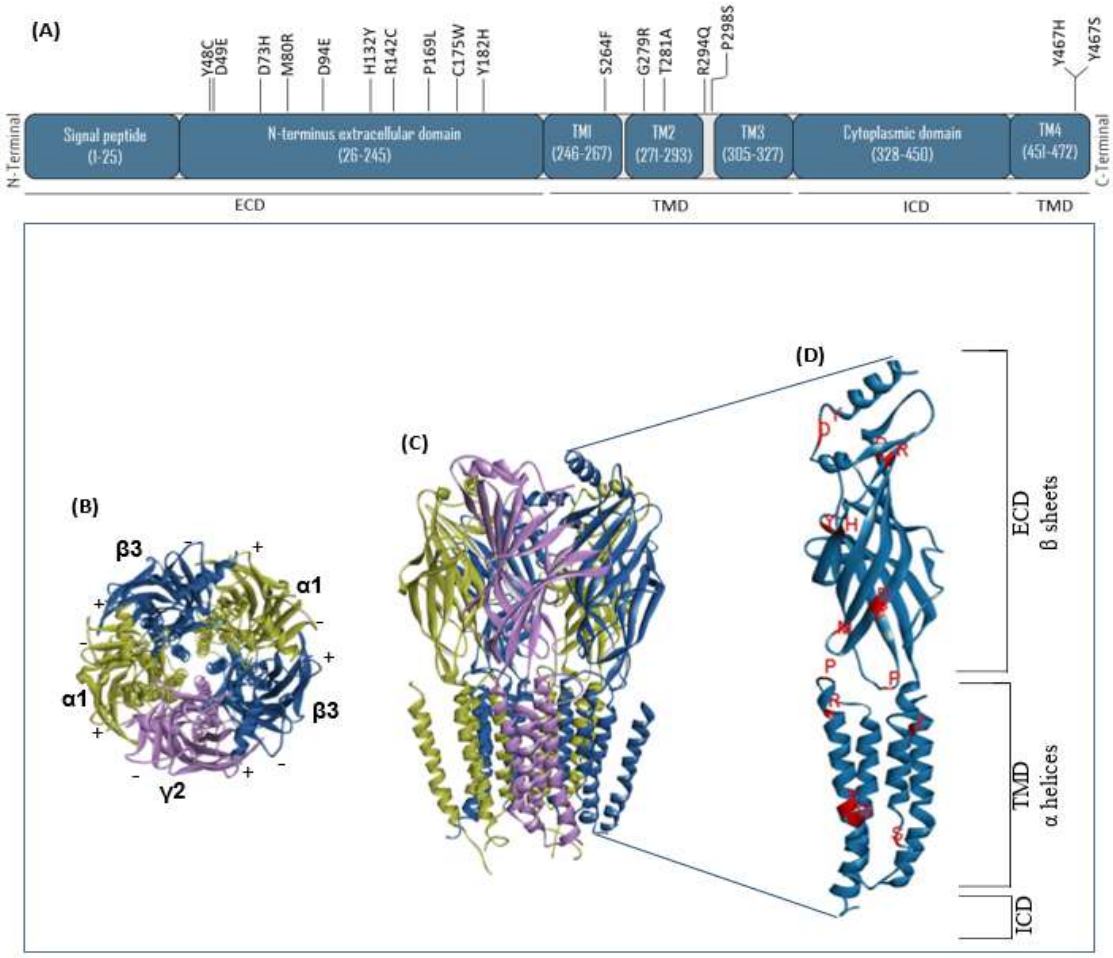

Figure 11. Structural mapping of β3 subunit

Structural features of GABRB3 showing the assembly with β3 subunit and its domains. (A) The protein diagram of β3subunit showing the domain specific location of 17 VUS identified as having the highest risk of pathogenicity. The amino acid positions of each domain are shown in parentheses in the diagram. (B) 3D reconstruction of GABRB3 receptor colored by subunit (top view) showing the position of β3 subunit in the receptor co-assembly. (C) 3D reconstruction of GABRB3 receptor, showing the position of β3 subunit in the receptor co-assembly (side view). (D) 3D reconstruction of β3 subunit of GABA (A) receptor (side view, extended version) showing the positions of the wild type residues (marked in red), where the pathogenic variants are detected (ECD: Extracellular domain; ICD: Intracellular domain; TMD: Transmembrane domain; TM1: Transmembrane domain 1; TM2: Transmembrane domain 2; TM3: Transmembrane domain 3; TM4: Transmembrane domain 4; N, Amino (N)-Terminal Domain ; C, Carboxy (C)-Terminal Domain). Image not to scale.

The structural domains of GABRB3 are colored as shown in *figure 12* for easier distinction. The 17 missense SNPs of GABRB3 filtered as pathogenic are marked with red balls on the numbered GABRB3 amino acid sequence.

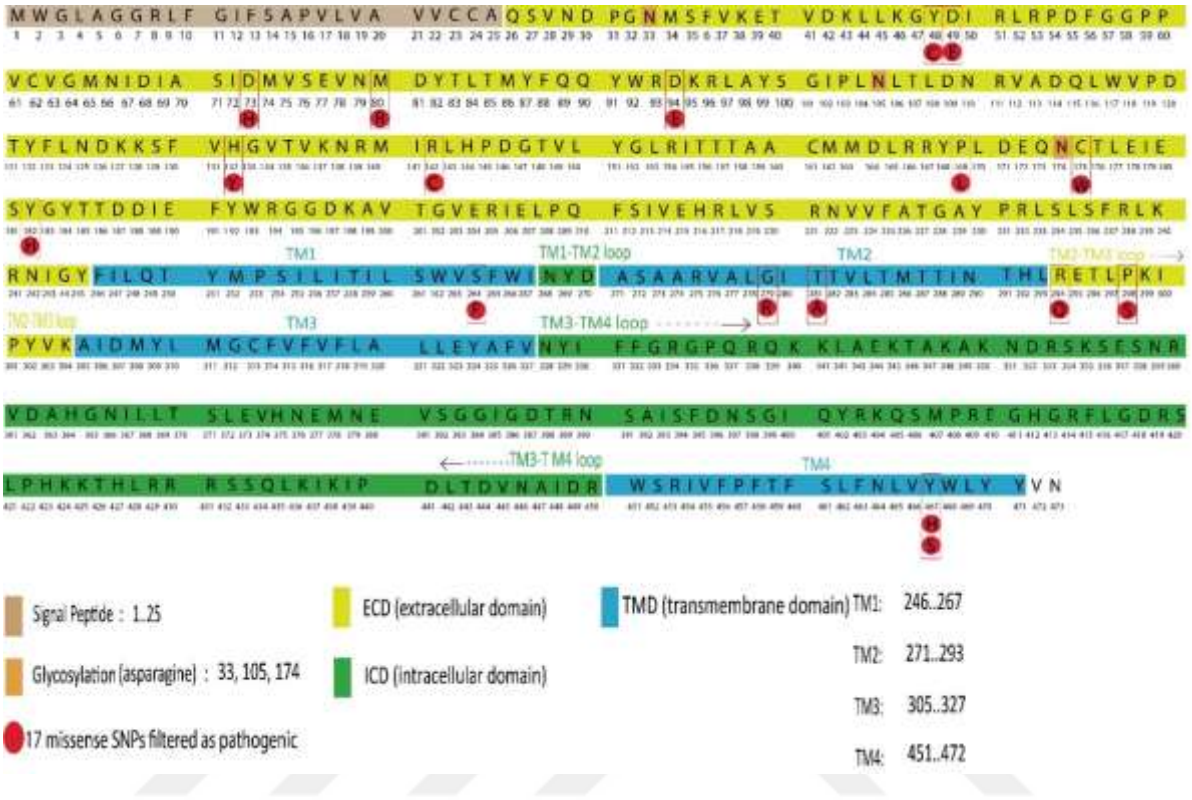

Figure 12. Representation of the GABRB3 protein sequence and variant domains

Representation of the 2D protein sequence encoded by acid receptor subunit beta-3 (GABRB3) / Isoform 1 precursor (homo sapiens) by protein domains (NCBI Reference Sequence : NP_000805.1).

4.4. 3D Visualization of Structural Conformation

HOPE server presents the results on the structural conformation and function of HOPE server presents the results on the structural conformation and function of proteins by analyzing them with 3D visualization. In the study, all 17 predicted pathogenic SNPs of GABRB3 were analyzed by the HOPE server according to different features such as size, hydrophobic interactions, charge, etc by comparing WT and MT (*Data Sheet 2*).

This step of the study focused on analyzing whether GABRB3 missense SNPs were located in the GABA binding region. Information was obtained by scanning the literature about the binding site of GABA, which was determined as the ligand in the study, on the

protein. As a result of the literature review, data on the GABA (referred to as ABU in the PDBe database) binding sites of GABRB3 were obtained from the PDBe database *(https://www.ebi.ac.uk/pdbe/)*. The data obtained are as follows; TYR122 (PDB range: Y97), GLU180 (PDB range: E155), SER181 (PDB range: S156), TYR182 (PDB range: Y157), PHE225 (PDB range: F200) , THR227 (PDB range: T202) and TYR230 (PDB range: Y205). Four of the seven amino acids position in this binding site corresponded to the VUSs in our study (*Table 7*). Six VUSs; Y182H, Y182C, F225V, T227P, T227A and Y230C, are located in GABA binding site. Among these variants, two different variants were observed at Y182 and T227 (Y182C, Y182H, T227A, T227P).

Table 7. GABA binding sites corresponding to VUSs

Amino Acid Position (UniProt Range)	Domain	UniProt Code	Ligand	Reference Structure (chain/residue range/PDB ID)	Reference
Y 182	Exracellular	P28472 · GBRB3_HUMAN	GAMMA-AMINO-BUTANOIC ACID	B,E / 26-473 / 6hup	Masiulis et al., 2019
				B,E / 26-473 / 6huo	Masiulis et al., 2019
				B,E/26-473/6huj	Masiulis et al., 2019
				B /1-332 / 6a96	Liu et al., 2018
				B / 1-473 / 7qn7	Sente et al., 2022
				B / 1-473 / 7qnb	Sente et al., 2022
				B / 1-473 / 7qna	Sente et al., 2022
				B,E /26-332,447-473/7pbz	Kasaragod et al., 2022
F 225	Exracellular	P28472 · GBRB3_HUMAN	GAMMA-AMINO-BUTANOIC ACID	B/1-332 / 6a96	Liu et al., 2018
				B,E/26-332,447-473/7pbz	Kasaragod et al., 2022
T 227	Exracellular	P28472 · GBRB3_HUMAN	GAMMA-AMINO-BUTANOIC ACID	B,E / 26-473 / 6hup	Masiulis et al., 2019
				B,E / 26-473 / 6huo	Masiulis et al., 2019
				B,E/26-473/6huj	Masiulis et al., 2019
				B /1-332 / 6a96	Liu et al., 2018
				B,E /33-332, 447-473/7pbd	Kasaragod et al., 2022
				B / 1-473 / 7qn7	Sente et al., 2022
				B / 1-473 / 7qna	Sente et al., 2022
				B,E /26-332,447-473/7pbz	Kasaragod et al., 2022
Y 230	Exracellular	P28472 · GBRB3_HUMAN	GAMMA-AMINO-BUTANOIC ACID	B,E / 26-473 / 6hup	Masiulis et al., 2019
				B,E / 26-473 / 6huo	Masiulis et al., 2019
				B,E/26-473/6huj	Masiulis et al., 2019
				B /1-332 / 6a96	Liu et al., 2018
				B / 1-473 / 7qn7	Sente et al., 2022
				B / 1-473 / 7qna	Sente et al., 2022
				B / 1-473 / 7qnb	Sente et al., 2022
				B,E /26-332,447-473/7pbz	Kasaragod et al., 2022

As seen in the results table, it was considered a striking result that the only missense SNP that was both predicted to be pathogenic and located in the gene binding site was Y182H (*Table 6*). Additionally, variants of uncertain significance (VUSs) located in the GABA binding site (Y182C, F225V, T227A, T227P, Y230C) but not listed in *Table 6*, were also included in the study for further docking analyses regardless of their pathogenity. The impact of the change is shown in *Data Sheet 3*. Images of overlaid atoms in *Data Sheet 3* were generated in UCSF Chimera 1.17.3 and SWISS MODEL to validate the images on the HOPE server. For this purpose, firstly, the GABRB3 FASTA sequence obtained from UniProt (*https://www.uniprot.org/*) was sent to SWISS-MODEL for

homology study. The obtained homology model of MT was superimposed with WT using the UCSF Chimera 1.17.3 program.

The location of the predicted amino acids as pathogenic (center) and the superposition of the variants with the WT GABRB3 protein are presented in *figure 13.*

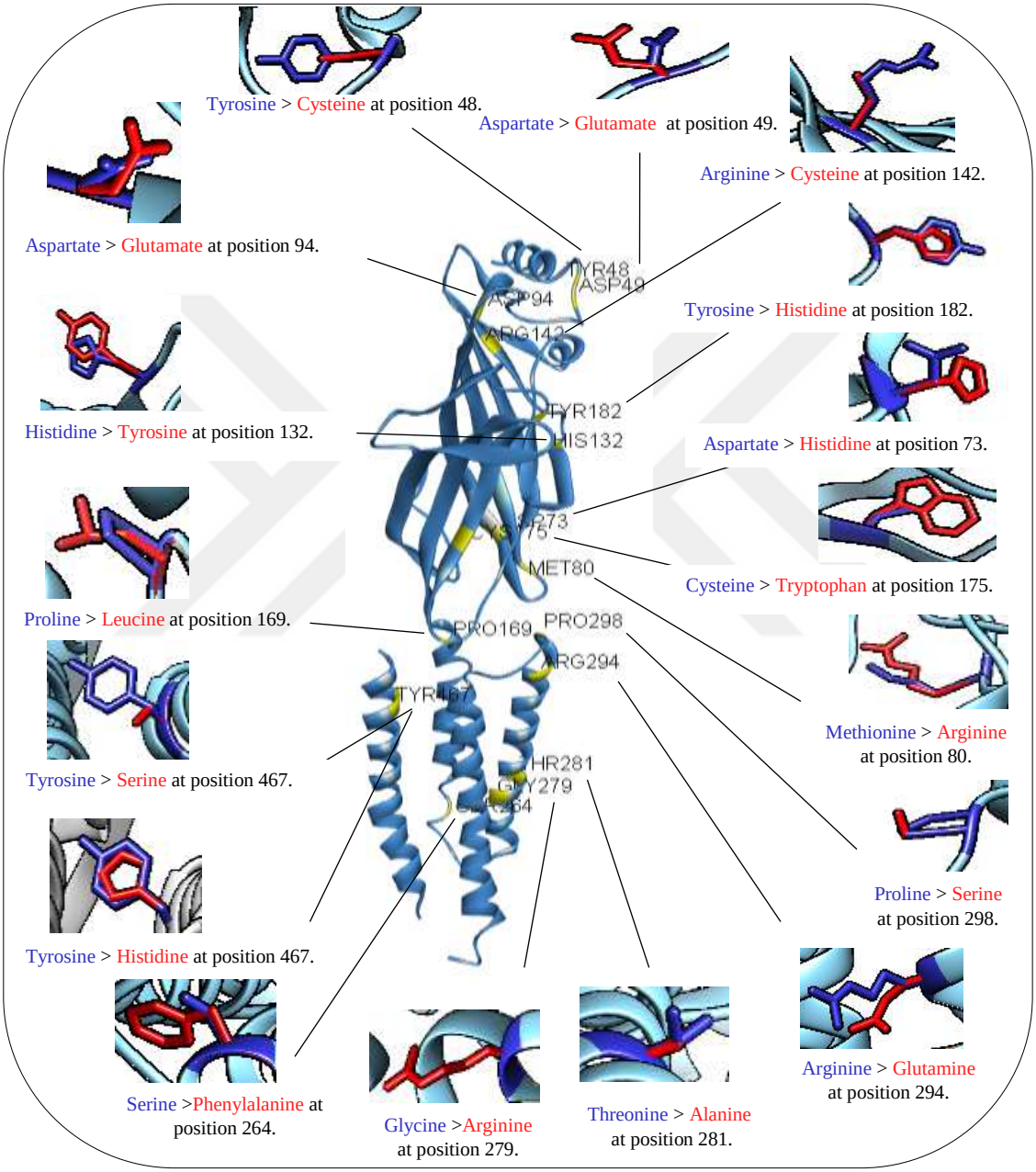

Figure 13. Superimpositions with the variants.

The superimpositions are shown as blue for the wild type and red for the mutant type.

4.5. Molecular Docking

4.5.1. Ligand Preparation

The ligand obtained from the DrugBank website is downloaded in PDB format with 3D coordinates. There are certain requirements to accurately predict the protein's target ligand binding compatibility and energy. Energy minimization is completed and then we activate the option that will determine the torsion locations for different conformations of the ligand. Next, the format is converted from PDB to PDBQT to optimize the ligand geometry with MGL Tools (AutodDockTools-1.5.7).

A docking analysis was used to investigate the effects of six filtered variants (Y182H, Y182C, F225V, T227A, T227P and Y230C) on binding affinity to the GABA molecule. As a first step, The GABA molecule to be used as a ligand (*DrugBank accession number: DB02530*) was downloaded from DrugBank *(https://go.drugbank.com/)* as shown in *figure 14*. DrugBank is a comprehensive, free accessible online database containing information on drugs and drug targets (*Wishart et al., 2018*).

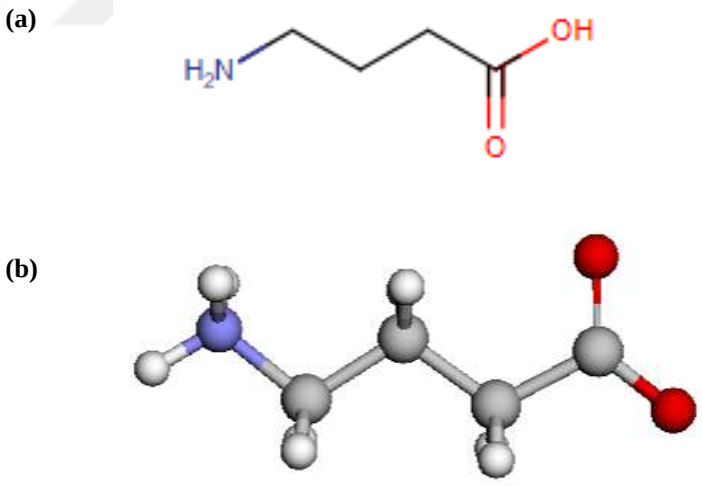

Figure 14. 2D (a) and 3D (b) structure for ligand gamma-Aminobutyric acid

(DrugBank Accession Number :DB02530)

4.5.2. Protein Preparation

In order to perform molecular docking , the three-dimensional (3D) structures of GABRB3 were searched in the Protein Data Bank (PDB, *https://www.rcsb.org/*). PDB provides free access to 3D structure data of molecules found in all organism on the planet through its downloadable data archive. The amino acids in the GABA binding site and the data obtained as a result of the literature review confirmed each other. Cryo-EM crystal structure data of human GABRB3 were obtained from the Protein Data Bank *(https://www.rcsb.org/)* in PDB format, coded 7QN7 *(Sente et al., 2022).* Since the image of the protein is obtained by crystallization technique in a watery environment, water molecules in the file must be removed. Discovery Studio Visualizer was used to remove water molecules. Then respectively; missing atoms were repaired, Kollman charges and polar hydrogens are added to the structure by AutoDockVina 1.5.7. In the final stage, this is converted into a PDBQT output file.

The crystal structure of GABA(A)R-beta3 homopentamer, derived from five identical monomers, was not preferred for use in the study. Rather than the homopentamer, the GABA(A)R-beta3 heteropentamer, derived from two or more different (but similar) monomers, was preferred for analysis. Another important criterion was that they were of homo sapiens origin and their resolution was not lower than 3.00 Å. The structure of *PDB entry ID: 7QN7* was compatible with these criteria (*fig. 15*).

Molecular docking studies were performed on AutoDock Vina. AutoDock Vina was downloaded from the web page of MGLTools *(https://ccsb.scripps.edu/mgltools/downloads/)* which comprises AutoDockTools 1.5.7. One of the program requirements for molecular docking in AutoDock Vina is structure format (PDBQT) in which it should be saved. For analysis of each MT or WT, 2 PDBQT files were created, one from the ligand molecule and the other from the receptor molecule.

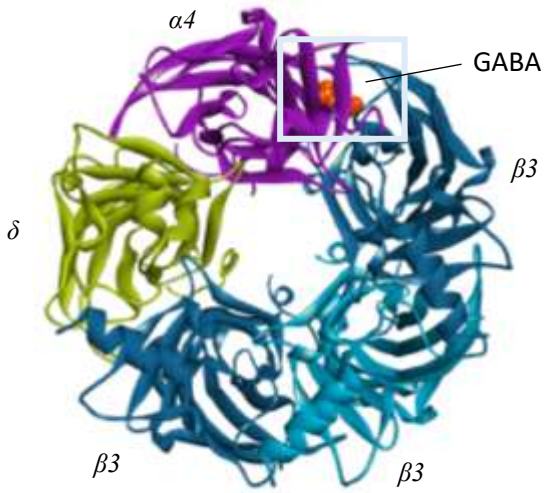

Figure 15. GABA binding site

According to data from PDB ID: 7QN7, $GABA_AR$ *(α4β3δ) includes one putative GABA binding site at the β3+/α4– interface (Model was recolored in BIOVIA DSV). GABA is modeled as red balls inside the light blue square.*

The amino acids in the protein (GABRB3) binding region of the ligand (GABA) were obtained from PDB as a result of literature review (*Table 7*). MGLTools-1.5.7 includes the software package that creates files like PDBQT specifically for AutoDock Vina. The grid box size x, y, z values are 10.0 × 10.0 × 10.0. The grid box center x,y,z values are 145.880429 × 107.889286 × 106.158571 at the binding site of *PDB ID:7QN7 (B chain).*

4.5.3. Value of ΔΔG between WT and MT

The process involves applying docking algorithms that position small molecules into the active site. The simulation box (grid box) and the coordinates (x, y, z) where the placement will be made are specified. Before placement, a file containing this information (txt=grid parameters file) and another file showing the placement parameters (txt=layout parameters file) are created. The results of the interaction energies are shown in a .txt file. The last stage is performed on the command prompt, the previously prepared txt files are entered into the command prompt screen and scanning for affinity values is started.

Validation of the molecular docking reliability, the best docking pose was selected among the change in binding free energy score (ΔΔG - Kcal/mol) of nine options obtained from the AutoDock Vina output (*Trott and Olson, 2010*). For this, the placement pose simulation was done in Discovery Studio Visualizer. Since it is known that the binding energies calculated by docking with AutoDock Vina are the forces that affect the binding

process of H-bonds, electrostatic interactions and pi-pi interactions, these forces were taken into account in choosing the most accurate pose.

As a result, while Y182H (Y157 PDB range) was determined as pathogenic in our study, the rest Y182C (Y157 PDB range), F225V (F200 PDB range), T227A (T202 PDB range), T227P (T202 PDB range), Y230C (Y205 PDB range) were actually not predicted as pathogenic. Neverteless, all of these four variants have impacted on the interaction with GABA as determined by docking simulations regardless of their pathogenicity (*fig. 16)*

As a result, the docking results revealed different values of binding energies expressed in kcal/mol (*Table 8*). The results for Y182H were critical to the function of the receptor. GABA selected as ligand appears to interact well with wild-type GABRB3 (ΔΔG = -5.3 Kcal/mol), which was studied as receptor. It was concluded that this interaction was reduced for the mutant GABRB3 type containing the H182 amino acid (ΔΔG = -4.9 Kcal/mol). AutoDock Vina binding energy scores were simulated by BIOVIA Discovery Studio Visualizer (*fig. 16*). It was observed that Y182H (PDB range Y157H) decreased binding affinity.

Table 8. Binding affinity table of the best docked poses

Wild Type	**Affinity (Kcal/mol)**
WT	-5.3
Mutant Residue	**Binding Affinity (ΔΔG - Kcal/mol)**
Y182H	-4.9
Y182C	-4.8
F225V	-5.1
T227P	-5.0
T227A	-5.0
Y230C	-5.1

The results were slightly more critical for Y182C (PDB range Y157C). It was concluded that this interaction was reduced by the mutant type amino acid C157 ΔΔG = -4.8 Kcal/mol). This is the lowest binding affinity value in this study. Moreover ıt was observed that there was no conventional hydrogen bond with GABA at position 157 (*fig.17*).

The values of other mutant variants are as follows; F225V (PDB range F200V) ΔΔG = -5.1 Kcal/mol , T227P (PDB range T202P) ΔΔG = -5.0 Kcal/mol, T227A (PDB range T202A) ΔΔG = -5.0 Kcal/mol and Y230C (PDB range Y205C) ΔΔG = -5.1 Kcal/mol. The binding affinity energy values and their RMSD values (rmsd l.b and rmsd u.b) were given for one WT amino acid; Y182 and six variants; H182, C182, V225, A227, P227, C230 *(Data Sheet 4).*

The ligand-receptor residue interactions, distances (Å) and bond types between GABRB3 (PDB ID: 7QN7) and GABA are shown in the Table 9.

Table 9. Ligand-receptor residue interactions.

Interactions between GABRB3 (PDB ID: 7QN7) and GABA are illustrated in the Discovery Sudio Visualizer program according to AutoDock Vina.

WT	Name of Interactions	Distance	Bond Type
	A:ARG100:HE - :UNK0:O	2Å	Conventional Hydrogen Bond
	A:ARG100:HH21 - :UNK0:O	2,41Å	Conventional Hydrogen Bond
	:UNK0:N - B:TYR157:O	3,38Å	Conventional Hydrogen Bond
	:UNK0:O - B:THR202:OG1	2,73Å	Conventional Hydrogen Bond
	:UNK0:O - B:TYR205:OH	2,97Å	Conventional Hydrogen Bond
	:UNK0:N - B:TYR205	3,44Å	Pi-Donor Hydrogen Bond

Y157H	Name of Interactions	Distance	Bond Type
	A:ARG100:HH21 - :UNK0:O	1,94Å	Conventional Hydrogen Bond
	B:TYR97:HH - :UNK0:N	2,7Å	Conventional Hydrogen Bond
	B:THR202:HG1 - :UNK0:O	2,45Å	Conventional Hydrogen Bond
	:UNK0:N - B:GLU155:OE2	3,29Å	Conventional Hydrogen Bond
	:UNK0:N - B:SER156:O	3,36Å	Conventional Hydrogen Bond
	:UNK0:N - B:TYR157:O	3,36Å	Conventional Hydrogen Bond
	:UNK0:N - B:TYR205	3,56Å	Pi-Donor Hydrogen Bond
	:UNK0:C - A:PHE98	3,82Å	Pi-Sigma

(Continued table 9)

Y157C Name of Interactions	Distance	Bond Type
A:ARG100:HH21 - :UNK0:O	1,93Å	Conventional Hydrogen Bond
B:TYR97:HH - :UNK0:N	2,65Å	Conventional Hydrogen Bond
B:THR202:HG1 - :UNK0:O	2,45Å	Conventional Hydrogen Bond
:UNK0:N - B:GLU155:OE2	3,22Å	Conventional Hydrogen Bond
:UNK0:N - B:SER156:O	3,33Å	Conventional Hydrogen Bond
:UNK0:N - B:TYR205	3,6Å	Pi-Donor Hydrogen Bond

F200V Name of Interactions	Distance	Bond Type
A:ARG100:HE - :UNK0:O	2Å	Conventional Hydrogen Bond
A:ARG100:HH21 - :UNK0:O	2,37Å	Conventional Hydrogen Bond
:UNK0:N - B:GLU155:OE2	3,36Å	Conventional Hydrogen Bond
:UNK0:N - B:TYR157:O	3,35Å	Conventional Hydrogen Bond
:UNK0:O - B:THR202:OG1	2,74Å	Conventional Hydrogen Bond
:UNK0:O - B:TYR205:OH	2,96Å	Conventional Hydrogen Bond
:UNK0:N - B:TYR205	3,51Å	Pi-Donor Hydrogen Bond

T202P Name of Interactions	Distance	Bond Type
A:ARG100:HE - :UNK0:O	1,94Å	Conventional Hydrogen Bond
A:ARG100:HH21 - :UNK0:O	3,03Å	Conventional Hydrogen Bond
B:TYR157:HH - :UNK0:O	2,49Å	Conventional Hydrogen Bond
:UNK0:N - B:GLU155:OE2	3,33Å	Conventional Hydrogen Bond
:UNK0:N - B:TYR157:O	3,39Å	Conventional Hydrogen Bond
:UNK0:N - B:TYR205	3,53Å	Pi-Donor Hydrogen Bond
:UNK0:O - A:PHE98	3,63Å	Pi-Donor Hydrogen Bond
:UNK0:O - B:TYR157	3,8Å	Pi-Donor Hydrogen Bond

T202A Name of Interactions	Distance	Bond Type
A:ARG100:HE - :UNK0:O	2,02Å	Conventional Hydrogen Bond
A:ARG100:HH21 - :UNK0:O	2,43Å	Conventional Hydrogen Bond
:UNK0:N - B:GLU155:OE2	3,35Å	Conventional Hydrogen Bond
:UNK0:N - B:TYR157:O	3,39Å	Conventional Hydrogen Bond
:UNK0:O - B:TYR205:OH	2,98Å	Conventional Hydrogen Bond
:UNK0:N - B:TYR205	3,48Å	Pi-Donor Hydrogen Bond

(Continued table 9)

Y205C Name of Interactions	Distance	Bond Type
A:ARG100:HE - :UNK0:O	1,89Å	Conventional Hydrogen Bond
A:ARG100:HH21 - :UNK0:O	2,45Å	Conventional Hydrogen Bond
B:TYR157:HH - :UNK0:O	2,33Å	Conventional Hydrogen Bond
:UNK0:N - B:GLU155:OE2	3,34Å	Conventional Hydrogen Bond
:UNK0:N - B:SER156:O	3,20Å	Conventional Hydrogen Bond
:UNK0:N - B:TYR157:O	3,24Å	Conventional Hydrogen Bond
:UNK0:N - B:CYS205:SG	3,76Å	Conventional Hydrogen Bond
:UNK0:O - A:THR163:OG1	2,90Å	Conventional Hydrogen Bond
:UNK0:O - A:PHE98	3,75Å	Pi-Donor Hydrogen Bond
:UNK0:O - B:TYR157	3,93Å	Pi-Donor Hydrogen Bond

In summary, it was proven that the binding affinity of WT GABRB3 protein to GABA (ΔΔG =-5.3 Kcal/mol) was higher than that of GABRB3 variants. It has also been proven that two variants in Y182 (Y182H and Y182C) reduces the binding affinity more than other variants (F225V, T227P, T227A, Y230C) in the GABA binding site.

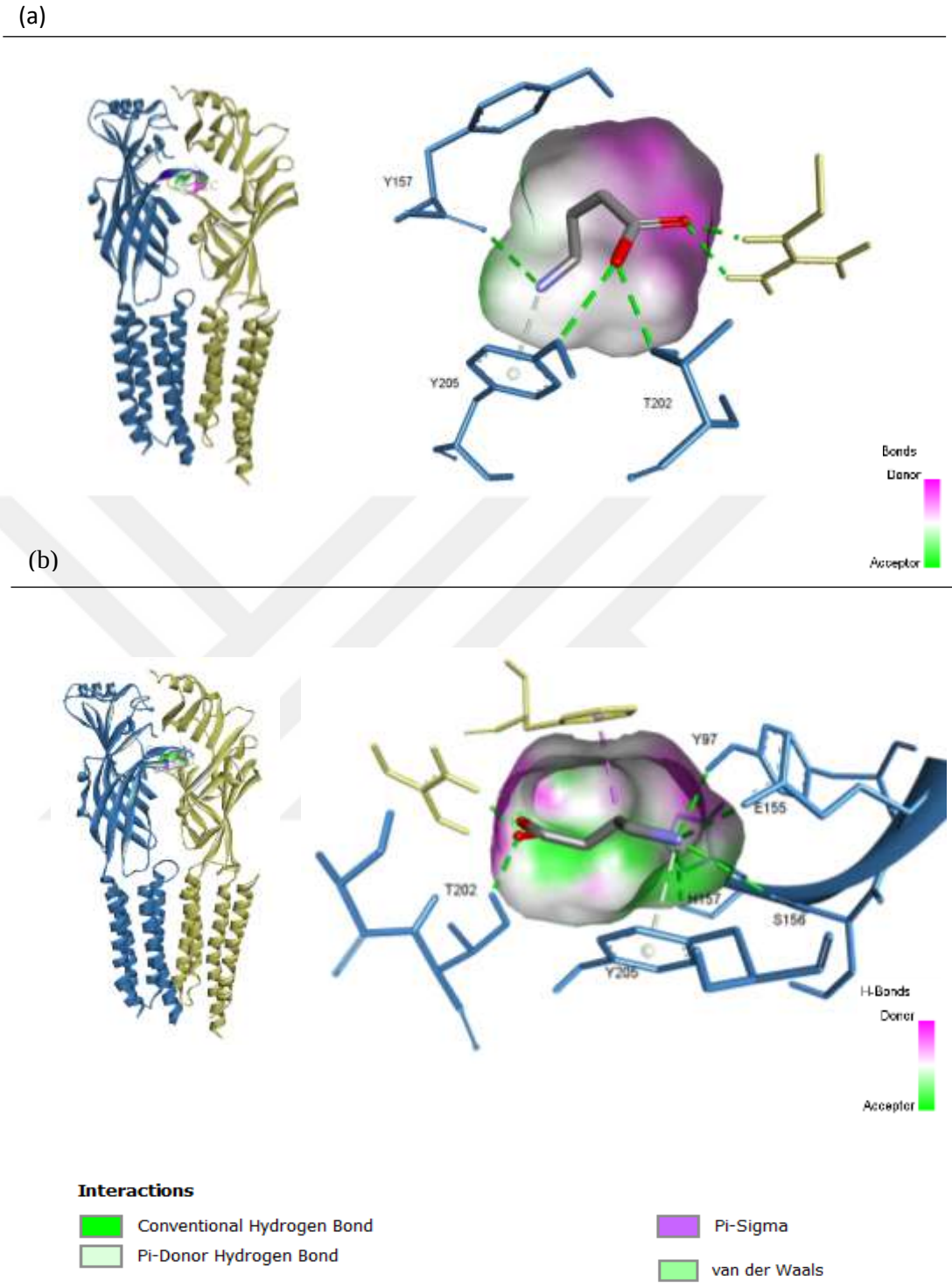

Figure 16. Molecular docking interactions

Molecular docking interaction of (a) WT, (b) MT H157 (UniProt range is H182) (c) MT C157 (UniProt range is C182), (d) MT V200 (UniProt range is V225), (e) MT P202 (UniProt range is P227), (f) MT A202 (UniProt range is A227) and (g) MT C205 (UniProt range is C230) of GABRB3 with GABA . The difference of amino acids number is due to the reference structure in PDB (PDB ID: 7QN7). UniProt range of amino acids : (a) WT, (b) H182, (c) C182, (d) V225, (e) A227, (f) P227 and (g) C230. The chain shown in blue belongs to the GABRB3 / B chain. The chain shown in yellow belongs to GABRA4 / A chain according to PDB ID: 7QN7.

(Continued figure 16)

(c)

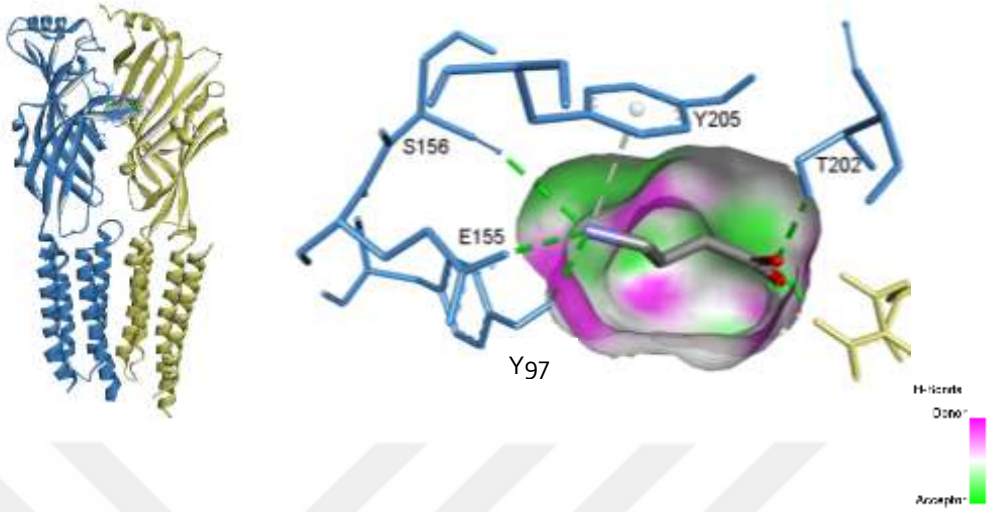

(d)

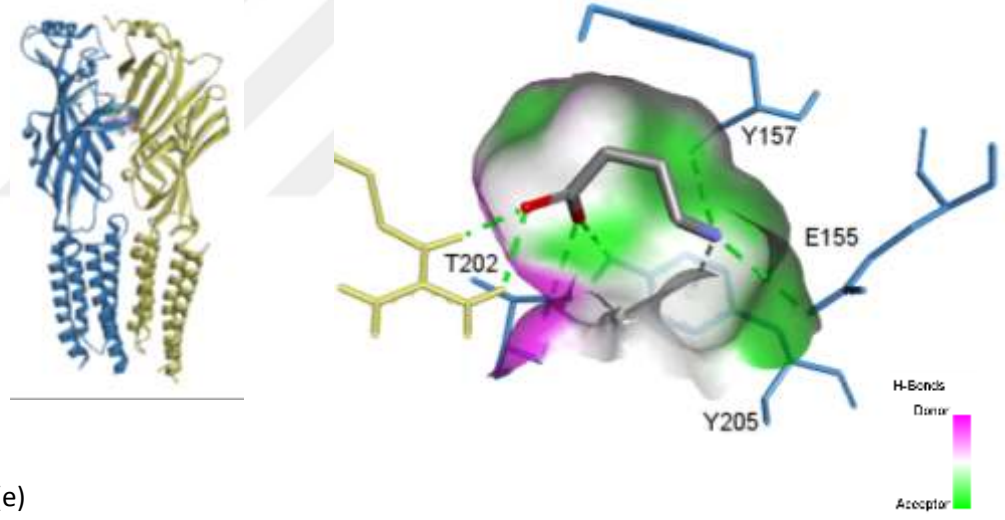

(e)

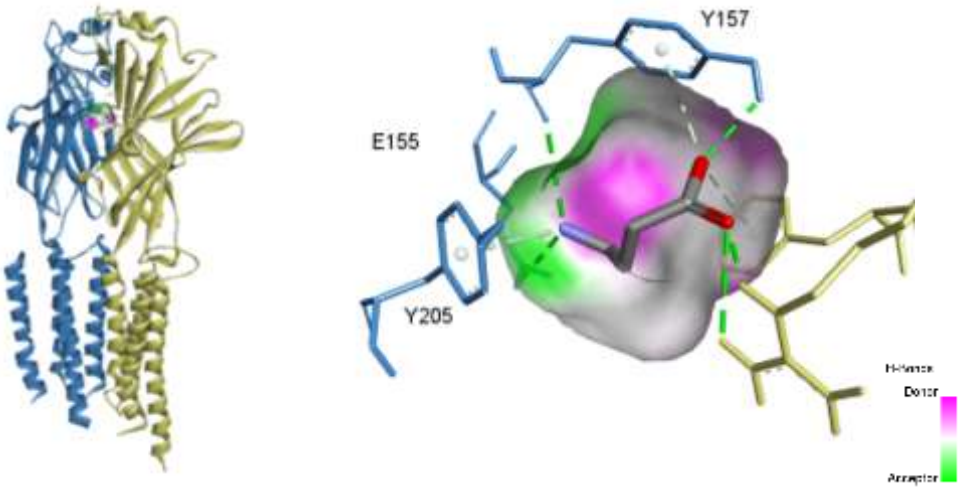

(Continued figure 16)

(f)

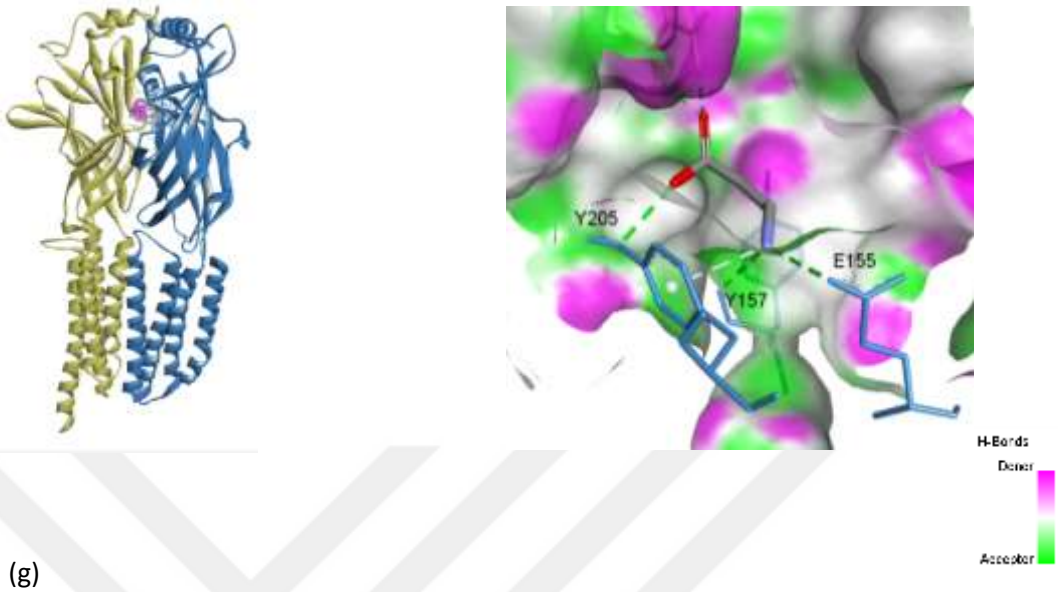

(g)

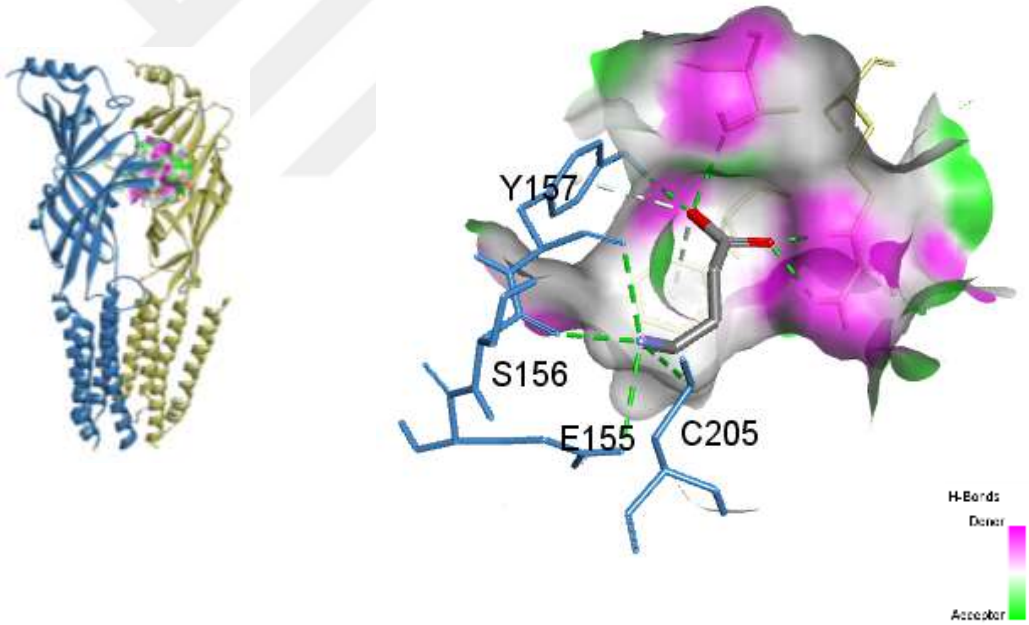

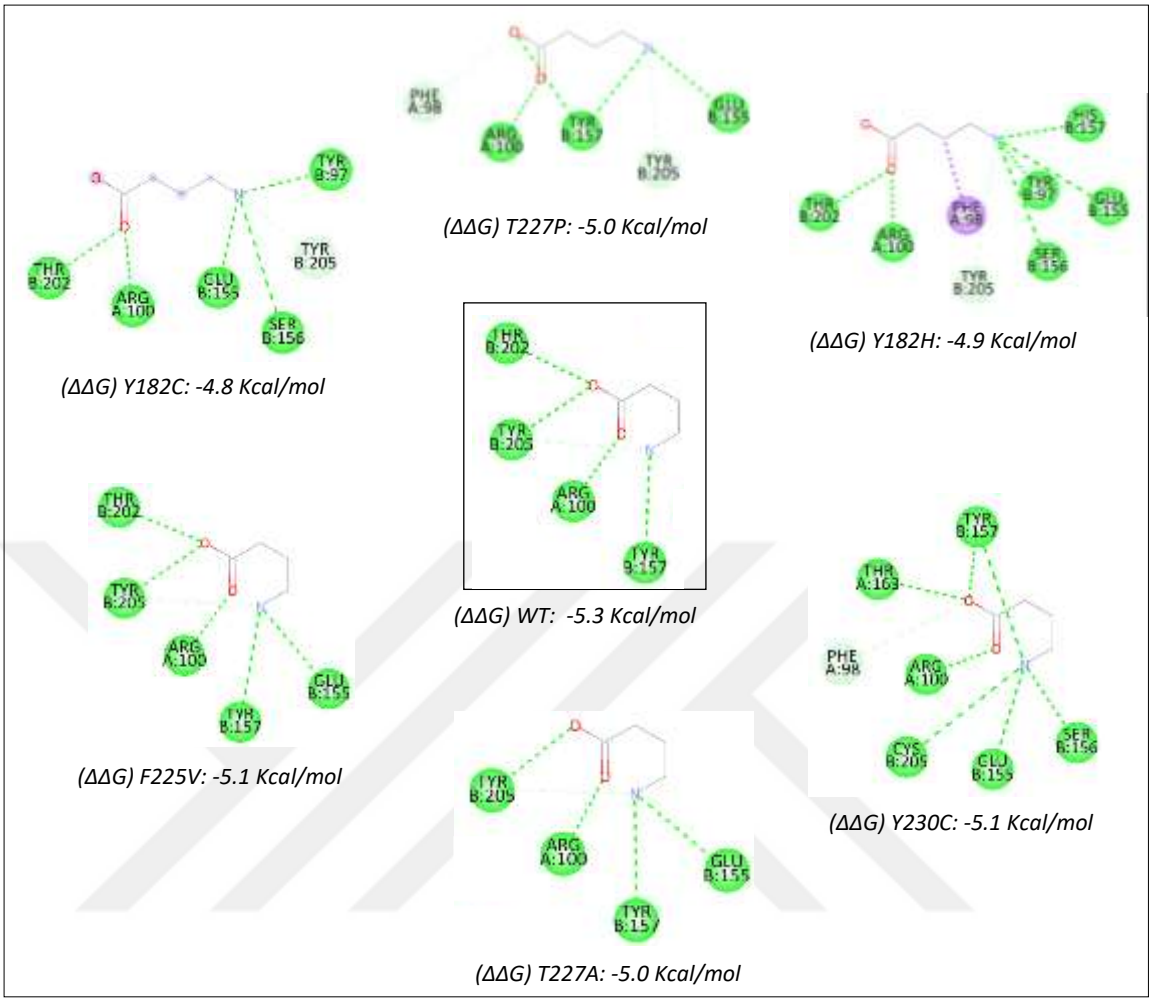

Figure 17. Binding affinities (ΔΔG).

The best docking pose of the GABA molecule with GABRB3 variants located in the GABA binding site. The residue numbers are given according to (A) shows 2D visualization highlighting the detailed interactions observed in the best pose of GABA-GABRB3 (WT) resulted in binding affinity (ΔΔG) of -5.3 Kcal/mol. The change in binding free energy (ΔΔG) of all variants located in the GABA binding sites are greater than the ΔΔG of the wild type (WT) conformation bounded to GABA (WT: -5.3 Kcal/mol). Y182C> Y182H> T227P= T227A> F225V= Y230C> WT -5.3 Kcal/mol

5. DISCUSSION

In this study, seventeen variants of uncertain significance (VUSs); *Y467S, Y467H, P298S, R294Q, T281A, G279R, S264F, Y182H, C175W, P169L, R142C, H132Y, D94E, M80R, D73H, D49E, Y48C* were predicted to be pathogenic, based on various prediction methods with integrative and computational analysis. These VUSs, which were predicted to be pathogenic as a result of their protein function effects, molecular mechanisms and molecular docking analyses, were scanned in the NCBI/ClinVar database and were found to have epilepsy-related effects (*Moller et al., 2017; Hernandez et al., 2017; Myers CT et al., 2016*). In this context, 17 VUSs have been suggested to be critical variants for understanding the genetic underlying motive of epileptogenic process mechanisms.

Considering that 30% of the etiological causes of epilepsy are genetically based, the knowledge that approximately 25% of the identified genes associated with epilepsy encode ion channels has revealed the necessity of defining the pathogenicity of the $GABA_AR$ variants (*Hebbar and Mefford, 2020;* Oyrer et al., 2018). Concordance with the study by Berkovic and friends in 1998, the significant influence of genetic factors in the etiology of epilepsy was confirmed in an unselected sample of twins from the population-based Danish Twin Registry (*Kjeldsen et al., 2001*). In another study using two cohorts of case-control samples from Hong Kong and Taiwan showed that two SNPs in CAMSAP1L1 at 1q32.1 were associated with epilepsy (*Guo et al., 2012*). In fact, the first twin study of epilepsy to provide a genetic basis was conducted by Lennox in 1940 and 1950 and is still valid today. A single nucleotide polymorphism (SNP)-based linkage study of familial mesial frontal lobe epilepsy (FLE) yielded (Fanciulli et al., 2014) a significant linkage to chromosome 3q26, very similar to that described by *Berkovic et al.*

The genetic discovery of Dravet Syndrome, an archetypal condition among Developmental and Epileptic Encephalopaties (DEEs), is of fundamental importance for understanding the genotype-phenotype relationship of epilepsy types (*Claes et al., 2001; Dravet, 2011*). SCN1A, which encodes the alpha 1 subunit of the sodium channel, is known to be associated with various epilepsy syndromes and a number of other diseases (*Scheffer and Nabbout, 2019; Lagae, 2021; Chilcott et al., 2022*). In approximately 90% of patients, Dravet syndrome is caused by nonsense mutations in the SCN1A gene. It is known that mutations in Dravet syndrome, one of the epileptic encephalopathies, are not

hereditary in most cases (*Selmer et al. 2009*). One study showed that common variation within and near SCN1A may increase susceptibility to mesial temporal lobe epilepsy with hippocampal sclerosis with febrile seizures (MTLEHS+FS), a typically severe epilepsy syndrome. MTLEHS is one of the common types of drug-resistant epilepsy (*Berg et al., 2010; Kasperaviciute et al., 2013*). In the study conducted on 870 patients with Dravet syndrome with next-generation sequencing technology in 2021, nine variants were identified in the α1, β2 or γ2 subunit subtypes of $GABA_AR$ (*Hernandez et al., 2021*).

GEFS+, linked to chromosomal locus 2q24, has been associated with mutations in three sodium channel genes and two gamma-aminobutyric acid $GABA_AR$ genes. This locus is characterized by both GEFS+ and familial febrile seizures (*Moulard et al., 1999; Kullmann, 2002*).

Any step that affects traffic to the cell membrane or lateral movement of receptors between synaptic and extrasynaptic locations can cause epilepsy. Identifying such a variant that may cause epilepsy is extremely important in terms of elucidating the genetic causes. Based on current clinical-genetic evidence, the identification of $GABA_AR$ genes associated with epilepsy first began in 2001, and studies have begun to gain momentum today (*Baulac et al., 2001; Cossette et al., 2002; Kang and Barnes2013; Orenstein et al., 2018; Zhang et al., 2023*). Findings of SNPs in the $GABA_A$Rin studies on epilepsy or other genetic diseases have shown that these SNPs exhibit phenotypes such as DEE, CAE, JME, FS, GEFS+ (*Absalom et al.,2022; Kumari et al., 2011; ; Gurba et al., 2012; Yang et al., 2020; Lien et al., 2016; Niturad et al., 2017; Bai et al., 2019*). In conclusion, literature information motivating to focus on SNPs in the $GABA_AR$ to better understand the underlying genetic causes of epilepsy has been supported by very satisfactory clinical results (*Arslan, 2023*).

In a 2017 study by Hernandez and friends, three SNPs (A305V, T288N and L170R) in the $GABA_AR$ β3 subunit gene (GABRB3) were associated with patients with early-onset epileptic encephalopathy (EOEE) and profound developmental delay. Shi and friends's research identified that GABRB3 variants can disable the partnering function of γ2 subunits, which are critical for synaptic clustering. In the same study, GABRB3 (N328D) or GABRB3 (E357K) variants were found to reduce GABA-evoked peak current amplitude. This suggests that the number of functional receptors on the cell surface is reduced (*Shi et al., 2019*). Another study reported that impaired GABRB3

receptor function would compromise the synaptogenesis process associated with neurodegenerative diseases (*Oh et al., 2016*). In the context of these studies, it has begun to be discovered that clinical features of epilepsy patients, especially DEE and CEA, are compatible with GABRB3 variants, and this has revealed the need to be supported by in silico studies on GABRB3 SNPs. The association of GABRB3 variants not only with epilepsy but also with other genetic diseases has motivated us to understand their impact on protein function (*Kim et al., 2006; Delahanthy et al., 2011; Warrier et al., 2013; Le et al., 2017; Coşkunpınar et al., 2023; Babij et al., 2023*). Although GABRB3 variants have been discovered in recent years and it has been understood that GABRB3 is associated with a wide phenotypic spectrum of epilepsy, in silico studies are still insufficient. Conducting in silico studies for GABRB3, which stands out as the underlying cause of loss of function causing GABAergic disinhibition, is very important for future clinical studies and personalized medicine (*Moller et al., 2017*). As a result of literature searches, the clinical identification of GABRB3 missense SNPs was accelerated and these SNPs were found to be associated with epilepsy and variable treatment response (*Chuang and Reddy, 2018; Braat and Kooy, 2015*). Although the discovery of GABRB3 missense SNPs associated with epilepsy has gained momentum in recent years, most of these identified variants have been reported without any analysis of their functional impact. In *2019, Laverty et al*. performed the binding affinity of WT β3 in the $GABA_AR$ cryo-EM structure (PDB ID: 6HUO) to GABA by computational docking. In this thesis study, in order to contribute to filling this lack in the literature, we combined various prediction algorithms with a specific logic to predict the effect of GABRB3 variants on protein function. In order to evaluate the strength of the response to GABA, we calculated the binding affinity values of six VUSs (Y182H, Y182C, F225V, T227A, T227P, Y230C) which located in the binding site. In this context, the standards and guidelines of the American College of Medical Genetics and Genomics (ACMG) were taken as reference in the evaluation of pathogenic evidence for GABRB3 variants (*Richards et al., 2015*).

In conclusion, the number and domain distribution of 17 SNPs predicted as pathogenic are as follows: 10 are located in the ECD (Y48C, D49E, D73H, M80R, D94E, H132Y, R142C, P169L, C175W, Y182H); one is located in the TM1 (S264F); two are located in the TM2 (G279R, T281A); two are located in the TM2-TM3 Loop (R294Q, P298S); two are located in located in the TM4 (Y467H, Y467S). Among these predicted pathogen variants of GABRB3, Y182H is the only variant that located in the GABA

binding site. In this context, to understand whether variant Y182H would cause a loss of function on protein, it was investigated whether it would cause a decrease in its binding affinity to GABA. The GABA binding affinity of Y182H variant of GABRB3 (ΔΔG: -4.9 Kcal/mol) was reduced compared to WT GABRB3 (ΔΔG: -5.3 Kcal/mol). This decrease in binding affinity may be due to a defect in GABRB3 receptor function due to the effect of the Y182H variant. In the variant effect analysis, binding affinities were calculated for five VUSs (Y182C, F225V, T227A, T227P, Y230C) that did not have the highest common score among all predictors but were located in the GABA binding site, and the results were respectively; ΔΔG: -4.8 Kcal/mol, ΔΔG = -5.1 Kcal/mol, ΔΔG =-5.0 Kcal/mol, ΔΔG=-5.0 Kcal/mol, ΔΔG =-5.1 Kcal/mol. The change in binding free energy (ΔΔG) of all variants located in the GABA binding sites are greater than the ΔΔG of the wild type (WT: -5.3 Kcal/mol) conformation bounded to GABA; Y182C> Y182H> T227P= T227A> F225V= Y230C> WT. It was observed that variant Y182C exhibited the most critical decrease of binding affinity. While WT and five variants (Y182H, T227P, T227A, F225V, Y230C) had hydrogen bonds with GABA at codon 182 and 230, only the Y182C amino acid change did not show any hydrogen bond interaction with GABA at codon 182. The results indicate that GABRB3 containing variants *Y182C* and *Y182H* will bind with less attractive force to the γ-Aminobutyric acid (GABA) ligand, the most common inhibitory neurotransmitter in the mammalian brain. In this context, we predicted that these variants in GABRB3 (Y182C and Y182H) may cause greater loss of function in GABA ligand-dependent neurotransmitter inhibition compared to other variants. In addition, 17 variants may led to change the conformation of the protein by affecting the three-dimensional shape orientation of the receptor, which may also change ion channel behavior and consequently play an important role in the pathogenesis of epilepsy.

The American College of Medical Genetics and Genomics (ACMG) and the Association for Molecular Pathology (AMP) have been accepted as references for providing the framework for the use of in silico tools to evaluate the impact of genetic variants (*Richards et al., 2015; Arslan, 2023*). In the evaluation of the variants in our study, two criteria (PP3 and PM1) in the ACMG-AMP standards were classified. If all in silico programs tested agree on the pathogenicity prediction, PP3 is considered evidence supporting. In this study, seventeen variants of uncertain significance (VUSs); Y467S, Y467H, P298S, R294Q, T281A, G279R, S264F, Y182H, C175W, P169L, R142C,

H132Y, D94E, M80R, D73H, D49E, Y48C were predicted to be pathogenic, based on various prediction methods (*SIFT, PolyPhen-2, PANTHER-PSEP, PHD SNP, ConSurf, MutPred2, FATHMM-XF, SNAP2, I-Mutant 3.0 and MUpro*). All prediction methods reported variants as pathogenic without exception in accordance with ACMG standards. The other criterion we will contribute to variant evaluation is PM1, which is considered as evidence of moderate pathogenicity for variants found in mutational hotspots, based on our literature searches. In this context, the ECD-TMD interface, an important region of the $GABA_AR$ β3 subunit, is the structural connection region between subunits. When it binds to a neurotransmitter binding site, it transmits its signal through the ECD-TMD interface. In this context, variants in this coupling region are thought to cause attenuation of signal transmission and thus have a possible risky function for epilepsy (*Absalom et al., 2022*). In this study, the variants that are both predicted to be pathogenic and found in the coupling region are as follows; *M80R, P169L, C175W* (located in the ECD), *P298S* (located in the TM2-TM3 loop). In addition, the proline amino acid provides conformational rigidity to its structure compared to other amino acids, so variations of proline at codons P169 and P298 (*P169L* and *P298S)* can disrupt the backbone structure of the protein. Considering the effect of the cysteine disulfide bridge ("Cys-loop") and the rigidity provided by the proline amino acid in the shaping of the ECD, *P169L* may affect receptor assembly and trafficking (*Goetz et al., 2007; Ghit et al., 2021*). The second transmembrane (TM2) domain of the $GABA_AR$ forms the inner surface of the ion channel. It is known that the amino acid sequences of the TM2 domain of almost all subunits of the $GABA_ARs$ are highly conserved (*Xu et al., 1996*). $GABA_AR$ opens the channel gate through conformational changes in TM2 channel-lining segments for appropriate regulation of GABAergic transmission (*Bera and Akabas, 2005*). TM2 channel lining segments could affect the channel gate opening mechanism through inappropriate conformational changes due to *G279R and T281A* variants in the GABRB3. In conclusion, among the VUSs predicted as pathogens in our study, especially those localized in the hotspots, may impair fast synaptic inhibition by reducing GABRB3 function and therefore increase susceptibility to seizure activity. When combining the criteria of ACMG standards, our variants M80R, P169L, C175W, Y182H, T281A, P298S and G279R predicted as pathogenic, met the classify of very strong pathogenic with 1 moderate (PM1) and 1 supporting (PP3). Our predicted pathogenic variants contribute to providing consistent and reliable genetic testing for ‘’Clinical Genetics Laboratories’’ by referencing the ACMG-AMP standards.

It is necessary to carefully evaluate the limitations of in silico applications. Although molecular docking programs are generally developed for the same purpose, they may perform differently in some applications. In binding affinity calculation, criteria such as internal energy, charge polarization, entropy and flexibility are critical for the accuracy of scoring. In order to get the most ideal docking prediction, the structure of the ligand and receptor should be flexible, have more accuracy valuable, have less system requirements and be less tiring on the processor. In molecular docking approaches, proteins are commonly assumed to be rigid. Considering that proteins are naturally flexible, flexibility will be an important criterion in ligand binding calculations. Because binding affinity prediction of GABRB3 to GABA may affect the accuracy of the result due to the complex atomic interactions between these two molecules. Despite this limitation, AutoDock Vina allows GABRB3 side chains to be considered flexible during docking with GABA, as well as providing torsion conformations for the ligand with its semi-flexible feature (*Trott and Olson, 2010*). Although flexible placement provides more realistic results, it should be noted that there is a risk of obtaining less accurate values. From this perspective, we chose the semi-flexible application, which is the most reliable option for this study.

The complexity of the genetic and phenotypic architecture underlying epilepsy complicates matters somewhat. Although there are many literature-based relationships between type of variation and functional effect, it is possible that a variant predicted as LOF (loss of function/plof) may not result in the phenotype because there is no clear correlation between them (*MacArthur et al., 2012; Vihinen, 2021; Takata et al., 2019*). This may be due to polygenic inheritance. Polygenic inheritance, unlike Mendelian genetics, refers to a phenotypic trait that arises through the interaction of two or more different genes (*Leu et al., 2019*). It should also be noted that protein sequences can tolerate many variations. One of the challenges yet to be overcome in the treatment of epilepsy is the heterogeneity of the patient population. Therefore, a better understanding of genotype–phenotype relationships should be accelerated to classify these patients according to their possible susceptibility to different therapeutic interventions.

6. CONCLUSIONS and RECOMMENDATIONS

Considering that one of the underlying causes of drug resistance is etiologically genetic mechanisms and that these genetic mechanisms affect approximately one-third of the treatment of individuals with epilepsy, developing new treatment methods is critical for public health. One strategy to overcome drug resistance caused by variant proteins based on genetic variation is to develop drugs that directly target the effects of predicted pathogenic variation.

In order for experimental methods to elucidate the genetic mechanisms underlying diseases, they must match the data speed of methods GWAS. The fact that experimental methods cannot keep up with the speed of such as NGS has led to the need for alternative computational predictors. In this context, using computational approaches, we predicted pathogenic variants of the GABRB3 protein that could change the conformation of the protein by affecting its three-dimensional shape orientation, thus changing the ion channel behavior, due to its role in inhibition. In addition, We reveal in silico that variants located in the GABA binding domain will bind with a less attractive force to the γ-Aminobutyric acid ligand, the most common inhibitory neurotransmitter in the mammalian brain. Consequently, we predict that these variants may play an important role in the pathogenesis of epilepsy.

For more accurate interpretation of protein variant effects through computational predictions, annotated machine learning algorithms need to be developed that provide a more realistic prediction rather than a binary output with tolerance/intolerance as with most predictors.

Looking ahead, to keep pace with the output of GWAS technologies aimed at determining the association of genotypes with phenotypes, the development of computational prediction algorithms through global collaborations could help elucidate a number of largely unanswered fundamental questions regarding the genetic mechanisms of epilepsy. In order to make significant progress in the development of personalized sensitive treatments for specific genetic etiologies, it is recommended that the variants we predicted in our study be prioritized.

7. REFERENCES

Absalom, N. L., Ahring, P. K., Liao, V. W., Balle, T., Jiang, T., Anderson, L. L., Arnold, J. C., McGregor, I. S., Bowen, M. T., & Chebib, M. (2019). Functional genomics of epilepsy-associated mutations in the $GABA_A$ receptor subunits reveal that one mutation impairs function and two are catastrophic. *The Journal of biological chemistry*, *294*(15), 6157–6171. https://doi.org/10.1074/jbc.RA118.005697

Absalom, N. L., Liao, V. W. Y., Kothur, K., Indurthi, D. C., Bennetts, B., Troedson, C., Mohammad, S. S., Gupta, S., McGregor, I. S., Bowen, M. T., Lederer, D., Mary, S., De Waele, L., Jansen, K., Gill, D., Kurian, M. A., McTague, A., Møller, R. S., Ahring, P. K., Dale, R. C., … Chebib, M. (2020). Gain-of-function *GABRB3* variants identified in vigabatrin-hypersensitive epileptic encephalopathies. *Brain communications*, *2*(2), fcaa162. https://doi.org/10.1093/braincomms/fcaa162

Absalom, N. L., Liao, V. W. Y., Johannesen, K. M. H., Gardella, E., Jacobs, J., Lesca, G., Gokce-Samar, Z., Arzimanoglou, A., Zeidler, S., Striano, P., Meyer, P., Benkel-Herrenbrueck, I., Mero, I. L., Rummel, J., Chebib, M., Møller, R. S., & Ahring, P. K. (2022). Gain-of-function and loss-of-function GABRB3 variants lead to distinct clinical phenotypes in patients with developmental and epileptic encephalopathies. *Nature communications*, *13*(1), 1822. https://doi.org/10.1038/s41467-022-29280-x

Adzhubei IA, Schmidt S, Peshkin L, Ramensky VE, Gerasimova A, Bork P, Kondrashov AS, Sunyaev SR. Nat Methods **7**(4):248-249 (2010).

Adzhubei, I., Jordan, D. M., & Sunyaev, S. R. (2013). Predicting functional effect of human missense mutations using PolyPhen-2. *Current protocols in human genetics*, *Chapter 7*, Unit7.20. https://doi.org/10.1002/0471142905.hg0720s76

Akyuz, E., Polat, A. K., Eroglu, E., Kullu, I., Angelopoulou, E., & Paudel, Y. N. (2021). Revisiting the role of neurotransmitters in epilepsy: An updated review. *Life sciences*, *265*, 118826. https://doi.org/10.1016/j.lfs.2020.118826

Arslan, A., von Engelhardt, J., & Wisden, W. (2014). Cytoplasmic domain of δ subunit is important for the extra-synaptic targeting of GABAA receptor subtypes. *Journal of integrative neuroscience*, *13*(4), 617–631. https://doi.org/10.1142/S0219635214500228

Arslan A. Pathogenic variants of human GABRA1 gene associated with epilepsy: A computational approach. Heliyon. 2023 Sep 15;9(9):e20218. doi: 10.1016/j.heliyon.2023.e20218. PMID: 37809401; PMCID: PMC10559982.

Armon, A., Graur, D., & Ben-Tal, N. (2001). ConSurf: an algorithmic tool for the identification of functional regions in proteins by surface mapping of phylogenetic information. *Journal of molecular biology*, *307*(1), 447–463. https://doi.org/10.1006/jmbi.2000.4474

Ashkenazy, H., Abadi, S., Martz, E., Chay, O., Mayrose, I., Pupko, T., & Ben-Tal, N. (2016). ConSurf 2016: an improved methodology to estimate and visualize evolutionary conservation in macromolecules. *Nucleic acids research*, *44*(W1), W344–W350. https://doi.org/10.1093/nar/gkw408

Azizzadeh-Roodpish, S., Garzon, M. H., & Mainali, S. (2021). Classifying single nucleotide polymorphisms in humans. *Molecular genetics and genomics : MGG*, *296*(5), 1161–1173. https://doi.org/10.1007/s00438-021-01805-x

Babij, R., Ferrer, C., Donatelle, A., Wacks, S., Buch, A. M., Niemeyer, J. E., Ma, H., Duan, Z. R. S., Fetcho, R. N., Che, A., Otsuka, T., Schwartz, T. H., Huang, B. S., Liston, C., & De Marco García, N. V. (2023). Gabrb3 is required for the functional integration of pyramidal neuron subtypes in the somatosensory cortex. *Neuron*, *111*(2), 256–274.e10. https://doi.org/10.1016/j.neuron.2022.10.037

Baulac, S., Huberfeld, G., Gourfinkel-An, I., Mitropoulou, G., Beranger, A., Prud'homme, J. F., ... & LeGuern, E. (2001). First genetic evidence of GABAA receptor dysfunction in epilepsy: a mutation in the γ2-subunit gene. *Nature genetics*, *28*(1), 46-48.

Ben-Ari, Y., Khalilov, I., Kahle, K. T., & Cherubini, E. (2012). The GABA excitatory/inhibitory shift in brain maturation and neurological disorders. The Neuroscientist : a review journal bringing neurobiology, neurology and psychiatry, 18(5), 467–486. https://doi.org/10.1177/1073858412438697

Bera, A. K., & Akabas, M. H. (2005). Spontaneous thermal motion of the GABA(A) receptor M2 channel-lining segments. *The Journal of biological chemistry*, *280*(42), 35506–35512. https://doi.org/10.1074/jbc.M504645200

Berg, A. T., Berkovic, S. F., Brodie, M. J., Buchhalter, J., Cross, J. H., van Emde Boas, W., Engel, J., French, J., Glauser, T. A., Mathern, G. W., Moshé, S. L., Nordli, D., Plouin, P., & Scheffer, I. E. (2010). Revised terminology and concepts for organization of seizures and epilepsies: report of the ILAE Commission on Classification and Terminology, 2005-2009. *Epilepsia*, *51*(4), 676–685. https://doi.org/10.1111/j.1528-1167.2010.02522.x

Berkovic, S. F., Howell, R. A., Hay, D. A., & Hopper, J. L. (1998). Epilepsies in twins: genetics of the major epilepsy syndromes. *Annals of neurology*, *43*(4), 435-445.

Billakota, S., Andresen, J. M., Gay, B. C., Stewart, G. R., Fedorov, N. B., Gerlach, A. C., & Devinsky, O. (2019). Personalized medicine: Vinpocetine to reverse effects of GABRB3 mutation. *Epilepsia*, *60*(12), 2459–2465. https://doi.org/10.1111/epi.16394

Bowery, N. G., & Smart, T. G. (2006). GABA and glycine as neurotransmitters: a brief history. *British journal of pharmacology*, *147 Suppl 1*(Suppl 1), S109–S119. https://doi.org/10.1038/sj.bjp.0706443

Braat, S., & Kooy, R. F. (2015). The GABAA Receptor as a Therapeutic Target for Neurodevelopmental Disorders. *Neuron*, *86*(5), 1119–1130. https://doi.org/10.1016/j.neuron.2015.03.042

Brickley, S. G., & Mody, I. (2012). Extrasynaptic GABA(A) receptors: their function in the CNS and implications for disease. *Neuron*, *73*(1), 23–34. https://doi.org/10.1016/j.neuron.2011.12.012

Bryson, A., Reid, C., & Petrou, S. (2023). Fundamental Neurochemistry Review: $GABA_A$ receptor neurotransmission and epilepsy: Principles, disease mechanisms and pharmacotherapy. *Journal of neurochemistry*, *165*(1), 6–28. https://doi.org/10.1111/jnc.15769

Capriotti, E., Calabrese, R., & Casadio, R. (2006). Predicting the insurgence of human genetic diseases associated to single point protein mutations with support vector machines and evolutionary information. *Bioinformatics (Oxford, England)*, *22*(22), 2729–2734. https://doi.org/10.1093/bioinformatics/btl423

Capriotti E, Fariselli P, Calabrese R, Casadio R (2005) Predicting protein stability changes from sequences using support vector machines. Bioinformatics 21(SUPPL. 2):54–58. https://doi.org/10.1093/bioinformatics/bti1109

Cargill, M., Altshuler, D., Ireland, J., Sklar, P., Ardlie, K., Patil, N., Shaw, N., Lane, C. R., Lim, E. P., Kalyanaraman, N., Nemesh, J., Ziaugra, L., Friedland, L., Rolfe, A., Warrington, J., Lipshutz, R., Daley, G. Q., & Lander, E. S. (1999). Characterization of single-nucleotide polymorphisms in coding regions of human genes. *Nature genetics*, *22*(3), 231–238. https://doi.org/10.1038/10290

Cecchini, M., & Changeux, J. P. (2015). The nicotinic acetylcholine receptor and its prokaryotic homologues: Structure, conformational transitions & allosteric modulation. *Neuropharmacology*, *96*(Pt B), 137–149. https://doi.org/10.1016/j.neuropharm.2014.12.006

Chen, T., Giri, M., Xia, Z., Subedi, Y. N., & Li, Y. (2017). Genetic and epigenetic mechanisms of epilepsy: a review. *Neuropsychiatric disease and treatment*, *13*, 1841–1859. https://doi.org/10.2147/NDT.S142032

Chilcott, E., Díaz, J. A., Bertram, C., Berti, M., & Karda, R. (2022). Genetic therapeutic advancements for Dravet Syndrome. *Epilepsy & behavior : E&B*, *132*, 108741. https://doi.org/10.1016/j.yebeh.2022.108741

Chuang, S. H., & Reddy, D. S. (2018). Genetic and Molecular Regulation of Extrasynaptic GABA-A Receptors in the Brain: Therapeutic Insights for Epilepsy. *The Journal of pharmacology and experimental therapeutics*, *364*(2), 180–197. https://doi.org/10.1124/jpet.117.244673

Claes, L., Del-Favero, J., Ceulemans, B., Lagae, L., Van Broeckhoven, C., & De Jonghe, P. (2001). De novo mutations in the sodium-channel gene SCN1A cause severe myoclonic epilepsy of infancy. *American journal of human genetics*, *68*(6), 1327–1332. https://doi.org/10.1086/320609

Cloix, J. F., & Hévor, T. (2009). Epilepsy, regulation of brain energy metabolism and neurotransmission. *Current medicinal chemistry*, *16*(7), 841–853. https://doi.org/10.2174/092986709787549316

Cheng, J., Randall, A., & Baldi, P. (2006). Prediction of protein stability changes for single-site mutations using support vector machines. *Proteins*, *62*(4), 1125–1132. https://doi.org/10.1002/prot.20810

Collins, F. S., & Fink, L. (1995). The Human Genome Project. *Alcohol health and research world*, *19*(3), 190–195.

Coskunpinar, E. M., Tur, S., Cevher Binici, N., & Yazan Songür, C. (2023). Association of GABRG3, GABRB3, HTR2A gene variants with autism spectrum disorder. *Gene*, *870*, 147399. https://doi.org/10.1016/j.gene.2023.147399

Cossette, P., Liu, L., Brisebois, K., Dong, H., Lortie, A., Vanasse, M., ... & Rouleau, G. A. (2002). Mutation of GABRA1 in an autosomal dominant form of juvenile myoclonic epilepsy. *Nature genetics*, *31*(2), 184-189.

Delahanty, R. J., Kang, J. Q., Brune, C. W., Kistner, E. O., Courchesne, E., Cox, N. J., Cook, E. H., Jr, Macdonald, R. L., & Sutcliffe, J. S. (2011). Maternal transmission of a rare GABRB3 signal peptide variant is associated with autism. *Molecular psychiatry*, *16*(1), 86–96. https://doi.org/10.1038/mp.2009.118

Denommé-Pichon AS, Vitobello A, Olaso R, Ziegler A, Jeanne M, Tran Mau-Them F, Couturier V, Racine C, Isidor B, Poë C, Jouan T, Boland A, Fin B, Bacq-Daian D, Besse C, Garde A, Prost A, Garret P, …, Thauvin-Robinet C. Accelerated genome sequencing with controlled costs for infants in intensive care units: a feasibility study in a French hospital network. Eur J Hum Genet. 2022 May;30(5):567-576. doi: 10.1038/s41431-021-00998-4. Epub 2021 Nov 15. PMID: 34782754; PMCID: PMC9091203.

Devinsky, O., Vezzani, A., O'Brien, T. J., Jette, N., Scheffer, I. E., de Curtis, M., & Perucca, P. (2018). Epilepsy (primer). *Nature Reviews: Disease Primers*, *4*(1).

Distinct roles of gamma-aminobutyric acid type A receptor subtypes: A focus on phasic and tonic inhibition. A Arslan. Journal of Neurobehavioral Sciences 2, 72-76 3 2015

Dravet C. (2011). The core Dravet syndrome phenotype. *Epilepsia*, *52 Suppl 2*, 3–9. https://doi.org/10.1111/j.1528-1167.2011.02994.x

Eberhardt, J., Santos-Martins, D., Tillack, A. F., & Forli, S. (2021). AutoDock Vina 1.2.0: New Docking Methods, Expanded Force Field, and Python Bindings. *Journal of chemical information and modeling*, *61*(8), 3891–3898. https://doi.org/10.1021/acs.jcim.1c00203

Egawa, K., & Fukuda, A. (2013). Pathophysiological power of improper tonic GABA(A) conductances in mature and immature models. *Frontiers in neural circuits*, *7*, 170. https://doi.org/10.3389/fncir.2013.00170

Epi4K Consortium (2012). Epi4K: gene discovery in 4,000 genomes. *Epilepsia*, *53*(8), 1457–1467. https://doi.org/10.1111/j.1528-1167.2012.03511.x

Epi4K Consortium. De Novo Mutations in SLC1A2 and CACNA1A Are Important Causes of Epileptic Encephalopathies. Am J Hum Genet. 2016 Aug 4;99(2):287-98. doi: 10.1016/j.ajhg.2016.06.003. Epub 2016 Jul 28. PMID: 27476654; PMCID: PMC4974067.

Epi4K Consortium, Epilepsy Phenome/Genome Project, Allen, A. S., Berkovic, S. F., Cossette, P., Delanty, N., Dlugos, D., Eichler, E. E., Epstein, M. P., Glauser, T., Goldstein, D. B., Han, Y., Heinzen, E. L., Hitomi, Y., Howell, K. B., Johnson, M. R., Kuzniecky, R., Lowenstein, D. H., Lu, Y. F., Madou, M. R., … Winawer, M. R. (2013). De novo mutations in epileptic encephalopathies. *Nature*, *501*(7466), 217–221. https://doi.org/10.1038/nature12439

Epi4K Consortium (2017). Phenotypic analysis of 303 multiplex families with common epilepsies. *Brain : a journal of neurology*, *140*(8), 2144–2156. https://doi.org/10.1093/brain/awx129

Epi25 Collaborative. Electronic address: s.berkovic@unimelb.edu.au, & Epi25 Collaborative (2019). Ultra-Rare Genetic Variation in the Epilepsies: A Whole-Exome Sequencing Study of 17,606 Individuals. *American journal of human genetics*, *105*(2), 267–282. https://doi.org/10.1016/j.ajhg.2019.05.020

Fanciulli, M., Di Bonaventura, C., Egeo, G., Fattouch, J., Dazzo, E., Radovic, S., Spadotto, A., Giallonardo, A. T., & Nobile, C. (2014). Suggestive linkage of familial mesial temporal lobe epilepsy to chromosome 3q26. *Epilepsy research*, *108*(2), 232–240. https://doi.org/10.1016/j.eplepsyres.2013.11.002

Farrant, M., & Nusser, Z. (2005). Variations on an inhibitory theme: phasic and tonic activation of GABA(A) receptors. *Nature reviews. Neuroscience*, *6*(3), 215–229. https://doi.org/10.1038/nrn1625

GABRA5 and GABRB3 in a Chinese population affected by childhood absence epilepsy. *Chinese medical journal*, *117*(10), 1497–1501.

Ghit, A., Assal, D., Al-Shami, A. S., & Hussein, D. E. E. (2021). $GABA_A$ receptors: structure, function, pharmacology, and related disorders. *Journal, genetic engineering & biotechnology*, *19*(1), 123. https://doi.org/10.1186/s43141-021-00224-0

Goetz, T., Arslan, A., Wisden, W., & Wulff, P. (2007). GABA(A) receptors: structure and function in the basal ganglia. *Progress in brain research*, *160*, 21–41. https://doi.org/10.1016/S0079-6123(06)60003-4

Guo, Y., Baum, L. W., Sham, P. C., Wong, V., Ng, P. W., Lui, C. H., Sin, N. C., Tsoi, T. H., Tang, C. S., Kwan, J. S., Yip, B. H., Xiao, S. M., Thomas, G. N., Lau, Y. L., Yang, W., Cherny, S. S., & Kwan, P. (2012). Two-stage genome-wide association study identifies variants in CAMSAP1L1 as susceptibility loci for epilepsy in Chinese. *Human molecular genetics*, *21*(5), 1184–1189. https://doi.org/10.1093/hmg/ddr550

Gurba, K. N., Hernandez, C. C., Hu, N., & Macdonald, R. L. (2012). GABRB3 mutation, G32R, associated with childhood absence epilepsy alters α1β3γ2L γ-aminobutyric acid type A (GABAA) receptor expression and channel gating. *The Journal of biological chemistry*, *287*(15), 12083–12097. https://doi.org/10.1074/jbc.M111.332528

Hebbar, M., & Mefford, H. C. (2020). Recent advances in epilepsy genomics and genetic testing. *F1000Research*, *9*, F1000 Faculty Rev-185. https://doi.org/10.12688/f1000research.21366.1

Hecht, M., Bromberg, Y., & Rost, B. (2015). Better prediction of functional effects for sequence variants. *BMC genomics*, *16 Suppl 8*(Suppl 8), S1. https://doi.org/10.1186/1471-2164-16-S8-S1

Hernandez C.C., Zhang Y., Hu N., Shen D., Shen W., et. al.: GABA $_A$ Receptor Coupling Junction and Pore *GABRB3* Mutations are Linked to Early-Onset Epileptic Encephalopathy. Sci. Rep. 2017; 7: pp. 15903.

Hernandez, C. C., Zhang, Y., Hu, N., Shen, D., Shen, W., Liu, X., Kong, W., Jiang, Y., & Macdonald, R. L. (2017). GABA $_A$ Receptor Coupling Junction and Pore GABRB3 Mutations are Linked to Early-Onset Epileptic Encephalopathy. *Scientific reports*, *7*(1), 15903. https://doi.org/10.1038/s41598-017-16010-3

Hernandez, C. C., Tian, X., Hu, N., Shen, W., Catron, M. A., Yang, Y., Chen, J., Jiang, Y., Zhang, Y., & Macdonald, R. L. (2021). Dravet syndrome-associated mutations

in *GABRA1*, *GABRB2* and *GABRG2* define the genetic landscape of defects of $GABA_A$ receptors. *Brain communications*, *3*(2), fcab033. https://doi.org/10.1093/braincomms/fcab033

Hines, R. M., Davies, P. A., Moss, S. J., & Maguire, J. (2012). Functional regulation of GABAA receptors in nervous system pathologies. *Current opinion in neurobiology*, *22*(3), 552–558. https://doi.org/10.1016/j.conb.2011.10.007

Homanics, G. E., DeLorey, T. M., Firestone, L. L., Quinlan, J. J., Handforth, A., Harrison, N. L., Krasowski, M. D., Rick, C. E., Korpi, E. R., Mäkelä, R., Brilliant, M. H., Hagiwara, N., Ferguson, C., Snyder, K., & Olsen, R. W. (1997). Mice devoid of gamma-aminobutyrate type A receptor beta3 subunit have epilepsy, cleft palate, and hypersensitive behavior. *Proceedings of the National Academy of Sciences of the United States of America*, *94*(8), 4143–4148. https://doi.org/10.1073/pnas.94.8.4143

International League Against Epilepsy Consortium on Complex Epilepsies (2018). Genome-wide mega-analysis identifies 16 loci and highlights diverse biological mechanisms in the common epilepsies. *Nature communications*, *9*(1), 5269. https://doi.org/10.1038/s41467-018-07524-z

International League Against Epilepsy Consortium on Complex Epilepsies (2023). GWAS meta-analysis of over 29,000 people with epilepsy identifies 26 risk loci and subtype-specific genetic architecture. *Nature genetics*, *55*(9), 1471–1482. https://doi.org/10.1038/s41588-023-01485-w

Jacob, T. C., Moss, S. J., & Jurd, R. (2008). GABA(A) receptor trafficking and its role in the dynamic modulation of neuronal inhibition. *Nature reviews. Neuroscience*, *9*(5), 331–343. https://doi.org/10.1038/nrn2370

Janve, V. S., Hernandez, C. C., Verdier, K. M., Hu, N., & Macdonald, R. L. (2016). Epileptic encephalopathy de novo GABRB mutations impair γ-aminobutyric acid type A receptor function. *Annals of neurology*, *79*(5), 806–825. https://doi.org/10.1002/ana.24631

Joo, K., Yoon, S. H., Rhie, D. J., & Jang, H. J. (2014). Phasic and Tonic Inhibition are Maintained Respectively by CaMKII and PKA in the Rat Visual Cortex. *The Korean journal of physiology & pharmacology : official journal of the Korean Physiological Society and the Korean Society of Pharmacology*, *18*(6), 517–524. https://doi.org/10.4196/kjpp.2014.18.6.517

Kaculini, C. M., Tate-Looney, A. J., & Seifi, A. (2021). The History of Epilepsy: From Ancient Mystery to Modern Misconception. *Cureus*, *13*(3), e13953. https://doi.org/10.7759/cureus.13953

Kang, J. Q., & Barnes, G. (2013). A common susceptibility factor of both autism and epilepsy: functional deficiency of GABA A receptors. *Journal of autism and developmental disorders*, *43*(1), 68–79. https://doi.org/10.1007/s10803-012-1543-7

Kasperaviciute, D., Catarino, C. B., Matarin, M., Leu, C., Novy, J., Tostevin, A., Leal, B., Hessel, E. V., Hallmann, K., Hildebrand, M. S., Dahl, H. H., Ryten, M., Trabzuni, D., Ramasamy, A., Alhusaini, S., Doherty, C. P., Dorn, T., Hansen, J., Krämer, G., Steinhoff, B. J., … Sisodiya, S. M. (2013). Epilepsy, hippocampal sclerosis and febrile seizures linked by common genetic variation around SCN1A. *Brain : a journal of neurology*, *136*(Pt 10), 3140–3150. https://doi.org/10.1093/brain/awt233

Kasugai, Y., Swinny, J. D., Roberts, J. D., Dalezios, Y., Fukazawa, Y., Sieghart, W., Shigemoto, R., & Somogyi, P. (2010). Quantitative localisation of synaptic and extrasynaptic GABAA receptor subunits on hippocampal pyramidal cells by freeze-fracture replica immunolabelling. *The European journal of neuroscience*, *32*(11), 1868–1888. https://doi.org/10.1111/j.1460-9568.2010.07473.x

Katsonis, P., Wilhelm, K., Williams, A., & Lichtarge, O. (2022). Genome interpretation using in silico predictors of variant impact. *Human genetics*, *141*(10), 1549–1577. https://doi.org/10.1007/s00439-022-02457-6

Kim, S. A., Kim, J. H., Park, M., Cho, I. H., & Yoo, H. J. (2006). Association of GABRB3 polymorphisms with autism spectrum disorders in Korean trios. *Neuropsychobiology*, *54*(3), 160–165. https://doi.org/10.1159/000098651

Kim, S. A., Kim, J. H., Park, M., Cho, I. H., & Yoo, H. J. (2006). Association of GABRB3 polymorphisms with autism spectrum disorders in Korean trios. *Neuropsychobiology*, *54*(3), 160–165. https://doi.org/10.1159/000098651

Kitchen, D. B., Decornez, H., Furr, J. R., & Bajorath, J. (2004). Docking and scoring in virtual screening for drug discovery: methods and applications. *Nature reviews. Drug discovery*, *3*(11), 935–949. https://doi.org/10.1038/nrd1549

Kjeldsen, M. J., Kyvik, K. O., Christensen, K., & Friis, M. L. (2001). Genetic and environmental factors in epilepsy: a population-based study of 11900 Danish twin pairs. *Epilepsy research*, *44*(2-3), 167–178. https://doi.org/10.1016/s0920-1211(01)00196-6

Kroemer R. T. (2007). Structure-based drug design: docking and scoring. *Current protein & peptide science*, *8*(4), 312–328. https://doi.org/10.2174/138920307781369382

Kullmann D. M. (2002). Genetics of epilepsy. *Journal of neurology, neurosurgery, and psychiatry*, *73 Suppl 2*(Suppl 2), II32–II35. https://doi.org/10.1136/jnnp.73.suppl_2.ii32

Kumari, R., Lakhan, R., Kalita, J., Garg, R. K., Misra, U. K., & Mittal, B. (2011). Potential role of GABAA receptor subunit; GABRA6, GABRB2 and GABRR2 gene polymorphisms in epilepsy susceptibility and pharmacotherapy in North Indian population. *Clinica chimica acta; international journal of clinical chemistry*, *412*(13-14), 1244–1248. https://doi.org/10.1016/j.cca.2011.03.018

Lagae L. (2021). Dravet syndrome. *Current opinion in neurology*, *34*(2), 213–218. https://doi.org/10.1097/WCO.0000000000000902

Landrum MJ, Lee JM, Riley GR, Jang W, Rubinstein WS, Church DM, Maglott DR. ClinVar: public archive of relationships among sequence variation and human phenotype. Nucleic Acids Res. 2014 Jan 1;42(1):D980-5. doi: 10.1093/nar/gkt1113. [PubMed PMID: 24234437]

Laurie, D. J., Wisden, W., & Seeburg, P. H. (1992). The distribution of thirteen GABAA receptor subunit mRNAs in the rat brain. III. Embryonic and postnatal development. *The Journal of neuroscience : the official journal of the Society for Neuroscience*, *12*(11), 4151–4172. https://doi.org/10.1523/JNEUROSCI.12-11-04151.1992

Laverty, D., Desai, R., Uchański, T., Masiulis, S., Stec, W. J., Malinauskas, T., Zivanov, J., Pardon, E., Steyaert, J., Miller, K. W., & Aricescu, A. R. (2019). Cryo-EM structure of the human α1β3γ2 $GABA_A$ receptor in a lipid bilayer. Nature, 565(7740), 516–520. https://doi.org/10.1038/s41586-018-0833-4

Le SV, Le PHT, Le TKV, Kieu Huynh TT, Hang Do TT. A mutation in GABRB3 associated with Dravet syndrome. Am J Med Genet A. 2017 Aug;173(8):2126-2131. doi: 10.1002/ajmg.a.38282. Epub 2017 May 24. PMID: 28544625.

Lee, S. E., Lee, Y., & Lee, G. H. (2019). The regulation of glutamic acid decarboxylases in GABA neurotransmission in the brain. *Archives of pharmacal research*, *42*(12), 1031–1039. https://doi.org/10.1007/s12272-019-01196-z

Lengauer, T., & Rarey, M. (1996). Computational methods for biomolecular docking. *Current opinion in structural biology*, *6*(3), 402–406. https://doi.org/10.1016/s0959-440x(96)80061-3

Lerche H. (2020). Drug-resistant epilepsy - time to target mechanisms. *Nature reviews. Neurology*, *16*(11), 595–596. https://doi.org/10.1038/s41582-020-00419-y

Leu, C., Stevelink, R., Smith, A. W., Goleva, S. B., Kanai, M., Ferguson, L., Campbell, C., Kamatani, Y., Okada, Y., Sisodiya, S. M., Cavalleri, G. L., Koeleman, B. P. C., Lerche, H., Jehi, L., Davis, L. K., Najm, I. M., Palotie, A., Daly, M. J., Busch, R. M., Epi25 Consortium, … Lal, D. (2019). Polygenic burden in focal and generalized epilepsies. *Brain : a journal of neurology*, *142*(11), 3473–3481. https://doi.org/10.1093/brain/awz292

Libby, A. M., Ghushchyan, V., McQueen, R. B., Slejko, J. F., Bainbridge, J. L., & Campbell, J. D. (2012). Economic differences in direct and indirect costs between people with epilepsy and without epilepsy. *Medical care*, *50*(11), 928–933. https://doi.org/10.1097/MLR.0b013e31826c8613

Lima LS, Galiciolli MEA, Pereira ME, Felisbino K, Machado-Souza C, de Oliveira CS, Guiloski IC. Modification by genetic polymorphism of lead-induced IQ alteration: a systematic review. Environ Sci Pollut Res Int. 2022 Jun;29(29):43435-43447. doi: 10.1007/s11356-022-19981-7. Epub 2022 Apr 6. PMID: 35386084.

Liu J, Tong L, Song S, Niu Y, Li J, Wu X, Zhang J, Zai CC, Luo F, Wu J, Li H, Wong AHC, Sun R, Liu F, Li B. Novel and de novo mutations in pediatric refractory epilepsy. Mol Brain. 2018 Sep 5;11(1):48. doi: 10.1186/s13041-018-0392-5. Erratum in: Mol Brain. 2018 Oct 16;11(1):59. PMID: 30185235; PMCID: PMC6125990.

Lorenz-Guertin, J. M., Bambino, M. J., & Jacob, T. C. (2018). γ2 $GABA_AR$ Trafficking and the Consequences of Human Genetic Variation. *Frontiers in cellular neuroscience*, *12*, 265. https://doi.org/10.3389/fncel.2018.00265

Lü, J. J., Zhang, Y. H., Pan, H., Chen, Y. C., Liu, X. Y., Jiang, Y. W., Bao, X. H., Shen, Y., Wu, H. S., Xu, K. M., & Wu, X. R. (2004). Case-control study and transmission/disequilibrium tests of the genes encoding

Löscher, W., Potschka, H., Sisodiya, S. M., & Vezzani, A. (2020). Drug resistance in epilepsy: clinical impact, potential mechanisms, and new innovative treatment options. *Pharmacological reviews*, *72*(3), 606-638.

MacArthur, D. G., Balasubramanian, S., Frankish, A., Huang, N., Morris, J., Walter, K., Jostins, L., Habegger, L., Pickrell, J. K., Montgomery, S. B., Albers, C. A., Zhang, Z. D., Conrad, D. F., Lunter, G., Zheng, H., Ayub, Q., DePristo, M. A., Banks, E., Hu, M., Handsaker, R. E., … Tyler-Smith, C. (2012). A systematic survey of loss-of-function variants in human protein-coding genes. *Science (New York, N.Y.)*, *335*(6070), 823–828. https://doi.org/10.1126/science.1215040

Maillard, P. Y., Baer, S., Schaefer, É., Desnous, B., Villeneuve, N., Lépine, A., Fabre, A., Lacoste, C., El Chehadeh, S., Piton, A., Porter, L. F., Perriard, C., Wardé, M. A., Spitz, M. A., Laugel, V., Lesca, G., Putoux, A., Ville, D., Mignot, C., Héron, D., … Milh, M. (2022). Molecular and clinical descriptions of patients with $GABA_A$ receptor gene variants (GABRA1, GABRB2, GABRB3, GABRG2): A cohort study, review of literature, and genotype-phenotype correlation. *Epilepsia*, *63*(10), 2519–2533. https://doi.org/10.1111/epi.17336

Masiulis, S., Desai, R., Uchański, T., Serna Martin, I., Laverty, D., Karia, D., Malinauskas, T., Zivanov, J., Pardon, E., Kotecha, A., Steyaert, J., Miller, K. W., & Aricescu, A. R. (2019). CryoEM structure of human full-length heteromeric alpha1beta3gamma2L GABA(A)R in complex with alprazolam (Xanax), GABA and megabody Mb38. https://www.wwpdb.org/pdb?id=pdb_00006huo

Mead O, Thynne E, Winterberg B, Solomon PS. Characterising the role of GABA and its metabolism in the wheat pathogen Stagonospora nodorum. PLoS One. 2013 Nov 12;8(11):e78368. doi: 10.1371/journal.pone.0078368. PMID: 24265684; PMCID: PMC3827059.

Miller, P. S., & Aricescu, A. R. (2014). Crystal structure of a human GABAA receptor. *Nature*, *512*(7514), 270–275. https://doi.org/10.1038/nature13293

Moller R.S., Wuttke T.V., Helbig I., Marini C., Johannesen K.M., et. al.: Mutations in *GABRB3* : from febrile seizures to epileptic encephalopathies. Neurology 2017; 88: pp. 483-492.

Myers C.T.M.J., Schneider A.L., Petrovski S., Allen A.S., Carvill G.L., Zemel M., Saykally J.E., LaCroix A.J., Heinzen E.L., Hollingsworth G., Nikanorova M., Corbett M., Gecz J., Coman D., Freeman J., Calvert S, …. Mefford H.C De Novo Mutations in SLC1A2 and CACNA1A Are Important Causes of Epileptic Encephalopathies. Am. J. Hum. Genet. 2016; 99: pp. 287-298.

Moulard, B., Guipponi, M., Chaigne, D., Mouthon, D., Buresi, C., & Malafosse, A. (1999). Identification of a new locus for generalized epilepsy with febrile seizures plus (GEFS+) on chromosome 2q24-q33. *American journal of human genetics*, *65*(5), 1396–1400. https://doi.org/10.1086/302621

Ng, P. C., & Henikoff, S. (2001). Predicting deleterious amino acid substitutions. *Genome research*, *11*(5), 863–874. https://doi.org/10.1101/gr.176601

Nikolaus, S., Antke, C., Beu, M., & Müller, H. W. (2010). Cortical GABA, striatal dopamine and midbrain serotonin as the key players in compulsive and anxiety disorders--results from in vivo imaging studies. *Reviews in the neurosciences*, *21*(2), 119–139. https://doi.org/10.1515/revneuro.2010.21.2.119

Numis, A. L., da Gente, G., Sherr, E. H., & Glass, H. C. (2022). Whole-exome sequencing with targeted analysis and epilepsy after acute symptomatic neonatal seizures. *Pediatric research*, *91*(4), 896–902. https://doi.org/10.1038/s41390-021-01509-3

Nykamp, K., Anderson, M., Powers, M., Garcia, J., Herrera, B., Ho, Y. Y., Kobayashi, Y., Patil, N., Thusberg, J., Westbrook, M., Invitae Clinical Genomics Group, & Topper, S. (2017). Sherloc: a comprehensive refinement of the ACMG-AMP variant classification criteria. *Genetics in medicine : official journal of the American College of Medical Genetics*, *19*(10), 1105–1117. https://doi.org/10.1038/gim.2017.37

Oh, W. C., Lutzu, S., Castillo, P. E., & Kwon, H. B. (2016). De novo synaptogenesis induced by GABA in the developing mouse cortex. *Science (New York, N.Y.)*, *353*(6303), 1037–1040. https://doi.org/10.1126/science.aaf5206

Orenstein, N., Goldberg-Stern, H., Straussberg, R., Bazak, L., Hubshman, M. W., Kropach, N., ... & Basel-Salmon, L. (2018). A de novo GABRA2 missense mutation in severe early-onset epileptic encephalopathy with a choreiform movement disorder. *European journal of paediatric neurology*, *22*(3), 516-524.

Oyrer, J., Maljevic, S., Scheffer, I. E., Berkovic, S. F., Petrou, S., & Reid, C. A. (2018). Ion Channels in Genetic Epilepsy: From Genes and Mechanisms to Disease-Targeted Therapies. *Pharmacological reviews*, *70*(1), 142–173. https://doi.org/10.1124/pr.117.014456

Papandreou A, McTague A, Trump N, Ambegaonkar G, Ngoh A, Meyer E, Scott RH, Kurian MA. GABRB3 mutations: a new and emerging cause of early infantile epileptic encephalopathy. Dev Med Child Neurol. 2016 Apr;58(4):416-20. doi: 10.1111/dmcn.12976. Epub 2015 Dec 9. PMID: 26645412; PMCID: PMC4864756.

Parrini E, Marini C, Mei D, Galuppi A, Cellini E, Pucatti D, Chiti L, Rutigliano D, Bianchini C, Virdò S, De Vita D, Bigoni S, Barba C, Mari F, Montomoli M, Pisano T, Rosati A; Clinical Study Group; Guerrini R. Diagnostic Targeted Resequencing in 349 Patients with Drug-Resistant Pediatric Epilepsies Identifies Causative Mutations in 30 Different Genes. Hum Mutat. 2017 Feb;38(2):216-225. doi: 10.1002/humu.23149. Epub 2016 Dec 9. PMID: 27864847.

Pejaver, V., Urresti, J., Lugo-Martinez, J., Pagel, K. A., Lin, G. N., Nam, H. J., Mort, M., Cooper, D. N., Sebat, J., Iakoucheva, L. M., Mooney, S. D., & Radivojac, P. (2020). Inferring the molecular and phenotypic impact of amino acid variants with MutPred2. *Nature communications*, *11*(1), 5918. https://doi.org/10.1038/s41467-020-19669-x

Perucca, P., & Perucca, E. (2019). Identifying mutations in epilepsy genes: Impact on treatment selection. *Epilepsy research*, *152*, 18–30. https://doi.org/10.1016/j.eplepsyres.2019.03.001

Perucca, P., Bahlo, M., & Berkovic, S. F. (2020). The Genetics of Epilepsy. *Annual review of genomics and human genetics*, *21*, 205–230. https://doi.org/10.1146/annurev-genom-120219-074937

Pettersen, E. F., Goddard, T. D., Huang, C. C., Couch, G. S., Greenblatt, D. M., Meng, E. C., & Ferrin, T. E. (2004). UCSF Chimera--a visualization system for exploratory research and analysis. *Journal of computational chemistry*, *25*(13), 1605–1612. https://doi.org/10.1002/jcc.20084

Richards, S., Aziz, N., Bale, S., Bick, D., Das, S., Gastier-Foster, J., Grody, W. W., Hegde, M., Lyon, E., Spector, E., Voelkerding, K., Rehm, H. L., & ACMG Laboratory Quality Assurance Committee (2015). Standards and guidelines for the interpretation of sequence variants: a joint consensus

recommendation of the American College of Medical Genetics and Genomics and the Association for Molecular Pathology. *Genetics in medicine : official journal of the American College of Medical Genetics*, *17*(5), 405–424. https://doi.org/10.1038/gim.2015.30

Righes Marafiga, J., Vendramin Pasquetti, M., & Calcagnotto, M. E. (2021). GABAergic interneurons in epilepsy: More than a simple change in inhibition. *Epilepsy & behavior : E&B*, *121*(Pt B), 106935. https://doi.org/10.1016/j.yebeh.2020.106935

Roberts E, Frankel S. Gamma-aminobutyric acid in brain: its formation from glutamic acid. J Biol Chem 1950;187:55–63

Rogers, M. F., Shihab, H. A., Mort, M., Cooper, D. N., Gaunt, T. R., & Campbell, C. (2018). FATHMM-XF: accurate prediction of pathogenic point mutations via extended features. *Bioinformatics (Oxford, England)*, *34*(3), 511–513. https://doi.org/10.1093/bioinformatics/btx536

Satterstrom, F. K., Kosmicki, J. A., Wang, J., Breen, M. S., De Rubeis, S., An, J. Y., Peng, M., Collins, R., Grove, J., Klei, L., Stevens, C., Reichert, J., Mulhern, M. S., Artomov, M., Gerges, S., Sheppard, B., Xu, X., Bhaduri, A., Norman, U., Brand, H., … Buxbaum, J. D. (2020). Large-Scale Exome Sequencing Study Implicates Both Developmental and Functional Changes in the Neurobiology of Autism. *Cell*, *180*(3), 568–584.e23. https://doi.org/10.1016/j.cell.2019.12.036

Scheffer, I. E. et al. ILAE classification of the epilepsies: Position paper of the ILAE Commission for Classification and Terminology. *Epilepsia* **58**, 512–521 (2017).

Selmer, K. K., Eriksson, A. S., Brandal, K., Egeland, T., Tallaksen, C., & Undlien, D. E. (2009). Parental SCN1A mutation mosaicism in familial Dravet syndrome. *Clinical genetics*, *76*(4), 398–403. https://doi.org/10.1111/j.1399-0004.2009.01208.x

Scheffer, I. E., & Nabbout, R. (2019). SCN1A-related phenotypes: Epilepsy and beyond. *Epilepsia*, *60 Suppl 3*, S17–S24. https://doi.org/10.1111/epi.16386

Sente A, Desai R, Naydenova K, Malinauskas T, Jounaidi Y, Miehling J, Zhou X, Masiulis S, Hardwick SW, Chirgadze DY, Miller KW, Aricescu AR. Differential assembly diversifies $GABA_A$ receptor structures and signalling. Nature. 2022 Apr;604(7904):190-194. doi: 10.1038/s41586-022-04517-3. Epub 2022 Mar 30. PMID: 35355020; PMCID: PMC7612593.ACMG

Shastry B. S. (2009). SNPs: impact on gene function and phenotype. *Methods in molecular biology (Clifton, N.J.)*, *578*, 3–22. https://doi.org/10.1007/978-1-60327-411-1_1

Shi, Y. W., Zhang, Q., Cai, K., Poliquin, S., Shen, W., Winters, N., Yi, Y. H., Wang, J., Hu, N., Macdonald, R. L., Liao, W. P., & Kang, J. Q. (2019). Synaptic clustering differences due to different GABRB3 mutations cause variable epilepsy syndromes. *Brain : a journal of neurology*, *142*(10), 3028–3044. https://doi.org/10.1093/brain/awz250

Sieghart, W., Fuchs, K., Tretter, V., Ebert, V., Jechlinger, M., Höger, H., & Adamiker, D. (1999). Structure and subunit composition of GABA(A) receptors. *Neurochemistry international*, *34*(5), 379–385. https://doi.org/10.1016/s0197-0186(99)00045-5

Staley K. (2015). Molecular mechanisms of epilepsy. *Nature neuroscience*, *18*(3), 367–372. https://doi.org/10.1038/nn.3947

Stone, E. A., Cooper, G. M., & Sidow, A. (2005). Trade-offs in detecting evolutionarily constrained sequence by comparative genomics. Annual review of genomics and human genetics, 6, 143–164. https://doi.org/10.1146/annurev.genom.6.080604.162146

Takata, A., Nakashima, M., Saitsu, H., Mizuguchi, T., Mitsuhashi, S., Takahashi, Y., Okamoto, N., Osaka, H., Nakamura, K., Tohyama, J., Haginoya, K., Takeshita, S., Kuki, I., Okanishi, T., Goto, T., Sasaki, M., Sakai, Y., Miyake, N., Miyatake, S., Tsuchida, N., … Matsumoto, N. (2019). Comprehensive analysis of coding variants highlights genetic complexity in developmental and epileptic encephalopathy. *Nature communications*, *10*(1), 2506.https://doi.org/10.1038/s41467-019-10482 9

Tanaka, M., Olsen, R. W., Medina, M. T., Schwartz, E., Alonso, M. E., Duron, R. M., Castro-Ortega, R., Martinez-Juarez, I. E., Pascual-Castroviejo, I., Machado-Salas, J., Silva, R., Bailey, J. N., Bai, D.,

Ochoa, A., Jara-Prado, A., Pineda, G., Macdonald, R. L., & Delgado-Escueta, A. V. (2008). Hyperglycosylation and reduced GABA currents of mutated GABRB3 polypeptide in remitting childhood absence epilepsy. *American journal of human genetics*, *82*(6), 1249–1261. https://doi.org/10.1016/j.ajhg.2008.04.020

Tanaka, M., Bailey, J. N., Bai, D., Ishikawa-Brush, Y., Delgado-Escueta, A. V., & Olsen, R. W. (2012). Effects on promoter activity of common SNPs in 5' region of GABRB3 exon 1A. *Epilepsia*, *53*(8), 1450–1456. https://doi.org/10.1111/j.1528-1167.2012.03572.x

Tang, H., & Thomas, P. D. (2016). PANTHER-PSEP: predicting disease-causing genetic variants using position-specific evolutionary preservation. *Bioinformatics (Oxford, England)*, *32*(14), 2230–2232. https://doi.org/10.1093/bioinformatics/btw222

Tang, X., Jaenisch, R., & Sur, M. (2021). The role of GABAergic signalling in neurodevelopmental disorders. *Nature reviews. Neuroscience*, *22*(5), 290–307. https://doi.org/10.1038/s41583-021-00443-x

Terunuma M. (2018). Diversity of structure and function of $GABA_B$ receptors: a complexity of $GABA_B$-mediated signaling. *Proceedings of the Japan Academy. Series B, Physical and biological sciences*, *94*(10), 390–411. https://doi.org/10.2183/pjab.94.026

Trott, O., & Olson, A. J. (2010). AutoDock Vina: improving the speed and accuracy of docking with a new scoring function, efficient optimization, and multithreading. *Journal of computational chemistry*, *31*(2), 455–461. https://doi.org/10.1002/jcc.21334

Treiman D. M. (2001). GABAergic mechanisms in epilepsy. *Epilepsia*, *42 Suppl 3*, 8–12. https://doi.org/10.1046/j.1528-1157.2001.042suppl.3008.x

Trump N, McTague A, Brittain H, Papandreou A, Meyer E, Ngoh A, Palmer R, Morrogh D, Boustred C, Hurst JA, Jenkins L, Kurian MA, Scott RH. Improving diagnosis and broadening the phenotypes in early-onset seizure and severe developmental delay disorders through gene panel analysis. J Med Genet. 2016 May;53(5):310-7. doi: 10.1136/jmedgenet-2015-103263. Epub 2016 Mar 18. PMID: 26993267; PMCID: PMC4862068.

Velisetty, P., Chalamalasetti, S. V., & Chakrapani, S. (2014). Structural basis for allosteric coupling at the membrane-protein interface in Gloeobacter violaceus ligand-gated ion channel (GLIC). *The Journal of biological chemistry*, *289*(5), 3013–3025. https://doi.org/10.1074/jbc.M113.523050

Venselaar, H., Te Beek, T. A., Kuipers, R. K., Hekkelman, M. L., & Vriend, G. (2010). Protein structure analysis of mutations causing inheritable diseases. An e-Science approach with life scientist friendly interfaces. *BMC bioinformatics*, *11*, 548. https://doi.org/10.1186/1471-2105-11-548

Vihinen M. (2021). Functional effects of protein variants. *Biochimie*, *180*, 104–120. https://doi.org/10.1016/j.biochi.2020.10.009

Visscher, P. M., Wray, N. R., Zhang, Q., Sklar, P., McCarthy, M. I., Brown, M. A., & Yang, J. (2017). 10 Years of GWAS Discovery: Biology, Function, and Translation. *American journal of human genetics*, *101*(1), 5–22. https://doi.org/10.1016/j.ajhg.2017.06.005

Wang, D. D., & Kriegstein, A. R. (2008). GABA regulates excitatory synapse formation in the neocortex via NMDA receptor activation. *The Journal of neuroscience : the official journal of the Society for Neuroscience*, *28*(21), 5547–5558. https://doi.org/10.1523/JNEUROSCI.5599-07.2008

Wang, J., Lin, Z. J., Liu, L., Xu, H. Q., Shi, Y. W., Yi, Y. H., He, N., & Liao, W. P. (2017). Epilepsy-associated genes. *Seizure*, *44*, 11–20. https://doi.org/10.1016/j.seizure.2016.11.030

Warrier, V., Baron-Cohen, S., & Chakrabarti, B. (2013). Genetic variation in GABRB3 is associated with Asperger syndrome and multiple endophenotypes relevant to autism. *Molecular autism*, *4*(1), 48. https://doi.org/10.1186/2040-2392-4-48

Waterhouse, A., Bertoni, M., Bienert, S., Studer, G., Tauriello, G., Gumienny, R., Heer, F. T., de Beer, T. A. P., Rempfer, C., Bordoli, L., Lepore, R., & Schwede, T. (2018). SWISS-MODEL: homology

modelling of protein structures and complexes. *Nucleic acids research*, *46*(W1), W296–W303. https://doi.org/10.1093/nar/gky427

Wishart, D. S., Feunang, Y. D., Guo, A. C., Lo, E. J., Marcu, A., Grant, J. R., Sajed, T., Johnson, D., Li, C., Sayeeda, Z., Assempour, N., Iynkkaran, I., Liu, Y., Maciejewski, A., Gale, N., Wilson, A., Chin, L., Cummings, R., Le, D., Pon, A., … Wilson, M. (2018). DrugBank 5.0: a major update to the DrugBank database for 2018. *Nucleic acids research*, *46*(D1), D1074–D1082. https://doi.org/10.1093/nar/gkx1037

Wong, L. W., Tae, H. S., & Cromer, B. A. (2015). Assembly, trafficking and function of α1β2γ2 GABAA receptors are regulated by N-terminal regions, in a subunit-specific manner. *Journal of neurochemistry*, *134*(5), 819–832. https://doi.org/10.1111/jnc.13175

World Health Organization, Epilepsy. http://www.who.int/mediacentre/factsheets/fs999/en/. (Accessed 5 September 2023).

Xu, M. I. N. G., & Akabas, M. H. (1996). Identification of channel-lining residues in the M2 membrane-spanning segment of the GABA (A) receptor alpha1 subunit. *The Journal of General Physiology*, *107*(2), 195-205.

Yang, X., Pan, G., Li, W. H., Zhang, L. M., Wu, B. B., Wang, H. J., Zhang, P., & Zhou, S. Z. (2017). *Zhonghua er ke za zhi = Chinese journal of pediatrics*, *55*(11), 813–817. https://doi.org/10.3760/cma.j.issn.0578-1310.2017.11.004

Yang, Y., Xiangwei, W., Zhang, X., Xiao, J., Chen, J., Yang, X., Jia, T., Yang, Z., Jiang, Y., & Zhang, Y. (2020). Phenotypic spectrum of patients with GABRB2 variants: from mild febrile seizures to severe epileptic encephalopathy. *Developmental medicine and child neurology*, *62*(10), 1213–1220. https://doi.org/10.1111/dmcn.14614

Zhang, M. W., Liang, X. Y., Wang, J., Gao, L. D., Liao, H. J., He, Y. H., Yi, Y. H., He, N., Liao, W. P., & China Epilepsy Gene 1.0 Project (2023). Epilepsy-associated genes: an update. *Seizure*, S1059-1311(23)00254-6. Advance online publication. https://doi.org/10.1016/j.seizure.2023.09.021

Zhu, S., Noviello, C. M., Teng, J., Walsh, R. M., Jr, Kim, J. J., & Hibbs, R. E. (2018). Structure of a human synaptic $GABA_A$ receptor. *Nature*, *559*(7712), 67–72. https://doi.org/10.1038/s41586-018-0255-3

APENDIXES

Data Sheet 1. *Protein stability*

AA Change	MUpro	I-Mutant 3.0	AA Change	MUpro	I-Mutant 3.0
Y471C	Decrease	Decrease	**C175W**	Decrease	Decrease
Y467S	Decrease	Decrease	**P169L**	Decrease	Decrease
Y467H	Decrease	Decrease	**A160E**	Decrease	Decrease
Y329H	Decrease	Decrease	**A160V**	Decrease	Decrease
A320T	Decrease	Decrease	**L153P**	Decrease	Decrease
V317A	Decrease	Decrease	**Y151C**	Decrease	Decrease
K304E	Decrease	Decrease	**V149M**	Decrease	Decrease
P298S	Decrease	Decrease	**D146A**	Decrease	Decrease
R294Q	Decrease	Decrease	**L143R**	Decrease	Decrease
L293P	Decrease	Decrease	**R142C**	Decrease	Decrease
V283M	Decrease	Decrease	**N138T**	Decrease	Decrease
T282A	Decrease	Decrease	**H132Y**	Decrease	Decrease
T281A	Decrease	Decrease	**Y99C**	Decrease	Decrease
G279R	Decrease	Decrease	**D94E**	Decrease	Decrease
N268K	Decrease	Decrease	**Y82S**	Decrease	Decrease
S264F	Decrease	Decrease	**Y82C**	Decrease	Decrease
S234L	Decrease	Decrease	**M80R**	Decrease	Decrease
Y230C	Decrease	Decrease	**D73H**	Decrease	Decrease
T227P	Decrease	Decrease	**G57R**	Decrease	Decrease
D188V	Decrease	Decrease	**R51G**	Decrease	Decrease
Y182H	Decrease	Decrease	**D49E**	Decrease	Decrease
			Y48C	Decrease	Decrease

Data Sheet 2. *Presentation of the superimposed structure*

17 pathogenic SNPs in GABRB3 with comments from HOPE. SWISS MODEL (Homology Modeling) & UCSF Chimera 1.16 (Validation of Visualizing).

Y467S

Tyrosine **Serine**

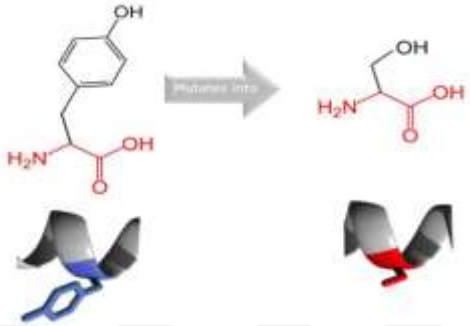

The mutant residue appears smaller than the wild type residue.Therefore an empty space wil form in the core of the protein.This size difference can affect the contacts with the lipid-membrane.

As a result of both the Consurf and HOPE score results, it can be said with high confidence that the mutant residue is located near a highly conserved location.

Y467H

Tyrosine **Histidine**

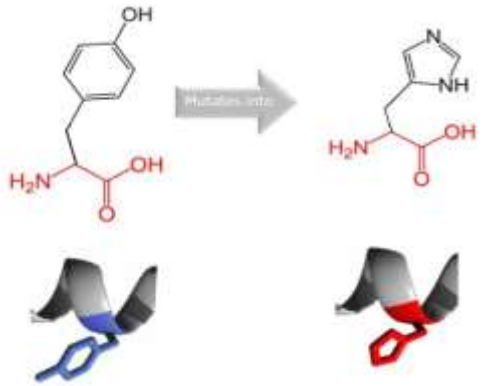

The mutant residue is smaller than the wild-type. This size difference can affect the contacts with the lipid-membrane.

The wild type residue is more hyrdophobic than the mutant residue.

The difference in hydrophobicity will affect hydrogen bond formation. This differences in hydrophobicity can affect the hydrophobic interactions with the membrane lipids.

The difference in size between the two residues ensures that the new residue is not in the right position to make the same hydrogen bond as the original wild-type residue did.

P298S

Proline **Serine**

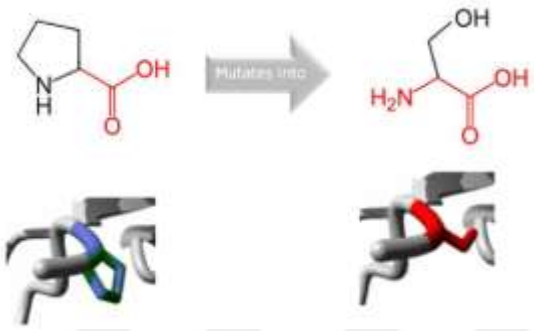

The mutant residue is smaller than the wild-type residue.

The wild-type residue is more hydrophobic than the mutant residue.

The wild-type residue is a proline. Prolines are known to be very rigid and therefore induce a special backbone conformation which might be required at this position. The mutation can disturb this special conformation.

R294Q

Arginine **Glutamine**

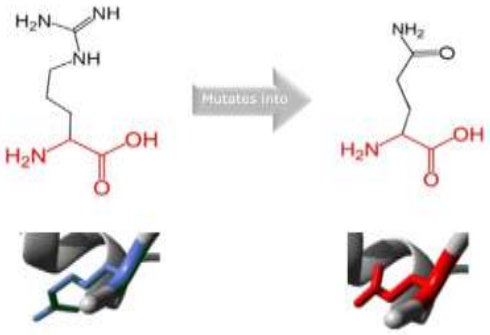

The mutant residue is smaller than the wild-type residue.

The size difference between wild-type and mutant residue makes that the new residue is not in the correct position to make the same hydrogen bond as the original wild-type residue did.

The wild-type residue charge was POSITIVE, the mutant residue charge is NEUTRAL.

The difference in charge will disturb the ionic interaction made by the original, wild-type residue.

T281A

Threonine **Alanine**

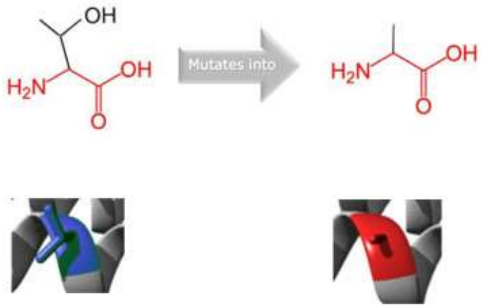

The mutant residue is smaller than the wild-type residue. The new residue might be too small to make multimer contacts.
This size difference can affect the contacts with the lipid-membrane.

The mutant residue is more hydrophobic than the wild-type residue. The difference in hydrophobicity will affect hydrogen bond formation. This differences in hydrophobicity can affect the hydrophobic interactions with the membrane lipids

---

G279R

Glycine **Arginine**

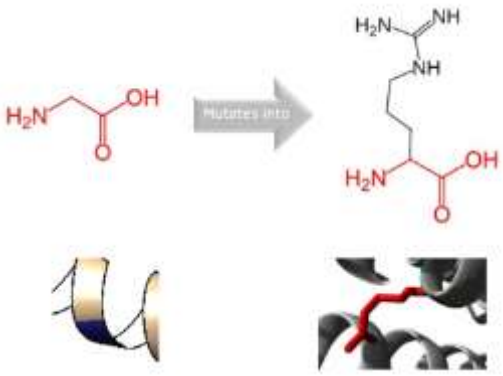

The mutant residue is bigger than the wild-type residue.

This size difference can affect the contacts with the lipid membrane.

The wild-type residue was buried in the core of the protein.
The mutant residue is bigger and probably will not fit.

The wild-type residue is more hydrophobic than the mutant residue. This differences in hydrophobicity can affect the hydrophobic interactions with the membrane lipids.

The wild-type residue charge was NEUTRAL, the mutant residue charge is POSITIVE. The mutant residue introduces a charge in a buried residue which can lead to protein folding problems.

S264F

Serine **Phenylalanine**

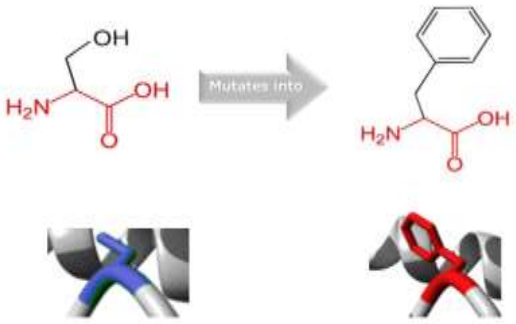

The mutant residue is bigger than the wild-type residue.This size difference can affect the contacts with the lipid-membrane.The wild-type residue was buried in the core of the protein. The mutant residue is bigger and probably will not fit.
The mutant residue is more hydrophobic than the wild-type residue.This differences in hydrophobicity can affect the hydrophobic interactions with the membrane lipids. The difference in hydrophobicity will affect hydrogen bond formation.

Y182H

Tyrosine **Histidine**

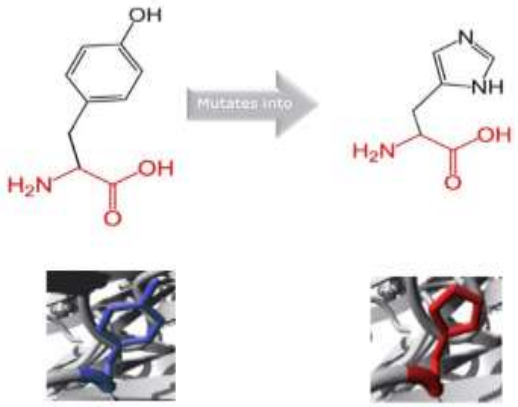

The wild-type and mutant amino acids differ in size.The mutant residue is smaller than the wild-type residue.The mutation will cause an empty space in the core of the protein.

The hydrophobicity of the wild-type and mutant residue differs.The mutation will cause loss of hydrophobic interactions in the core of the protein.

The mutant residue is located near a highly conserved position.

C175W

Cysteine **Tryptophan**

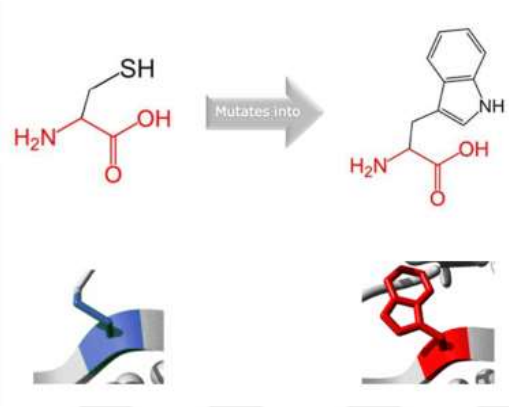

The mutant residue is bigger than the wild-type residue.The wild-type residue was buried in the core of the protein. The mutant residue is bigger and probably will not fit.

Together with loss of the cysteine bond, the differences between the old and new residue can cause destabilization of the structure.

The wild-type residue is very conserved.

P169L

Proline **Leucine**

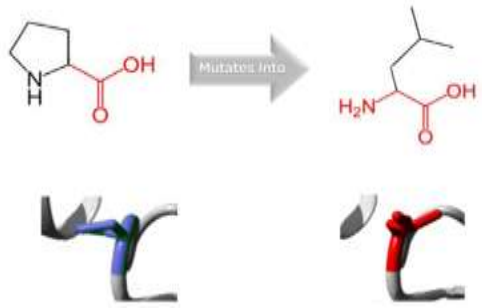

The wild-type residue is a proline. Prolines are known to be very rigid and therefore induce a special backbone conformation which might be required at this position. The mutation can disturb this special conformation.

The mutant residue is bigger than the wild-type residue. The wild-type residue was buried in the core of the protein. The mutant residue is bigger and probably will not fit.

The wild-type residue is very conserved.

R142C

Arginine **Cysteine**

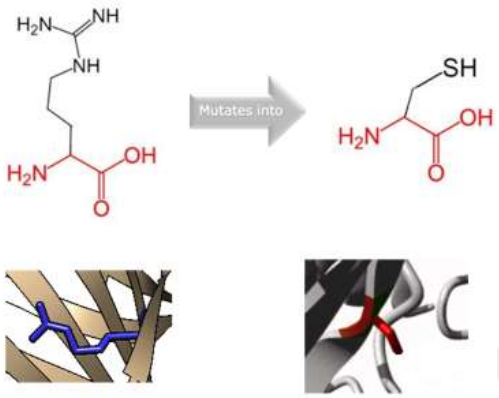

The mutant residue is smaller than the wild-type residue.The new residue might be too small to make multimer contacts.

The wild-type residue charge was POSITIVE, the mutant residue charge is NEUTRAL. The charge of the buried wild-type residue is lost by this mutation.

The mutant residue is more hydrophobic than the wild-type residue. The difference in hydrophobicity will affect hydrogen bond formation. A more hydrophobic residue is introduced here. Any hydrogen bond that could be made by the wild-type residue to other monomers will be lost now and affect the multimeric contacts.

H132Y

Histidine **Tyrosine**

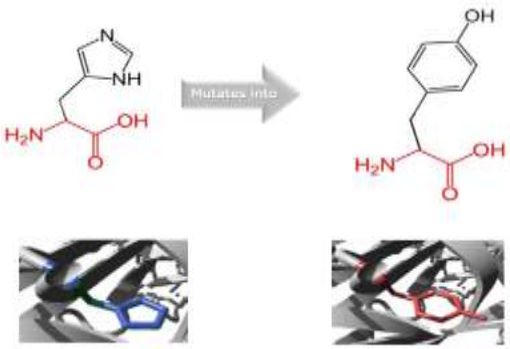

The mutant residue is bigger than the wild-type residue. The wild-type residue was buried in the core of the protein. The mutant residue is bigger and probably will not fit.

The hydrophobicity of the wild-type and mutant residue differs. The mutation will cause loss of hydrogen bonds in the core of the protein and as a result disturb correct folding.

D94E

Aspartic Acid **Glutamic Acid**

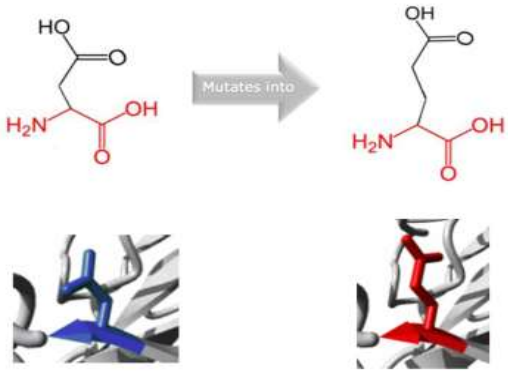

The mutant residue is bigger than the wild-type residue.The wild-type residue was buried in the core of the protein. The mutant residue is bigger and probably will not fit.

Only this residue type was found at this position. Mutation of a 100% conserved residue is usually damaging for the protein.

M80R

Methionine **Arginine**

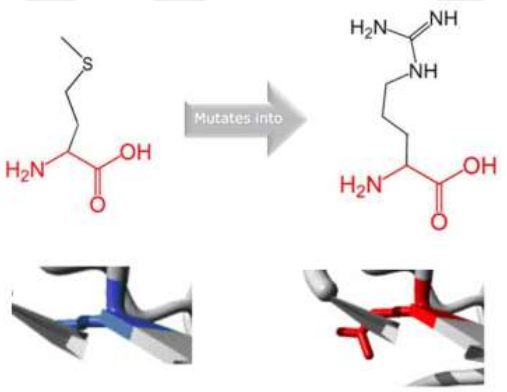

The mutant residue is bigger than the wild-type residue.The wild-type residue was buried in the core of the protein. The mutant residue is bigger and probably will not fit.

The wild-type residue charge was NEUTRAL, the mutant residue charge is POSITIVE.

The hydrophobicity of the wild-type and mutant residue differs.The mutation will cause loss of hydrophobic interactions in the core of the protein.

D73H

Aspartic Acid **Histidine**

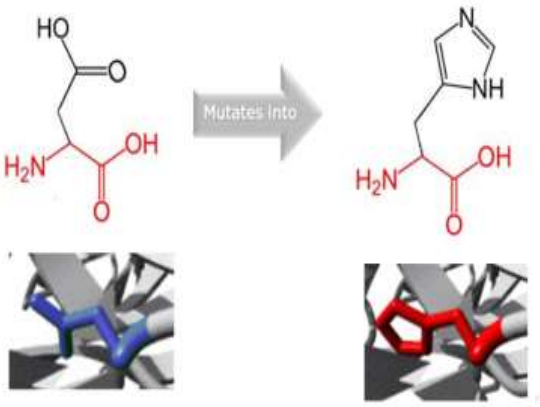

The mutant residue is bigger than the wild-type residue.

The residue is located on the surface of the protein, mutation of this residue can disturb interactions with other molecules or other parts of the protein.

The wild-type residue charge was NEGATIVE, the mutant residue charge is NEUTRAL.

The charge of the wild-type residue is lost by this mutation. This can cause loss of interactions with other molecules.

D49E

Aspartic Acid **Glutamic Acid**

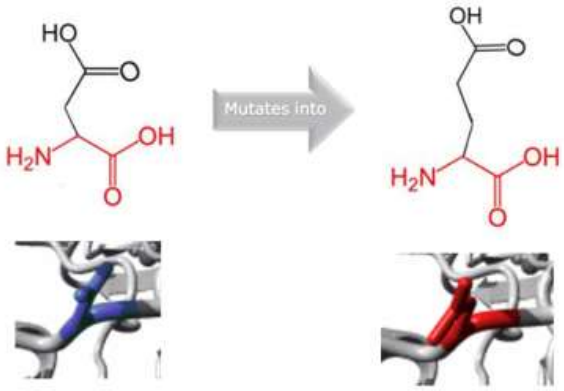

The mutant residue is bigger than the wild-type residue.The mutation introduces a bigger residue at this position, this can disturb the multimeric interactions.

Only this residue type was found at this position. Mutation of a 100% conserved residue is usually damaging for the protein. Mutant residue is located near a highly conserved position.

Y48C

Tyrosine **Cysteine**

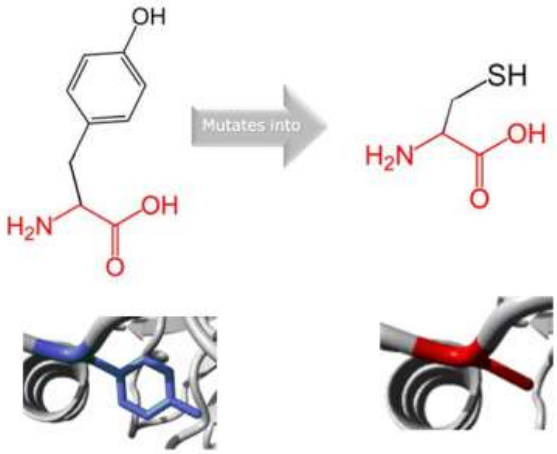

The mutant residue is smaller than the wild-type residue.This will cause a possible loss of external interactions.

The mutant residue is more hydrophobic than the wild-type residue.The difference in hydrophobicity will affect hydrogen bond formation.

Data Sheet 3. *Analysis of structural effects with images of superimposed atoms*

Y182H

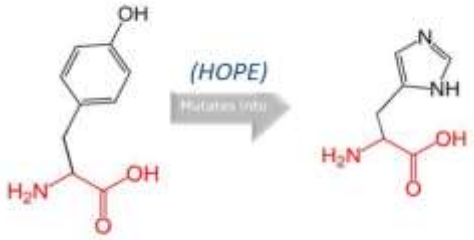

The wild-type and mutant amino acids differ in size.
The mutant residue is smaller than the wild-type residue.
This will cause a possible loss of external interactions.
The wild-type residue is more hydrophobic than the mutant residue.

(SWISS MODEL & UCSF Chimera)

Y182C

The wild-type and mutant amino acids differ in size.
The mutant residue is smaller than the wild-type residue.
This will cause a possible loss of external interactions.
The mutant residue is more hydrophobic than the wild-type residue.

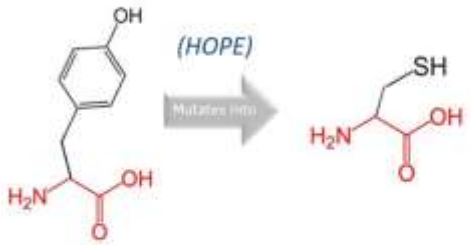

(SWISS MODEL & UCSF Chimera)

F225V

The wild-type and mutant amino acids differ in size.
The mutant residue is smaller than the wild-type residue.
This will cause a possible loss of external interactions.

(SWISS MODEL & UCSF Chimera)

T227A

The mutant residue is smaller than the wild-type residue.
The mutant residue is more hydrophobic than the wild-type residue.
The difference in hydrophobicity will affect hydrogen bond formation.

(SWISS MODEL & UCSF Chimera)

T227P

Each amino acid has its own specific size.
The mutant residue is more hydrophobic than the wild-type residue.
The difference in hydrophobicity will affect hydrogen bond formation.

(SWISS MODEL & UCSF Chimera)

Y230C

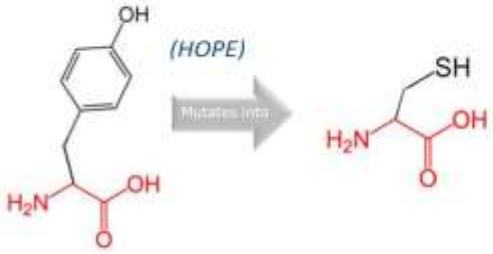

The wild-type and mutant amino acids differ in size.
The mutant residue is smaller than the wild-type residue.
The mutation will cause an empty space in the core of the protein.
The hydrophobicity of the wild-type and mutant residue differs.
The difference in properties between wild-type and mutation can easily cause loss of interactions with the ligand.

(SWISS MODEL & UCSF Chimera)

Data Sheet 4. Binding affinity outputs.

*Binding affinity of WT GABRB3 and GABRB3 containing variant residues (A) Cys 182, (B) His 182, (C) Val 225, (D) Pro 227, (E) Ala 227, and (F) Cys 230 to γ-Aminobutyric acid (GABA). *The docking interactions of the variants and WT of GABRB3 were examined, it was calculated as ΔΔG = -4.8 Kcal/mol, ΔΔG= -4.9 Kcal/mol, ΔΔG= -5.0 Kcal/mol, ΔΔG= -5.0 Kcal/mol, ΔΔG= -5.1 Kcal/mol and ΔΔG= -5.3 Kcal/mol for the Y182C, Y182H, T227A, T227P, F225V, Y230C variants and WT, respectively. **RMSD: Root-Mean-Square Deviation (RMSD l.b /u.b: lower bound/ upper bound*

(A)	**WT-Tyr 182**			**Cys 182**			
Mode	Affinity (Kcal/mol)	Distance from best mode RMSD l.b	RMSD u.b	Mode	Affinity (Kcal/mol)	Distance from best mode RMSD l.b	RMSD u.b
1	-5.3	0.000	0.000	1	-4.8	0.000	0.000
2	-4.9	1.429	1.920	2	-4.7	1.651	1.834
3	-4.5	2.704	3.560	3	-4.4	3.332	4.137
4	-4.5	3.031	3.748	4	-4.3	2.699	3.373
5	-4.3	1.899	2.014	5	-4.1	2.494	2.674
6	-4.2	1.965	2.358	6	-4.1	3.170	4.007
7	-3.9	2.058	2.633	7	-4.1	2.382	2.884
8	-3.8	3.502	4.045	8	-3.9	2.923	3.560
9	-3.8	3.025	3.642	9	-3.7	3.388	3.938

(B)	**WT-Tyr 182**			**His 182**			
Mode	Affinity (Kcal/mol)	Distance from best mode RMSD l.b	RMSD u.b	Mode	Affinity (Kcal/mol)	Distance from best mode RMSD l.b	RMSD u.b
1	-5.3	0.000	0.000	1	-4.9	0.000	0.000
2	-4.9	1.429	1.920	2	-4.8	1.615	1.838
3	-4.5	2.704	3.560	3	-4.8	1.293	1.750
4	-4.5	3.031	3.748	4	-4.5	2.301	2.785
5	-4.3	1.899	2.014	5	-4.4	3.468	4.264
6	-4.2	1.965	2.358	6	-4.2	3.132	3.982
7	-3.9	2.058	2.633	7	-3.8	3.073	3.586
8	-3.8	3.502	4.045	8	-3.7	2.223	2.981
9	-3.8	3.025	3.642	9	-3.7	3.431	4.152

(C)	**WT-Phe 225**			**Val 225**			
Mode	Affinity (Kcal/mol)	Distance from best mode RMSD l.b	RMSD u.b	Mode	Affinity (Kcal/mol)	Distance from best mode RMSD l.b	RMSD u.b
1	-5.3	0.000	0.000	1	-5.1	0.000	0.000
2	-4.9	1.429	1.920	2	-5.1	0.077	1.428
3	-4.5	2.704	3.560	3	-4.9	1.494	1.836
4	-4.5	3.031	3.748	4	-4.5	2.838	3.653
5	-4.3	1.899	2.014	5	-4.4	3.341	3.975
6	-4.2	1.965	2.358	6	-4.4	1.575	2.186
7	-3.9	2.058	2.633	7	-4.2	3.541	4.265
8	-3.8	3.502	4.045	8	-4.2	2.224	2.722
9	-3.8	3.025	3.642	9	-4.0	2.106	2.498

Continued Data Sheet 4

(D)	WT-Thr 227			Pro 227			
Mode	Affinity (Kcal/mol)	Distance from best mode RMSD l.b	RMSD u.b	Mode	Affinity (Kcal/mol)	Distance from best mode RMSD l.b	RMSD u.b
1	-5.3	0.000	0.000	1	-5.0	0.000	0.000
2	-4.9	1.429	1.920	2	-5.0	1.438	1.760
3	-4.5	2.704	3.560	3	-4.7	2.788	3.670
4	-4.5	3.031	3.748	4	-4.6	1.543	1.747
5	-4.3	1.899	2.014	5	-4.5	3.193	3.876
6	-4.2	1.965	2.358	6	-4.0	1.783	2.249
7	-3.9	2.058	2.633	7	-2.9	3.098	3.923
8	-3.8	3.502	4.045				
9	-3.8	3.025	3.642				

(E)	WT-Thr 227			Ala 227			
Mode	Affinity (Kcal/mol)	Distance from best mode RMSD l.b	RMSD u.b	Mode	Affinity (Kcal/mol)	Distance from best mode RMSD l.b	RMSD u.b
1	-5.3	0.000	0.000	1	-5.0	0.000	0.000
2	-4.9	1.429	1.920	2	-4.9	1.478	1.962
3	-4.5	2.704	3.560	3	-4.5	3.047	3.975
4	-4.5	3.031	3.748	4	-4.5	2.796	3.440
5	-4.3	1.899	2.014	5	-4.2	1.149	1.784
6	-4.2	1.965	2.358	6	-4.1	2.086	2.744
7	-3.9	2.058	2.633	7	-4.0	1.941	2.105
8	-3.8	3.502	4.045	8	-3.5	0.774	1.631
9	-3.8	3.025	3.642				

(F)	WT-Tyr 230			Cys 230			
Mode	Affinity (Kcal/mol)	Distance from best mode RMSD l.b	RMSD u.b	Mode	Affinity (Kcal/mol)	Distance from best mode RMSD l.b	RMSD u.b
1	-5.3	0.000	0.000	1	-5.1	0.000	0.000
2	-4.9	1.429	1.920	2	-5.0	1.444	1.882
3	-4.5	2.704	3.560	3	-4.6	3.363	3.983
4	-4.5	3.031	3.748	4	-4.5	3.343	4.183
5	-4.3	1.899	2.014	5	-4.4	3.023	3.766
6	-4.2	1.965	2.358	6	-3.3	2.425	2.766
7	-3.9	2.058	2.633	7	-3.1	1.725	1.725
8	-3.8	3.502	4.045	8	-3.0	1.749	1.978
9	-3.8	3.025	3.642	9	-2.6	3.176	3.903